Chemical scale investigations of ligand-gated ion channels using unnatural amino acids

Thesis by

Darren Lee Beene

In Partial Fulfillment of the

Requirements for the Degree of

Doctor of Philosophy

California Institute of Technology

Pasadena, California

2005

(Defended December 9, 2004)

for V.A.B. and E.S.B.

. . . everyday.

Acknowledgments

so much depends
upon

a red wheel
barrow

glazed with rain
water

beside the white
chickens.
W.C. Williams

Well somehow, despite my reluctance to venture beyond the academic confines, I will soon no longer be a student. The salad days are over. Having spent nearly thirty years of my life in school, there are more than a few to thank. First I must give credit to public education. From elementary school to university, I have received quality instruction at these state institutions. I also must give thanks to the Caltech community for creating a research institute truly different from the rest. Much thanks and appreciation goes to my advisor, Dennis Dougherty. In addition to creating a research environment where it was always a pleasure to work, his scientific reasoning and interpretive insight never failed to amaze me. An added bonus of joining the Dougherty group has been the opportunity to work with Henry Lester, who is a dedicated mentor and a firm believer in scientific discussion. I have also had the pleasure of a very fruitful collaboration with the Sarah Lummis group at the University of Cambridge. I am very thankful for the time and effort they have contributed to our joint projects. I would also like to thank my committee, Peter Dervan, Richard Roberts, and Robert Grubbs for their time and commitment to my education.

One of the great pleasures of my time at Caltech has been working with the members of the Dougherty group, who are, to the last, some of the most positive and creative

people I know (and anyone who says different is itchin' for a fight). Of the historical members who were there when I arrived, Joshua Maurer and Gabriel Brandt deserve special mention. It is not hyperbole to say these two have had a lasting influence on group culture. During my time in the group, Josh and Gabe were the stewards of technical and scientific knowledge. Josh is perhaps the most generous and helpful curmudgeon I have had the pleasure of knowing, and Gabe is truly a renaissance man. I am also indebted to other past members of the group. Lintong Li (at least in my time) broke the baby barrier for the group and was an excellent example of how to balance research and family. Niki Zacharias is an incredibly humane person and I have always been impressed with her social commitment. Don Elmore, the other literature major, was consistently a source of interesting conversation and positive cheer. David Dahan and I became first-time parents around the same time and got to share the joys and trials of parenthood.

In addition to past members, I also owe gratitude to the current line-up of Dougherty all-stars. I entered the group with E. James Petersson, Sarah May (nee´ Monahan), and Steve Spronk. Whether it involves suppression in mammalian cells, swimming or photography, Sarah is one of the most indefatigable people I know, and I have often wished I had one-tenth of her energy. Steve and I were the resident sport fanatics and were it not for a bum knee on my part, would have likely rivaled Stockton-to-Malone in the Caltech Intramural Basketball League. While at Caltech, I have had the pleasure of becoming good friends with James. I am greatly appreciative for the support and assistance he has provided, and must say that due in large part to his expertise and generous nature, group research did not miss a beat with Josh and Gabe's departure.

Tingwei Mu with his good nature never seemed to mind when my teetering mess encroached on his desk. Amanda Cashin always made work enjoyable, in particular when trying to diagnose the sometimes fickle Opus. Lori Lee has kindly volunteered to ensure the thioamide work will not die an ignoble death and will in my absence, I am sure, keep Michael on the straight and narrow. Michael Torrice never seemed to mind my (I hope not too) relentless ribbing and was a welcome addition to the lunch crew. Amy Eastwood set a high bar for desk management and order, a talent I hope at least in part rubbed off on me. Erik Rodriguez is a very capable scientist who always impressed me with his technical skills. Joanne Xiu, Kiowa Bower, Katie McMenimen, and Ariele Hanek have been welcome additions to the lab and I am sure will continue the Dougherty group tradition in developing time-wasting technologies.

I have made several good friends (apart from Dougherty group members) who have contributed significant enjoyment to my time at Caltech. Oren Scherman, my first roommate at Caltech, is a loyal friend and always has a unique (some say slightly crazy) take on things. Chris Thomas, my second roommate at Caltech, is an impressive chemist and wise beyond his years. Greg Drummond and I made several memorable treks to the Sierras, and I appreciate his adventurous and self-reliant spirit.

I save my final thanks for family. I am deeply thankful to my parents. Their passion for learning and adventure set a continual example of a well-lived life. My sister has a very kind soul and is always ready to help. I am infinitely grateful to my wife and kids. Maxwell and Beckett have brought more joy to my life than I could have ever imagined and put simply, Wendy makes my world spin.

Abstract

The Cys loop receptors, a family of ligand-gated ion channels, mediate fast synaptic transmission throughout the peripheral and central nervous systems. These are large multisubunit proteins, whose primary function is to transduce a chemical signal, binding of a neurotransmitter, into an electrical signal, ion flux across the cell membrane. These receptors have been implicated in several disease states and represent major therapeutic targets. The work presented in this thesis focuses on the chemical-scale elucidation of Cys loop receptors. The main approach of this work is the structure-function study using *in vivo* nonsense suppression methods. This technique allows for the site-specific incorporation of an unnatural amino acid into a protein expressed in a living cell.

Nonsense suppression methods were used to incorporate a series of fluorinated tryptophan derivatives into the binding site of the 5-HT_3R. This study identified a cation-π interaction between Trp 183 and the neurotransmitter, serotonin. A similar study using fluorinated phenylalanine derivatives identified a cation-π binding site at Tyr 198 in the $GABA_C$ receptor. These studies build on previous work from our research group and provide further evidence that the cation-π interaction is a common feature in ligand recognition by Cys loop receptors.

Nonsense suppression was also used to examine the role of several tyrosine residues in the 5-HT_3R. Here the findings demonstrated that the side chains of Tyr 143 and 153 make functionally important hydrogen bonds. These data were used to refine several computational models of serotonin docked into the binding site.

Structure-function studies of two conserved prolines in the M2-M3 loop showed that this region of the receptor is involved in the conformational changes associated with

receptor activation. The data also provide preliminary evidence that Pro 308 may serve as hinge for the gating movement of the M2 helix.

Table of Contents

Acknowledgments iv

Abstract vii

List of Figures xi

List of Tables xii

List of Schemes xiii

Chapter 1. Introduction 1

1.1 Chemistry and the brain 1

1.2 The Cys loop family of ligand-gated ion channels 3

1.3 Unnatural amino acid mutagenesis 7

1.4 Structure-function studies 11

1.5 References 12

Chapter 2. Cation-π interactions in ligand recognition by serotonergic (5-HT_3) and nicotinic acetylcholine receptors 15

2.1 Introduction 15

2.2 Results 17

2.3 Discussion 34

2.4 Conclusions 39

2.5 Methods 40

2.6 References 41

Chapter 3. Structure-function studies of tyrosines in the ligand-binding pocket of the 5-HT_{3A}R 46

3.1 Introduction 46

3.2 Results 48

3.3 Discussion 60

3.4 Conclusions 66

3.5 Methods 67

3.6 References 68

Chapter 4. Conserved prolines in the M2-M3 loop 70

4.1 Introduction 70

4.2 Transmembrane domains and the M2-M3 loop 72

4.3 Potential dynamic role of proline 75

4.4 Experimental design 79

4.5 Results 80

4.6 Discussion 94

4.7 Future directions 98

4.8 Methods 98

4.9 References 102

Chapter 5. Miscellaneous studies 107

5.1 Introduction 107

5.2 $GABA_C$ studies 107

5.3 Phe 226 in the 5-HT$_3$R 114

5.4 Efforts towards the incorporation of a backbone thioamide 117

5.5 References 127

List of figures

Figure 1.1 Structure of Cys loop ligand-gated ion channels 5

Figure 1.2 High-resolution structural data on Cys loop.receptors 7

Figure 1.3 Unnatural amino acid mutagenesis 9

Figure 1.4 Residues incorporated into integral membrane proteins by nonsense suppression 11

Figure 2.1 Views of the nAChR based on X-ray crystallography of the AChBP. 16

Figure 2.2 Sequence alignment of binding-site residues.in muscle nAChRα, 5-HT$_{3A}$R, and AChBP 17

Figure 2.3 Structures and electrostatic potential surfaces of F$_n$Trp series. 19

Figure 2.4 Structtures and electrostatic potential surfaces of nicotinic and serotonergic agonists. 20

Figure 2.5 Electrophysiological analysis of 5-HT with F$_n$Trp series 22

Figure 2.6 Electrophysiological analysis of 5-HT analogs with F$_n$Trp series. 27

Figure 2.7 Fluorination plot of norACh and TMA 28

Figure 2.8 Electrophysiological analysis of nicotine and N-Me-nicotinium 29

Figure 3.1 Sturcture of side chains used in the study of binding-site tyrosines in 5-HT$_3$R 48

Figure 3.2 Representative current traces and I$_{max}$.values for suppression with the pGEMHE vector 50

Figure 3.3 Dose-response relations for suppression experiments at 141 and 143 52

Figure 3.4 Dose-response relations for suppression experiments at 143 and 234. 57

Figure 3.5 Computational model of 5-HT docked into the 5-HT$_3$R binding-site. 61

Figure 3.6 Comparison of homology models of the 5-HT$_3$R in the closed and open states. 63

Figure 4.1 Model of the 5-HT$_3$R based on the AChBP structure and cryo-EM images 73

Figure 4.2 Sequence alignment of the transmembrane domains M2 and M3 in Cys loop receptors. 76

Figure 4.3 Schematic of *trans* and *cis*.prolyl peptide bonds 78

Figure 4.4 Structures of proline analogs 79

Figure 4.5 Dose-response relations for suppression experiments at position 308 in 5-HT_3R 82

Figure 4.6 Plot of $\Delta\Delta G$ EC_{50} versus $\Delta\Delta G_{cis}$ for mutations at 308 84

Figure 4.7 Representative current traces showing TMB-8 blockable leak currents in dmP 308....86

Figure 4.8 Representative current traces illustrating rate changes observed in 308 mutants....87

Figure 4.9 Schematic of favored proline ring conformations....87

Figure 4.10 Immunofluorescent images of nonfunctional 308 mutants. 90

Figure 4.11 Dose-response relations for suppression experiments at 301 in 5-HT_3R....93

Figure 4.12 Representative current traces illustrating rate changes observed in 301 mutants....93

Figure 4.13 Cartoon of gating mechanism in 5-HT_3R iullustrating the possible role of 308. 97

Figure 5.1 Cation-π binding sites in Cys loop receptors. 109

Figure 5.2 Structures of side chains used in $GABA_C$ studies....110

Figure 5.3 Dose-response relations for suppression experiments at 198 in $GABA_C$. 112

Figure 5.4 Fluorination plots for $GABA_C$ and Cys loop receptors. 114

Figure 5.5 Structures of side chains used to probe Phe 226 in 5-HT_3R....115

Figure 5.6 Predicted location of Phe 226 in 5-HT_3R binding site....117

Figure 5.7 Protein backbone mutations....119

Figure 5.8 Thionation reagents....120

Figure 5.9 Schematic of aminoacyl dCA and amino-thionoacyl dCA....121

List of tables

Table 2.1 Dose-response data for 5-HT_3R with F_nTrp series 24

Table 2.2 Dose-response data for nAChR with F_nTrp series....31

Table 2.3 Efficacy studies of 5-HT_3R and nAChR agonists....33

Table 3.1 Dose-response data for suppression experiments at 141 and 143 in 5-HT_3R.....56

Table 3.2 Dose-response data for suppression experiments at 141 and 143 in 5-HT_3R.....56

Table 3.3 Dose-response data for conventional mutagenesis experiments in 5-HT_3R.....59

Table 4.1 Electrophysiology data for suppression experiments at 308 in 5-HT_3R.....84

Table 4.2 Thermodynamic data for proline analogs. 85

Table 4.3 Electrophysiology data for suppression at 301 in 5-HT_3R.....94

Table 5.1 Dose-response data for suppression experiments at 198 in $GABA_C$. 112

Table 5.2 Dose-response data for suppression experiments at 226 in 5-HT_3R.....115

List of schemes

Schemes 4.1 Synthetic route for NVOV-DL-5,5-dimethylproline 99

Schemes 5.1 Synthetic route for amino-thionoacyl dCA based on solid-phase synthesis strategies 122

Schemes 5.2 Synthetic route for amino-thionoacyl dCA using standard dCA coupling chemistry.....122

Chapter 1. Introduction

1.1 Chemistry and the brain

In terms of speed and complexity, the nervous systems of higher organisms likely represent the pinnacle of intercellular communication. The human brain alone has roughly 10^{12} neurons and each neuron typically makes 10^{3}-10^{4} connections or synapses with other neurons. This means that there are approximately 10^{15}-10^{16} synapses in the human brain, with each synapse representing an intercellular connection for communication between two neurons. Thus, on one level, the brain is essentially a vast network for cell-to-cell communication. Astonishingly, signaling in this massive synaptic network operates on the *millisecond* timescale. It is this speed and complexity that gives rise to human thought and consciousness. An amazing feature of intercellular communication in the nervous system, and ultimately thought and consciousness, is that the events governing their function occur at the molecular level.

The primary mode of synaptic transmission (interneuronal communication) in the nervous system is chemical. In other words, the information conveyed between neurons is encoded in a small molecule, the neurotransmitter. This is recognized and bound by specific receptor molecules that translate the chemical information into cellular processes. The presynaptic neuron initiates synaptic transmission by releasing a neurotransmitter into the synaptic cleft. The neurotransmitter diffuses across the cleft where it binds to a neuroreceptor embedded in the membrane of the postsynaptic neuron. Binding of the neurotransmitter activates the receptor, conveying the synaptic signal across the cell membrane and resulting in the modulation of the postsynaptic neuron.

There are a wide variety of neurotransmitters and many different neuroreceptors. The majority of neuroreceptors can be divided between two main classes: the G-protein coupled receptors which mediate slow synaptic transmission and act through second messenger pathways, and the ligand-gated ion channels (LGIC) which mediate fast synaptic transmission. In LGICs, binding of the neurotransmitter induces a conformational change in the protein, opening an ion permeant channel that spans the cell membrane. The ion channel is fully contained within the LGIC, and once open, ion flow through the channel alters the postsynaptic neuron's membrane potential. This then either encourages or discourages the firing of an action potential in the postsynaptic neuron, depending on whether the LGIC is excitatory (cation selective) or inhibitory (anion selective).

The primary goal of the work presented in this thesis is the chemical-scale elucidation of the structure and function of LGICs. In particular, the studies focus on elucidation of a serotonin-gated ion channel, the 5-hydroxytryptamine-3 receptor ($5\text{-}HT_3R$)[1], a member of the Cys loop family of LGICs. This family of receptors mediates fast synaptic transmission throughout the peripheral and central nervous systems. They are also the targets for therapeutic treatments of Alzheimer's disease, Parkinson's, disease, schizophrenia, stroke, learning and attention deficit disorder, and drug addiction. The motivations for these studies are twofold. The Cys loop receptors are biologically and therapeutically significant, and they are of fundamental interest from a chemical perspective. Their study addresses important concerns in drug-receptor interactions and molecular recognition, and the structural rearrangement associated with activation of the ion channel poses an intriguing chemical question: How does the

noncovalent binding of a small molecule induce a large conformational change in a multisubunit protein?

1.2 The Cys loop family of ligand-gated ion channels

In addition to the 5-HT_3R, the Cys loop family of LGICs also includes the nicotinic acetylcholine (nAChR), gamma-amino butyric acid A ($GABA_A$), $GABA_C$, and glycine (GlyR) receptors.[2-8] These receptors can be separated into two subclasses based on their ion permeation properties: the cation-selective receptors including the nAChR and 5-HT_3R, and the anion-selective receptors including the $GABA_A$, $GABA_C$, and GlyR. The best-studied member of this family is the nAChR. These receptors are quite homologous with 25-30% conservation in the amino acid sequence identity among the various members. Thus, much of what is known about the structure and function of these receptors is inferred from studies of the nAChR.

The Cys loop receptors are multisubunit integral membrane proteins. Their quaternary structure is pentameric with five homologous subunits arranged in a pentagonal array around a central pore (Figure 1.1). Each subunit has a large extracellular N-terminal domain and four transmembrane domains, M1-M4. The M2 domains of each subunit line the interior of the channel lumen. The extracellular domain contains the ligand-binding site, as well as the Cys loop. The latter is a loop formed by two disulfide-bonded cysteines and is a common structural motif in all members of the family. Each receptor in the family has a variety of subunit isoforms. These combine in different compositions to form distinct receptor subtypes. For most of these receptors the exact subunit composition is unknown. The muscle receptor of the nAChR, however, has a well-understood composition of $(\alpha 1)_2\beta 1\gamma\delta$ (Figure 1.1). In this receptor, the ligand-

binding sites are located primarily in the α-subunits, and it is known both must be occupied to optimally activate the receptor (i.e., open the ion channel). For the 5-HT_3R, three subunits have been identified; *A*, *B*, and *C*.[1, 8, 9] The subunit stoichiometry for native receptors has yet to be determined, however, *A* subunits can form functional homomeric receptors, indicating that as with the muscle nAChR, the *A* subunit contains the majority of the ligand-binding determinants.

Being integral membrane proteins, the Cys loop receptors have been resistant to characterization by high-resolution structural techniques such as NMR and x-ray crystallography. A significant source of structural information concerning these receptors has come from cryo-electron microscopy (cryo-EM) studies on the *Torpedo* electric ray. The electric organ in these rays is highly enriched in nAChR-containing membranes. The high density of nAChR in this tissue is amenable to structural analysis by cryo-EM.[10-13] Recently, cryo-EM studies by Nigel Unwin have produced an image of the transmembrane domains at 4-Å resolution (Figure 1.2a).[14] This represents the highest resolution structure of this region of the protein, and is supported by much of the earlier structure-function studies in the Cys loop receptors. The structure revealed that each transmembrane domain forms a membrane-spanning α-helix. In addition, it provided strong evidence that the gate of the receptor is formed by the hydrophobic side chains of Leu 9' and Val 13' in M2 (numbering convention for residues in M2 starts with 1' at the C-terminal or cytoplasmic end of M2), confirming results from previous studies.[15, 16] A novel feature of this structure was the clear indication that the M2 domain extends two helical turns above the extracellular membrane. This contradicts the predictions based on

the hydropathy profile of the nAChR subunits, but results from earlier substituted cysteine accessibility studies support this conclusion.[17]

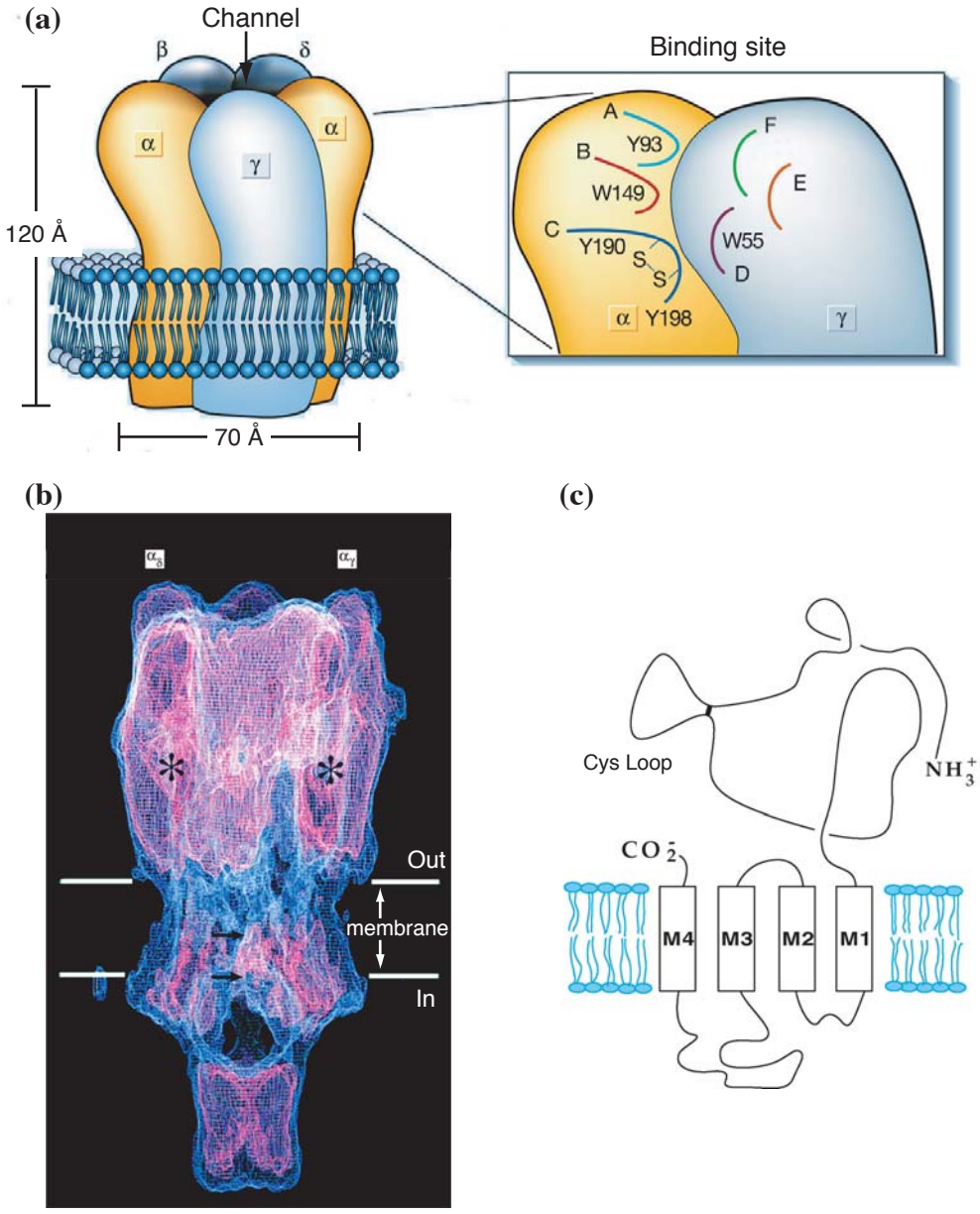

Unwin, *Phil T Soc B,* (2000) **335**.

Figure 1.1. Structure of Cys loop LGICs. (a) Cartoon of the nAChR showing general structural features of the receptor. Inset shows the location of the binding site at the subunit interface and the loops that contribute important aromatic residues to the primary binding site. (b) 4.6 Å cryo-EM of the nAChR. (c) Single subunit showing subunit topology.

While as yet, no x-ray crystal structure exists for these receptors, there is a crystal structure of an acetylcholine binding protein (AChBP) (Figure 1.2b).[18-20] This is a soluble protein from the snail, *Lymnaea helicalis*, and is highly homologous to the extracellular domain of the nAChR. The crystal structure of this protein has been a watershed event in the study of Cys loop LGICs, providing the first high-resolution structural data on the ligand-binding site. This structure confirmed much of the previous biochemical and biophysical studies on the nAChR, including the location of the ligand-binding site at subunit interfaces. In the muscle nAChR, the two binding sites are located at the α/γ and α/δ interfaces (Figure 1.1a and Figure 1.2b). Furthermore, the AChBP structure revealed that the binding site is composed of five noncontiguous loops (loops A-E), each of which contributes one or more aromatic residues to form the primary binding site (see chapters 2 and 3 for more details).

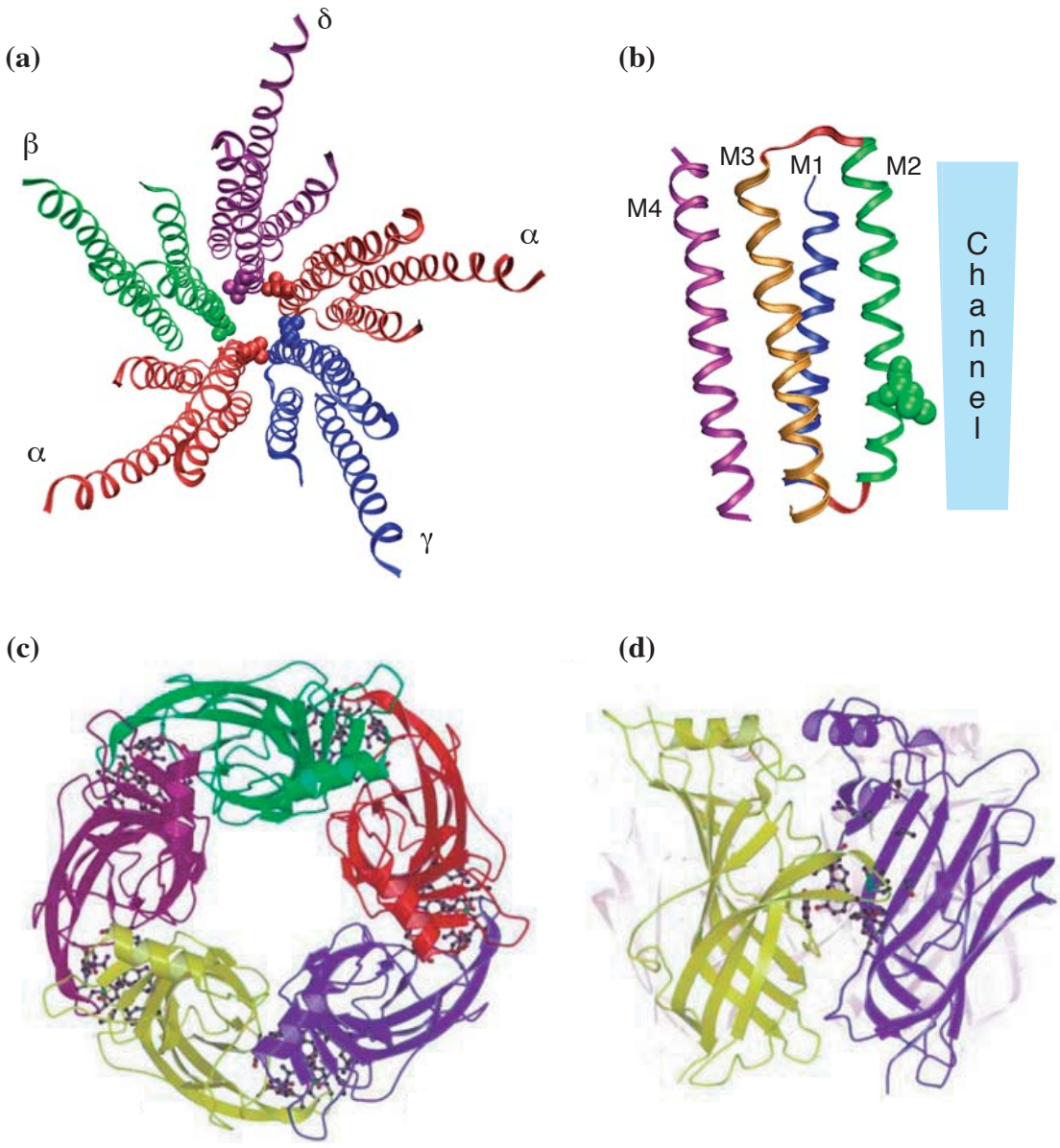

Figure 1.2. Cryo-EM structure of nAChR transmembrane domains and AChBP structure. (a) Top view (looking down from the extracellular side) of the transmembrane domains based on Unwin's 4.0Å images. Leu 9' for each subunit is shown in CPK representation. (b) Transmembrane domains of a single subunit. (c) Top view of the AChBP structure. (d) Side view of AChBP with two subunits highlighted and the binding site residues shown in ball-and-stick representation.

1.3 Unnatural amino acid mutagenesis

Although the recent structural breakthroughs detailed above have been invaluable to the study of Cys loop receptors, there are still many outstanding questions concerning

their function. By their very nature, these receptors are dynamic proteins undergoing large conformational changes and interconverting among multiple states (i.e., non-conducting closed state to conducting open state). X-ray crystal structures provide a starting point for evaluating these processes, but are only static snapshots. Structure-function studies are still necessary to determine what features revealed by the crystal structure are functionally significant. The central approach of the research presented here is the use of *in vivo* nonsense suppression for structure-function studies. This method allows for the site-specific incorporation of a synthetic amino acid into a protein expressed in a living cell. In many ways, this method is ideal for the study of ion channels. The ability to incorporate unnatural amino acids permits systematic structure-function studies, furnishing a chemical-scale precision unique among biochemical methods. In addition, the methodology allows for study in a cellular system, obviating the need for functional isolation of these multisubunit integral membrane proteins. One of the drawbacks of the nonsense suppression method (and in particular *in vivo* nonsense suppression) is the limited quantity of protein produced. This limitation is minimized, however, in the study of ion channels due to the extraordinary sensitivity of modern electrophysiology. Thus, the functional consequences of the introduced mutations can be readily assayed.

In 1989, Peter Schultz reported the first general method for the biosynthetic incorporation of unnatural amino acids using nonsense suppression.[21-24] The method works by commandeering a non-coding codon or 'nonsense codon' (Figure 1.3a). The commandeered codon– usually a stop codon– is placed in the gene at the site of interest. Typically, this would result in the premature termination of the protein's biosynthesis.

However, if the translation system is supplied with a suppressor tRNA (a tRNA whose anticodon recognizes the nonsense codon) that is charged with a synthetic amino acid, then translation proceeds with the unnatural amino acid incorporated into the protein at the site of interest. The *in vivo* nonsense suppression method extends this methodology for *in vivo* usage with the *Xenopus* oocyte expression system.[25-27]

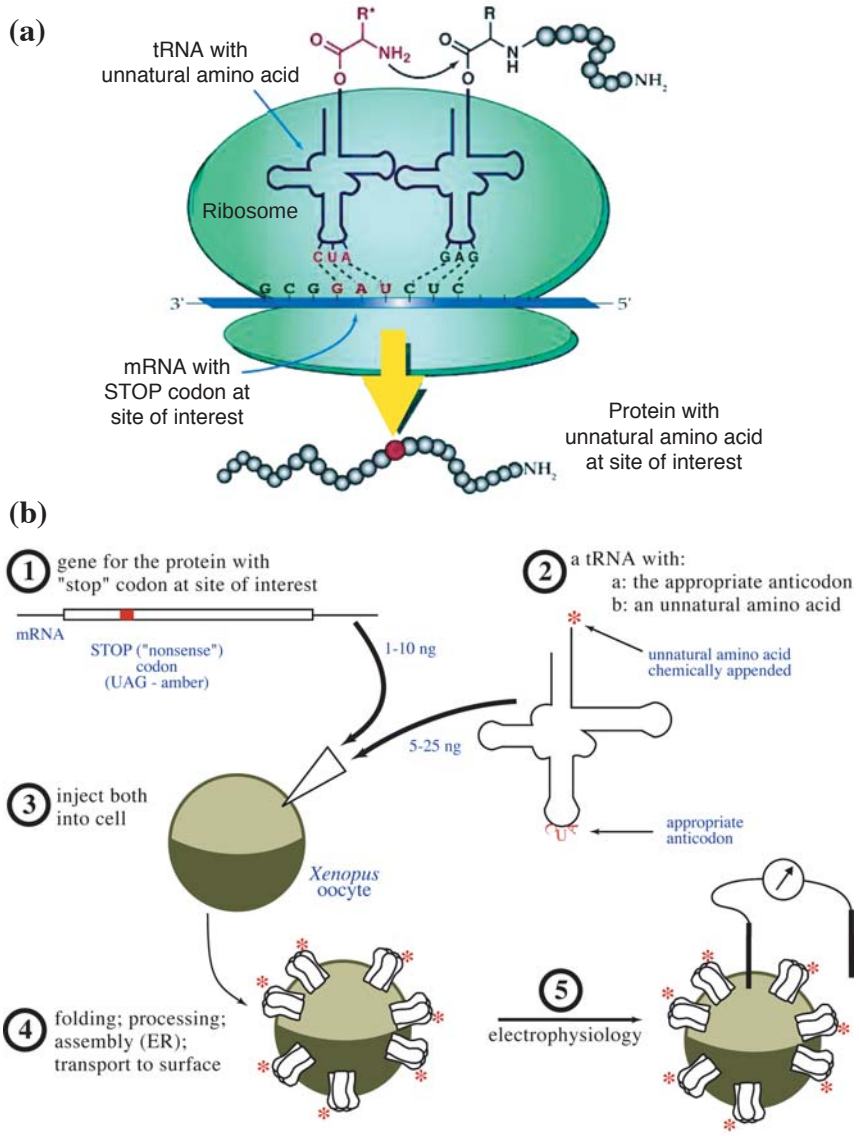

Figure 1.3. Nonsense suppression method. (a) Basic details of how nonsense suppression works. (b) *In vivo* nonsense suppression method.

The basic method for *in vivo* nonsense suppression first entails the placement of the amber stop codon (TAG) at the amino acid position of interest (Figure 1.3b). This is done using conventional site-directed mutagenesis, followed by *in vitro* transcription of UAG containing mRNA. Separately, a suppressor tRNA containing the appropriate anticodon (CUA), is prepared and chemically acylated with an unnatural amino acid. The tRNA and mRNA are then co-injected into a *Xenopus* oocyte. Protein synthesis and surface expression are carried out by the oocyte, allowing for electrophysiological study 24 to 72 hours later.

To date, more than eighty mutations (including both α-amino and α-hyroxy acids) have been incorporated into 15 different integral membrane proteins (Figure 1.4). In addition, the method has been extended for use with mammalian expression systems.[28] In our experience, the method is amenable to two sorts of studies: 1) detailed structure-function studies involving rational perturbation of the residue of interest[29-31] and 2) the introduction of unnatural side chains with novel chemical and biophysical properties such as fluorescent probes, 'caged' residues, and tethered agonists.[32-34] The limitations as to the variety of unnatural amino acids that can be incorporated have never been rigorously studied. There is, however, anecdotal evidence that hydrophobic residues suppress better than polar ones, and both D-amino acids and β-amino acids are poorly incorporated, if at all. Having noted this, the method can accommodate a wide variety of side chains, including several backbone mutations.[35-38]

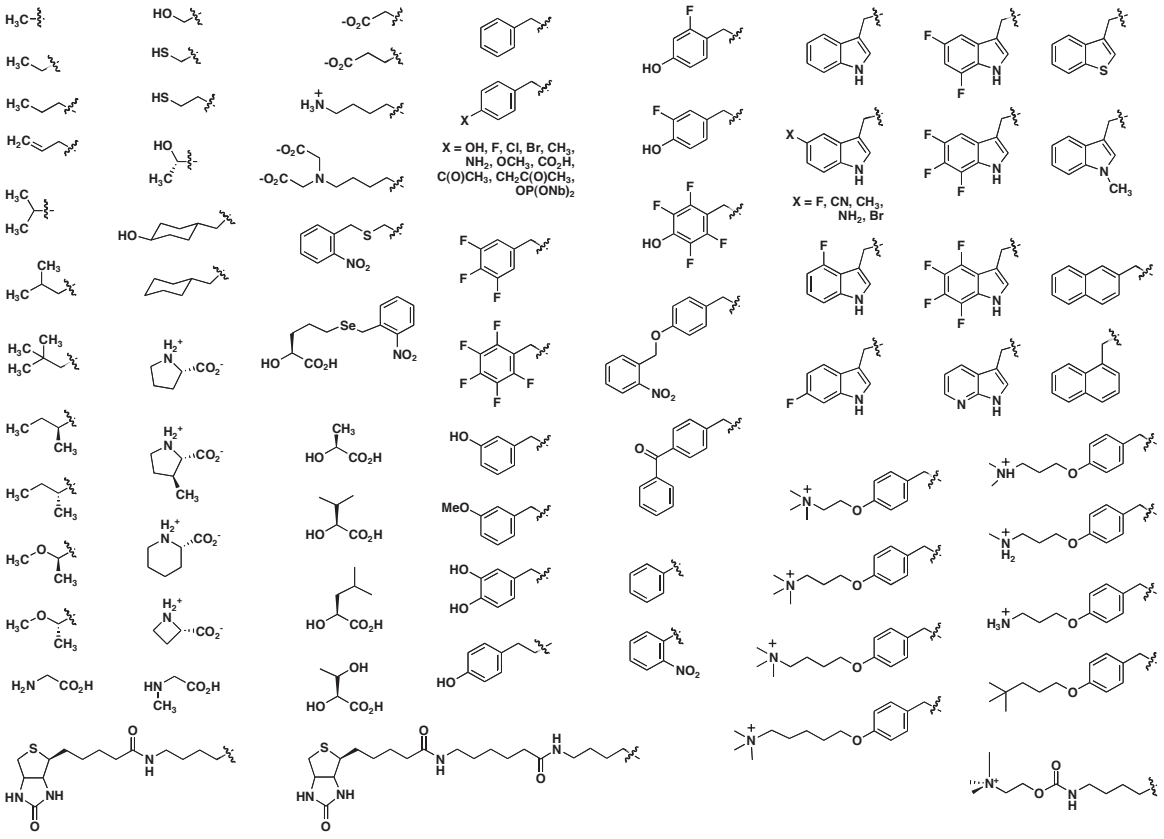

Figure 1.4. Representative α-amino and α-hydroxy acids incorporated into integral membrane proteins using *in vivo* nonsense suppression.

1.4 Structure-function studies

The nonsense suppression method is an excellent tool for structure-function studies. Much like conventional mutagenesis, it allows for site specificity in the mutations to be introduced. However, unlike conventional mutagenesis, it is not limited to the standard 20 amino acids. With the use of synthetic amino acids, one has rational control over the mutations to be introduced. In addition the chemical precision afforded by the technique is unique among biochemical methods. Consequently, it can provide chemical-scale information on the functional role and structural context of a given amino acid.

The majority of the work presented in this thesis centers on structure-function studies of the 5-HT_3R. Chapter 2 describes studies on the ligand-binding site in the

5-HT_3R and nAChR in which a series of progressively fluorinated tryptophans is used to identify the cation-π binding site of the 5-HT_3R and to compare and contrast ligand-recognition properties between the two receptors. This work is largely based on a *Biochemistry* paper written in collaboration with Gabriel Brandt, who performed all of the experiments on the nAChR.[39] The studies presented in Chapter 3 use a series of tyrosine analogs to probe the role of tyrosine residues near the ligand-binding site in the 5-HT_3R. Results from these studies are used to assess several models in which serotonin is computationally docked into the binding site. This chapter is based on a *Journal of Neuroscience* paper written in collaboration with the Sarah Lummis group at the University of Cambridge.[40] They performed all of the computational work, and Kerry Price in particular, contributed significant effort to this project. The work in Chapter 4 investigates the role of two conserved prolines in the M2-M3 loop of the 5-HT_3R. The findings from this work support a recently proposed model for the functional role of this loop in the gating pathway of Cys loop receptors. This work represents as well a collaboration with the Sarah Lummis group. Finally, Chapter 5 includes three miscellaneous studies: investigations of Phe 226 (Tyr 190 in the nAChR) in the 'aromatic box' of the 5-HT_3R; work identifying Tyr 198 (Trp 149 in the nAChR) as a cation-π binding site in the $GABA_C$ receptor; and efforts towards the incorporation of a backbone thioamide via nonsense suppression. The first two studies in Chapter 5 were done in collaboration with Sarah Lummis.

1.5 References

1. Maricq, A. V.; Peterson, A. S.; Brake, A. J.; Myers, R. M.; Julius, D., Primary structure and functional expression of the 5HT3 receptor, a serotonin-gated ion channel. *Science* **1991,** 254, (5030), 432-7.
2. Corringer, P. J.; Le Novere, N.; Changeux, J. P., Nicotinic receptors at the amino acid level. *Annu Rev Pharmacol Toxicol* **2000,** 40, 431-58.

3. Hucho, F.; Weise, C., Ligand-gated ion channels. *Angew. Chem. Int. Ed.* **2001,** 40, 3100-3116.
4. Jackson, M. B.; Yakel, J. L., The 5-HT3 receptor channel. *Annu Rev Physiol* **1995,** 57, 447-68.
5. Karlin, A., Emerging structure of the nicotinic acetylcholine receptors. *Nature Reviews Neuroscience* **2002,** 3, (2), 102-114.
6. Lester, H. A.; Dibas, M. I.; Dahan, D. S.; Leite, J. F.; Dougherty, D. A., Cys-loop receptors: new twists and turns. *Trends in Neurosciences* **2004,** 27, (6), 329-336.
7. Lummis, S. C. R., The transmembrane domain of the 5-HT3 receptor: its role in selectivity and gating. *Biochemical Society Transactions* **2004,** 32, 535-539.
8. Reeves, D. C.; Lummis, S. C. R., The molecular basis of the structure and function of the 5-HT3 receptor: a model ligand-gated ion channel (Review). *Molecular Membrane Biology* **2002,** 19, (1), 11-26.
9. Davies, P. A.; Pistis, M.; Hanna, M. C.; Peters, J. A.; Lambert, J. J.; Hales, T. G.; Kirkness, E. F., The 5-HT3B subunit is a major determinant of serotonin-receptor function. *Nature* **1999,** 397, (6717), 359-63.
10. Unwin, N.; Miyazawa, A.; Li, J.; Fujiyoshi, Y., Activation of the nicotinic acetylcholine receptor involves a switch in conformation of the a subunits. *Journal of Molecular Biology* **2002,** 319, (5), 1165-1176.
11. Unwin, N., The Croonian Lecture 2000. Nicotinic acetylcholine receptor and the structural basis of fast synaptic transmission. *Philosophical Transactions of the Royal Society of London Series B-Biological Sciences* **2000,** 355, (1404), 1813-1829.
12. Unwin, N., Nicotinic Acetylcholine-Receptor at 9-Angstrom Resolution. *Journal of Molecular Biology* **1993,** 229, (4), 1101-1124.
13. Miyazawa, A.; Fujiyoshi, Y.; Stowell, M.; Unwin, N., Nicotinic acetylcholine receptor at 4.6 angstrom resolution: Transverse tunnels in the channel wall. *Journal of Molecular Biology* **1999,** 288, (4), 765-786.
14. Miyazawa, A.; Fujiyoshi, Y.; Unwin, N., Structure and gating mechanism of the acetylcholine receptor pore. *Nature* **2003,** 423, (6943), 949-955.
15. Akabas, M. H.; Kaufmann, C.; Archdeacon, P.; Karlin, A., Identification of Acetylcholine-Receptor Channel-Lining Residues in the Entire M2 Segment of the Alpha-Subunit. *Neuron* **1994,** 13, (4), 919-927.
16. Labarca, C.; Nowak, M. W.; Zhang, H.; Tang, L.; Deshpande, P.; Lester, H. A., Channel gating governed symmetrically by conserved leucine residues in the M2 domain of nicotinic receptors. *Nature* **1995,** 376, (6540), 514-6.
17. Bera, A. K.; Chatav, M.; Akabas, M. H., GABA(A) receptor M2-M3 loop secondary structure and changes in accessibility during channel gating. *Journal of Biological Chemistry* **2002,** 277, (45), 43002-43010.
18. Brejc, K.; van Dijk, W. J.; Klaassen, R. V.; Schuurmans, M.; van der Oost, J.; Smit, A. B.; Sixma, T. K., Crystal structure of an ACh-binding protein reveals the ligand-binding domain of nicotinic receptors. *Nature* **2001,** 411, (6835), 269-276.
19. Celie, P. H. N.; van Rossum-Fikkert, S. E.; van Dijk, W. J.; Brejc, K.; Smit, A. B.; Sixma, T. K., Nicotine and carbamylcholine binding to nicotinic acetylcholine receptors as studied in AChBP crystal structures. *Neuron* **2004,** 41, (6), 907-914.
20. Dougherty, D. A.; Lester, H. A., Neurobiology - Snails, synapses and smokers. *Nature* **2001,** 411, (6835), 252-254.
21. Cornish, V. W.; Schultz, P. G., A New Tool for Studying Protein-Structure and Function. *Current Opinion in Structural Biology* **1994,** 4, (4), 601-607.
22. Dougherty, D. A., Unnatural amino acids as probes of protein structure and function. *Current Opinion in Chemical Biology* **2000,** 4, (6), 645-652.
23. Gilmore, M. A.; Steward, L. E.; Chamberlin, A. R., Incorporation of noncoded amino acids by in vitro protein biosynthesis. *Topics in Current Chemistry* **1999,** 202, 77-99.
24. Noren, C. J.; Anthonycahill, S. J.; Griffith, M. C.; Schultz, P. G., A General-Method for Site-Specific Incorporation of Unnatural Amino-Acids into Proteins. *Science* **1989,** 244, (4901), 182-188.
25. Beene, D. L.; Dougherty, D. A.; Lester, H. A., Unnatural amino acid mutagenesis in mapping ion channel function. *Current Opinion in Neurobiology* **2003,** 13, (3), 264-270.
26. Nowak, M. W.; Kearney, P. C.; Sampson, J. R.; Saks, M. E.; Labarca, C. G.; Silverman, S. K.; Zhong, W.; Thorson, J.; Abelson, J. N.; Davidson, N.; Schultz, P. G.; Dougherty, D. A.; Lester, H. A., Nicotinic Receptor-Binding Site Probed with Unnatural Amino-Acid-Incorporation in Intact-Cells. *Science* **1995,** 268, (5209), 439-442.

27. Nowak, M. W.; Gallivan, J. P.; Silverman, S. K.; Labarca, C. G.; Dougherty, D. A.; Lester, H. A., In vivo incorporation of unnatural amino acids into ion channels in Xenopus oocyte expression system. *Methods in Enzymology* **1998,** 293, 504-529.
28. Monahan, S. L.; Lester, H. A.; Dougherty, D. A., Site-specific incorporation of unnatural amino acids into receptors expressed in mammalian cells. *Chemistry & Biology* **2003,** 10, (6), 573-580.
29. Kearney, P. C.; Nowak, M. W.; Zhong, W.; Silverman, S. K.; Lester, H. A.; Dougherty, D. A., Agonist binding site of the nicotinic acetylcholine receptor: Tests with novel side chains and with several agonists. *Molecular Pharmacology* **1996,** 50, (5), 1401-1412.
30. Dang, H.; England, P. M.; Farivar, S. S.; Dougherty, D. A.; Lester, H. A., Probing the role of a conserved M1 proline residue in 5- hydroxytryptamine(3) receptor gating. *Molecular Pharmacology* **2000,** 57, (6), 1114-1122.
31. Zhong, W. G.; Gallivan, J. P.; Zhang, Y. O.; Li, L. T.; Lester, H. A.; Dougherty, D. A., From ab initio quantum mechanics to molecular neurobiology: A cation-pi binding site in the nicotinic receptor. *Proceedings of the National Academy of Sciences of the United States of America* **1998,** 95, (21), 12088-12093.
32. England, P. M.; Lester, H. A.; Davidson, N.; Dougherty, D. A., Site-specific, photochemical proteolysis applied to ion channels in vivo. *Proceedings of the National Academy of Sciences of the United States of America* **1997,** 94, (20), 11025-11030.
33. Li, L. T.; Zhong, W. G.; Zacharias, N.; Gibbs, C.; Lester, H. A.; Dougherty, D. A., The tethered agonist approach to mapping ion channel proteins toward a structural model for the agonist binding site of the nicotinic acetylcholine receptor. *Chemistry & Biology* **2001,** 8, (1), 47-58.
34. Miller, J. C.; Silverman, S. K.; England, P. M.; Dougherty, D. A.; Lester, H. A., Flash decaging of tyrosine sidechains in an ion channel. *Neuron* **1998,** 20, (4), 619-624.
35. England, P. M.; Zhang, Y. N.; Dougherty, D. A.; Lester, H. A., Backbone mutations in transmembrane domains of a ligand-gated ion channel: Implications for the mechanism of gating. *Cell* **1999,** 96, (1), 89-98.
36. Koh, J. T.; Cornish, V. W.; Schultz, P. G., An experimental approach to evaluating the role of backbone interactions in proteins using unnatural amino acid mutagenesis. *Biochemistry* **1997,** 36, (38), 11314-11322.
37. Killian, J. A.; Van Cleve, M. D.; Shayo, Y. F.; Hecht, S. M., Ribosome-mediated incorporation of hydrazinophenylalanine into modified peptide and protein analogues. *Journal of the American Chemical Society* **1998,** 120, (13), 3032-3042.
38. Eisenhauer, B. M.; Hecht, S. M., Site-specific incorporation of (aminooxy)acetic acid into proteins. *Biochemistry* **2002,** 41, (38), 11472-11478.
39. Beene, D. L.; Brandt, G. S.; Zhong, W. G.; Zacharias, N. M.; Lester, H. A.; Dougherty, D. A., Cation-pi interactions in ligand recognition by serotonergic (5-HT3A) and nicotinic acetylcholine receptors: The anomalous binding properties of nicotine. *Biochemistry* **2002,** 41, (32), 10262-10269.
40. Beene, D. L.; Price, K. L.; Lester, H. A.; Dougherty, D. A.; Lummis, S. C. R., Tyrosine residues that control binding and Gating in the 5-hydroxytryptamine(3) receptor revealed by unnatural amino acid mutagenesis. *Journal of Neuroscience* **2004,** 24, (41), 9097-9104.

Chapter 2. Cation-π interactions in ligand recognition by serotonergic ($5\text{-}HT_{3A}$) and nicotinic acetylcholine receptors

2.1 Introduction

Synaptic transmission is largely mediated by neurotransmitters and the receptors that bind them. At the core of this process is the selective recognition and binding of a small molecule by its protein host. Despite the pharmacological and clinical significance of compounds that modulate synaptic signaling, the chemical basis of neurotransmitter binding has been difficult to determine. High-resolution structural data on neuroreceptors with bound agonists are only just becoming available[1-5], and functional data are still needed to distinguish which agonist-receptor interactions are mechanistically significant.

Nearly all neurotransmitters contain a cationic center, and a common strategy for biological recognition of cations is the cation-π interaction, the stabilizing interaction between a cation and the negative electrostatic potential on the face of an aromatic ring.[6, 7] Earlier work in the Dougherty group introduced a technique for the *in situ* identification of cation-π binding sites.[8] This technique relies on nonsense suppression methodology for site-specific introduction of an unnatural amino acid into a functioning receptor expressed in a living cell.[9-12] In the first application of the technique, a series of fluorinated Trp derivatives was introduced at various positions in the binding region of the nicotinic acetylcholine receptor (nAChR). At Trp 149 of the α-subunit, the EC_{50} of ACh for receptor activation was strongly correlated to the degree of fluorination, providing a strong indication that ACh binds to the nAChR through a cation-π interaction with Trp α149. This assessment was subsequently confirmed in 2001 by the

crystallization of a soluble acetylcholine-binding protein (AChBP) from the snail, *Lymnaea helicalis*.[2] AChBP shares significant structural and sequence homology with the nAChR ligand-binding domain. (Figures 2.1 and 2.2) The crystal structure of AChBP revealed that the binding site is a box of aromatic residues, including the critical Trp α149. (Figure 2.1) Electron density corresponding to a molecule of HEPES was seen in this box with its ammonium center bound to Trp α149, as expected for a cation-π interaction.

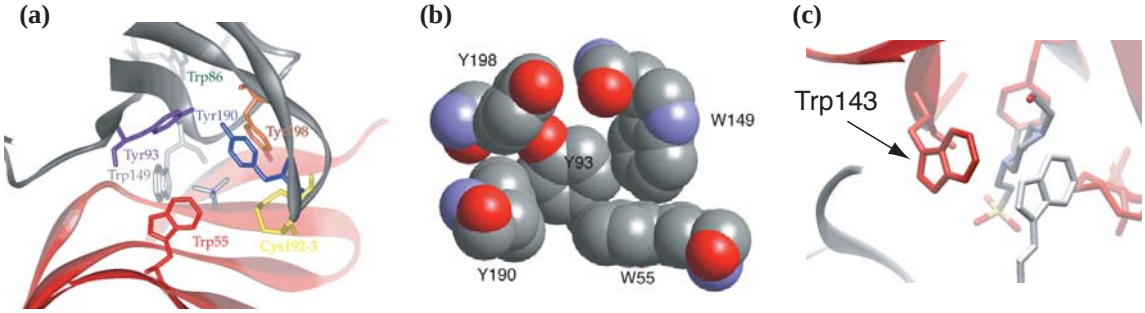

Figure 2.1. Several views of the nicotinic acetylcholine receptor (nAChR). (a) Details of the binding site illustrating the prevalence of aromatic residues. The coordinates come from X-ray diffraction of an ACh binding protein with high homology to nAChR. (b) The 'aromatic box' comprising the nAChR active site, based on AChBP coordinates. (c) Diffraction data from AChBP showing a HEPES molecule from the crystallization buffer bound to the face of Trp143, the homolog of muscle nAChR Trp149 and 5-HT_{3A}R Trp183.

In the work presented in this chapter, the F_n-Trp technique is utilized to examine the ligand-binding domain of the serotonin-gated ion channel, 5-HT_{3A}R. In addition, the cation-π interaction at the nAChR is further evaluated, considering nicotine and several other agonists. This work was done in collaboration with Gabriel Brandt who performed the majority of nAChR experiments. These studies generate two major findings. The first is that 5-HT_{3A}R Trp 183, which aligns with Trp α149 in the nAChR, binds the primary ammonium of serotonin (5-hydroxytryptamine, or 5-HT) via a cation–π

interaction. The second is that in the muscle nAChR, nicotine does not experience a strong cation-π interaction with Trp α149. The first result is consistent with the idea that the binding site of the serotonin channel is highly homologous to that of nAChR. The second result, however, is surprising in light of accepted pharmacophore models for the nicotinic receptor. Because of questions raised by these results, a series of both serotonin and nicotine derivatives were analyzed to better understand the role of the cation-π interaction in ligand recognition at these two receptors.

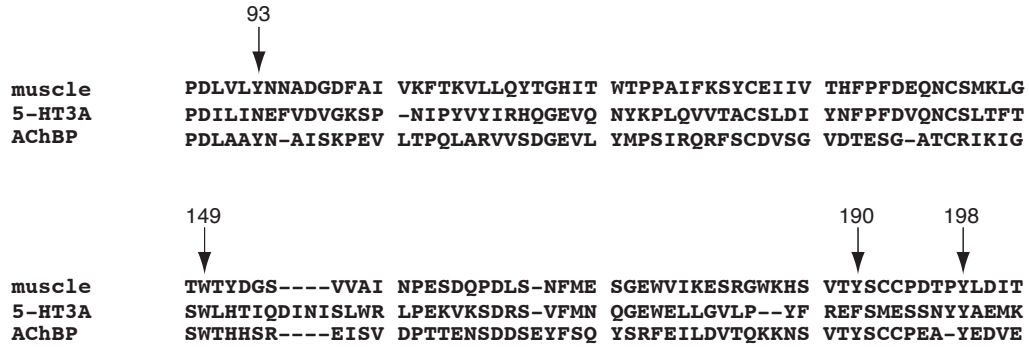

Figure 2.2. Sequence alignment of muscle nAChRα, 5-HT_{3A}R, and AChBP. The residues that comprise the aromatic box are indicated with arrows, with the exception of the Trp residue contributed by the interfacial subunit, which is conserved among all members of the nAChR receptor family and which is γ55 or δ57 in muscle nAChR and α90 in 5-HT_{3A}R.

2.2 Results

Unnatural amino acids were incorporated into the 5-HT_{3A}R and nAChR using *in vivo* nonsense suppression methods, and mutant receptors were evaluated electrophysiologically.[9-12] The structures and electrostatic potential surfaces of the side chains of the unnatural amino acids utilized are presented in Figure 2.3. Electrostatic potential surfaces provide a useful guide for evaluating the cation-π binding ability of an aromatic ring.[13, 14] These surfaces show how electron-withdrawing groups such as cyano

and fluoro substantially weaken the cation-π interaction. The agonists used in these studies are presented in Figure 2.4, along with their electrostatic potential surfaces. Note that the energy scales of the electrostatic potential plots are very different for Figures 2.3 and 2.4. For the side chains, the scale is ±25 kcal/mol, such that red is negative and blue is positive electrostatic potential. However, the structures of Figure 2.4 are all cations, and so the energy range is -5 to 160 kcal/mol. For a cation, the surface is positive everywhere; red simply represents relatively less positive, blue relatively more positive.

When studying weak agonists and/or receptors with diminished binding capability, we found it necessary to introduce a Leu to Ser mutation at a site known as 9' in the second transmembrane region of the receptor.[15, 16] This site is almost 50 Å from the binding site, and previous work has shown that each L9'S mutation lowers EC_{50} by a factor of roughly 10, with multiple L9'S mutations having an additive effect. Results from earlier studies and data reported below clearly demonstrate that trends in EC_{50} values are not perturbed by L9'S mutations[16]. For the present study, we used receptors that contain one or two L9'S mutations, as noted in the Tables and Figure captions.

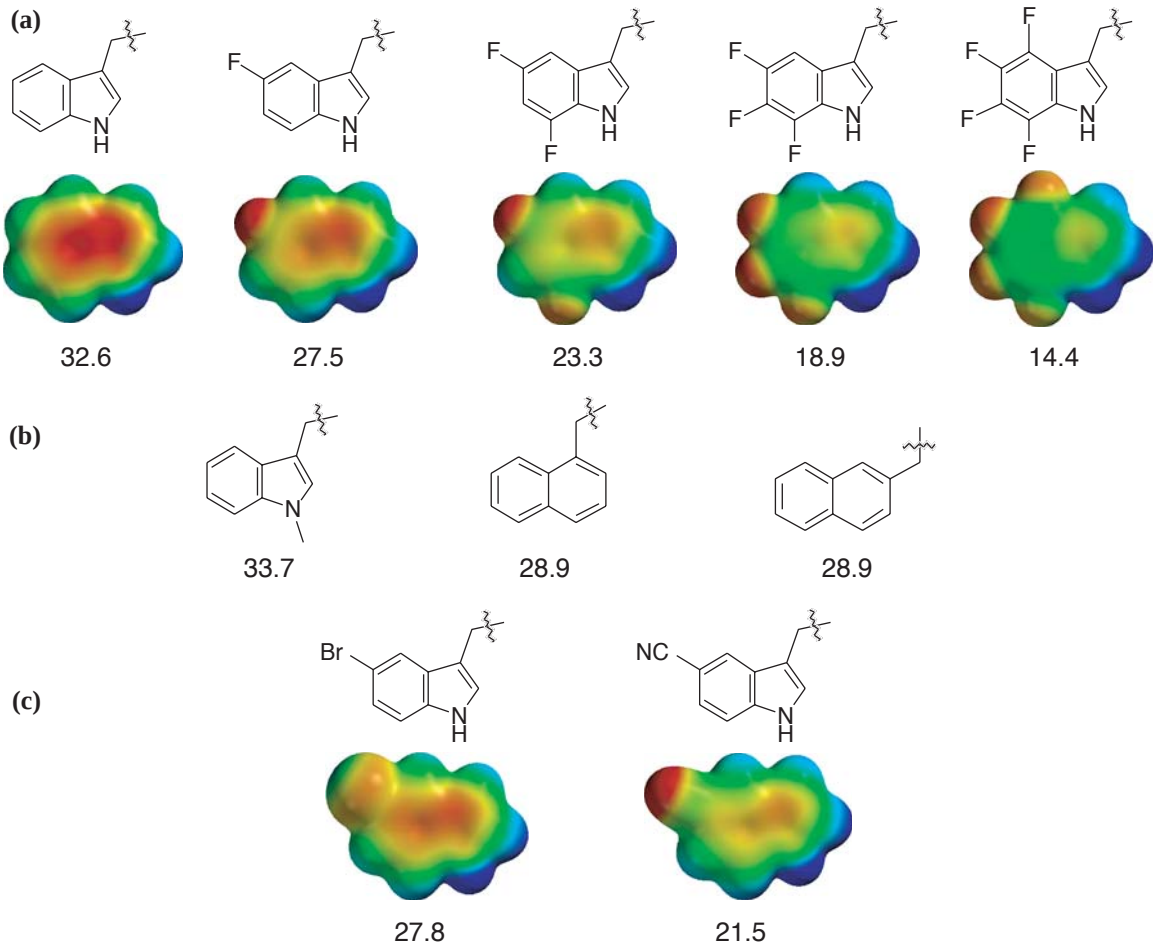

Figure 2.3. Side chains introduced in place of binding site Trp residues. (a) The series of fluorinated Trp analogs, with the gas-phase cation-π binding energy of fluoroindoles (HF 6-31G**) in kcal/mol. (b) Trp analogs without the indole nitrogen hydrogen bond donation ability, along with calculated cation-π binding energy. (c) Trp analogs for screening Trp sites for electrostatic interactions, with calculated cation-π binding ability. AM1 electrostatic surfaces are colored according to an energy scale corresponding to ±25 kcal/mol, where blue is positive and red negative.

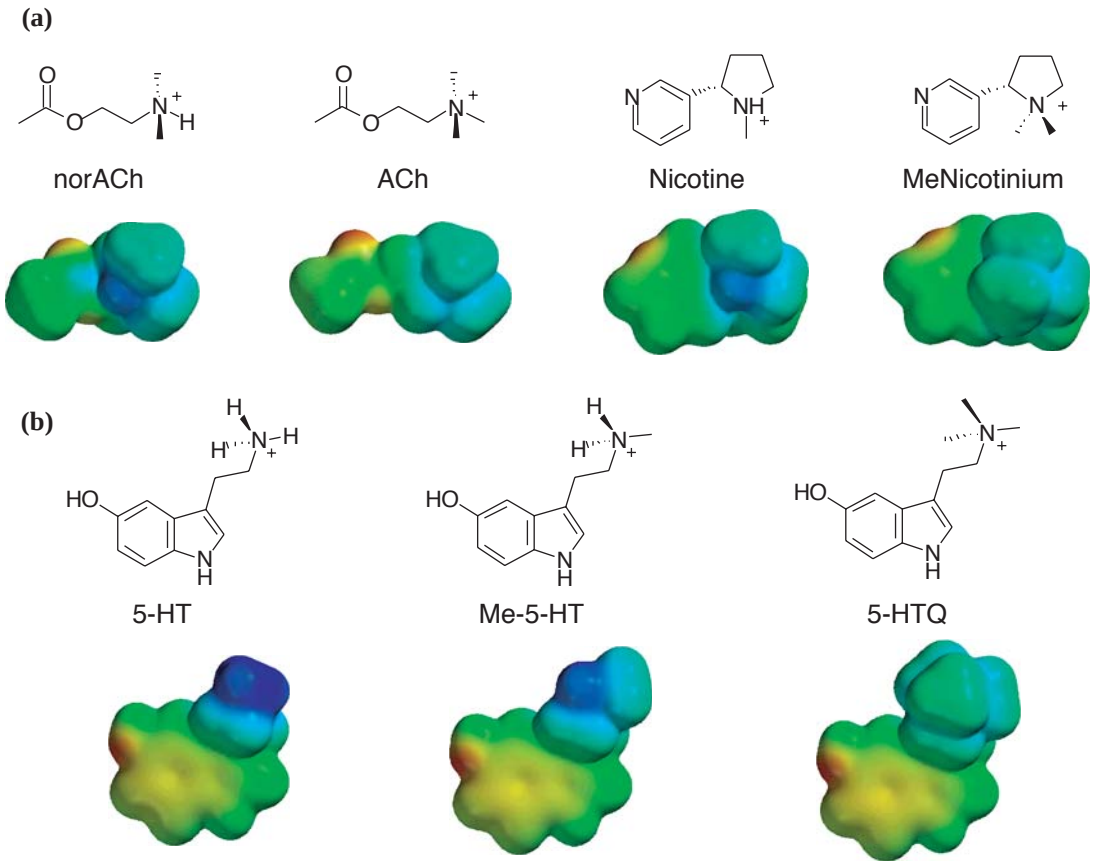

Figure 2.4. Agonists utilized in this study (a) nAChR agonists, with AM1 electrostatic surfaces calculated using Spartan showing the overall geometrical similarity of the structurally distinct nicotinoid and cholinergic agonists. (b) 5-HT_{3A}R agonists, with AM1 electrostatic surfaces showing the varying charge density around the nitrogen center. Electrostatic surfaces correspond to an energy range of –5 to +160 kcal/mol, where blue is positive and red negative.

Finally, it should be noted that the quantity reported here, EC_{50}, is not a binding constant, but a composite of equilibria for both binding and gating.[17] An advantage of EC_{50} is that it represents a *functional* assay; all mutant receptors reported here are fully functioning ligand-gated ion channels. This alleviates concerns that the mutations introduced cause a massive structural reorganization of the receptor. Because the subtle mutations we make are in the region of the agonist binding site, and the presumptive gate of the ion channel is almost 50 Å away, we assume variations in EC_{50} for the series of

unnatural residues reflect differential agonist-binding ability, and that the gating equilibrium is not substantially perturbed.

2.1.1 5-HT$_{3A}$R Studies

Two subunits, A and B, have been identified for the 5-HT$_3$R.[18, 19] Only the 5-HT$_{3A}$R when expressed alone in heterologous expression systems forms functional homomeric receptors, and the 5-HT$_3$R studies presented here were carried out using homomeric 5-HT$_{3A}$ receptors. Previous work has shown that the homomeric and heteromeric (A and B) receptors share a common pharmacology while differing somewhat in biophysical properties, such as conduction, kinetics, and desensitization characteristics.[20]

2.1.2 Position 183 in the 5-HT$_{3A}$R

Because of the well-established effect of fluorine substitution in modulating the cation-π interaction, a series of fluorinated Trp derivatives (5-F-Trp, 5,7-F$_2$-Trp, 5,6,7-F$_3$-Trp, and 4,5,6,7-F$_4$-Trp) was incorporated at position 183, the analog of Trp α149. Whole-cell currents and fits to the Hill equation, presented in Figure 2.5, demonstrate that these receptors display the functional hallmarks of 5-HT$_3$R's – desensitization to prolonged agonist exposure and Hill coefficients around two. The EC$_{50}$ values for the wild type and the mutants are given in Table 2.1. A clear trend can be seen from the data. Each additional fluorine produces an increase in EC$_{50}$. Re-introduction of the wild type residue, Trp, yielded an EC$_{50}$ of 1.21 μM, comparable to that obtained from the wild type receptor heterologously expressed in oocytes. If a single fluorine is added to the tryptophan ring EC$_{50}$ increases 5-fold to 6.03 μM. Addition of another fluorine to the

ring leads to a 31-fold increase (relative to wild type) in EC_{50}, 37.7 μM, and a third fluorine yields an EC_{50} of 244 μM, 201-fold greater than Trp.

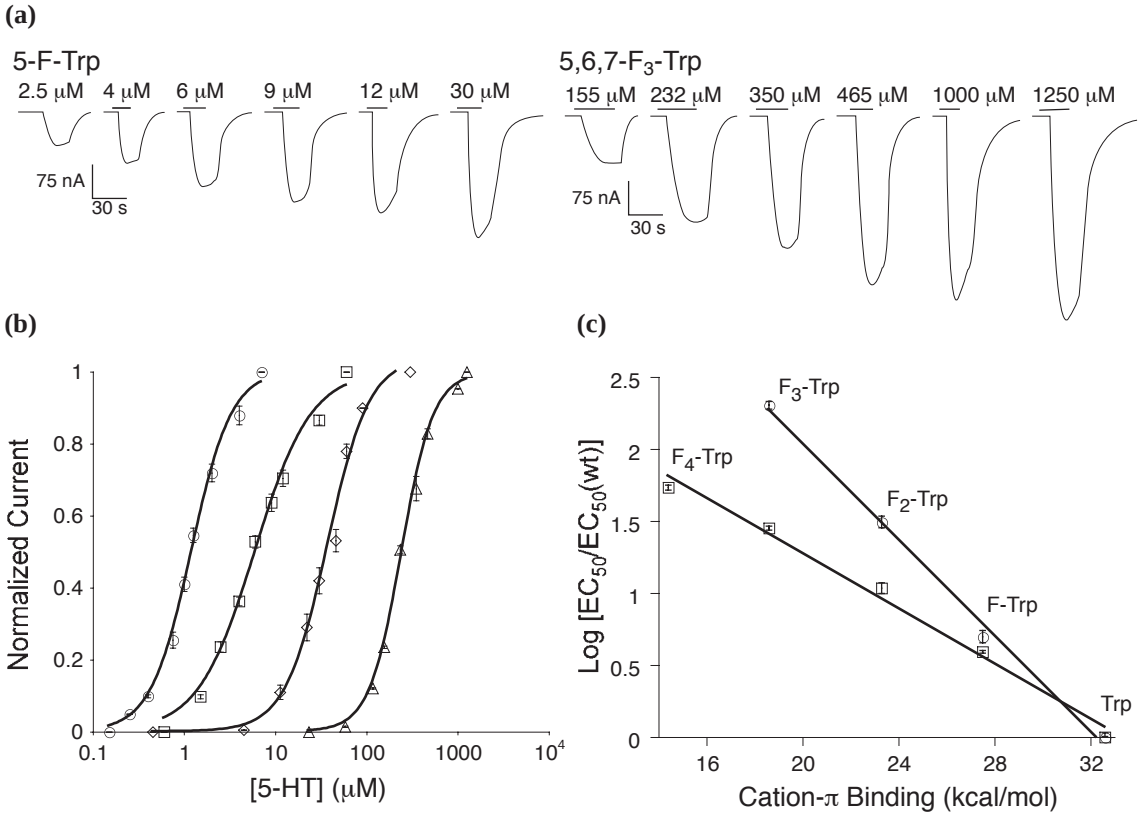

Figure 2.5. Electrophysiological analysis of 5-HT. (a) Representative voltage-clamp current traces for oocytes expressing suppressed 5-HT_{3A}R. Bars represent application of 5-HT. (b) 5-HT dose-response relations and fits to the Hill equation for 5-HT_{3A}R suppressed with Trp (*circles*), F–Trp (*squares*), F_2-Trp (*diamonds*), and F_3-Trp (*triangles*) at position 183. (c) Fluorination plot (log [EC_{50}/EC_{50} (wt)] versus calculated cation-π binding ability for the series of fluorinated Trp derivatives) for 5-HT (*circle*) at the 5-HT_{3A}R and ACh (*squares*) at the nAChR. 5-HT data fit the line y = 5.37 - 0.17x and ACh data fit the line y = 3.2 - 0.096x. The correlation for both linear fits is r = 0.99.

Attempts to record dose-response relations from the incorporation of 4,5,6,7-F_4-Trp at 183 were unsuccessful because this mutant required highly elevated concentrations of 5-HT— concentrations at which the agonist becomes an effective open channel-blocker. In a similar strategy to that used for the nAChR, a Val to Ser mutation was

introduced at position 13' in the M2 domain. This mutation has been shown to increase the agonist sensitivity of the 5-HT_3R.[21, 22] The EC_{50} values for the F_n-Trp series did show a progressive increase correlating with fluorination of the tryptophan ring, but did not entirely replicate the trend seen for receptors lacking this mutation (Table 2.1). Further analysis demonstrated that this mutation leads to standing currents that are reversible by addition of the open-channel blocker TMB-8, indicating this mutation produces constitutive activation of the receptor in the absence of agonist. For this reason, studies with the V13'S mutation were abandoned.

As in previous work on the nAChR, our measure for the cation-π binding ability of the fluorinated Trp derivatives is the calculated binding energy (kcal/mol) of a generic probe cation (Na^+) to the corresponding substituted indole.[8, 13] This provides a convenient way to express the clear trend in the dose-response data in a more quantitative way. Extensive studies of the cation-π interaction establish that *trends* in cation-π binding ability across a series of aromatics are independent of the identity of the cation, justifying the use of a simple probe ion. In order to also place the dose-response data for the channel on an energy scale, the logarithmic ratio of EC_{50} for mutants to EC_{50} for wild type is used. We refer to such representations as fluorination plots. A plot of this ratio versus cation-π binding ability for Trp183 reveals a compelling relationship (Figure 2.5c). Over a range of greater than two orders of magnitude in EC_{50}, there is a linear correlation between log (EC_{50}) and the cation-π binding ability of the side chains. This provides substantial evidence that Trp 183 binds 5-HT through a cation-π interaction arising from van der Waals contact between the agonist ammonium group and the indole side chain.

Table 2.1 Dose-response data for 5–HT_{3A}R and unnatural amino acids

	Residue	EC_{50}±SEM (μM)	Hill±SEM
	W183		
5-HT	Trp	1.21 ± 0.06	2.0 ± 0.16
	F-Trp	6.03 ± 0.5	1.4 ± 0.14
	F_2-Trp	37.7 ± 2.96	1.9 ± 0.23
	F_3-Trp	244 ± 8.4	2.5 ± 0.17
5-HT	Trp	0.04 ± 0.002	1.6 ± 0.06
V13'S	F-Trp	0.06 ± 0.003	1.8 ± 0.14
	F_2-Trp	0.27 ± 0.006	2.6 ± 0.13
	F_3-Trp	3.53 ± 0.141	2.2 ± 0.16
N-Me-5-HT	Trp	1.82 ± 0.10	2.5 ± 0.13
	F-Trp	2.70 ± 0.17	1.9 ± 0.19
	F_2-Trp	23.1 ± 2.73	2.6 ± 0.22
	F_3-Trp	368 ± 12	2.0 ± 0.10
5-HTQ	Trp	1.07 ± 0.07	2.1 ± 0.25
	F-Trp	1.65 ± 0.15	1.6 ± 0.19
	F_2-Trp	12.8 ± 0.95	1.8 ± 0.19
	F_3-Trp	284 ± 18.7	2.0 ± 0.15
5-HT	1-Np-Ala	30.4 ± 1.75	1.6 ± 0.10
	2-Np-Ala	32.0 ± 2.30	1.6 ± 0.12
	N-Me-Trp	25.6 ± 1.66	1.8 ± 0.16
	W90		
5-HT	Trp	1.21 ± 0.06	2.0 ± 0.16
	F_4-Trp	1.01 ± 0.05	1.6 ± 0.09

Along with modulating the cation-π interaction, fluorination also increases the ability of a Trp analog to donate a hydrogen bond.[23, 24] Therefore, an alternative interpretation of the above results would be that the hydrogen-bonding ability of the NH of the indole side chain of Trp 183 decreases receptor activation, and that fluorinated Trp analogs decrease activation by increasing the hydrogen-bond strength. This hypothesis suggests that EC_{50} would be decreased by side chains that remove the hydrogen bond, but

remain isosteric with Trp. To test this hypothesis, a series of Trp analogs lacking a hydrogen-bond donor at the nitrogen position of the indole was incorporated at position 183 (Figure 2.3b). The EC_{50} values for 2-Np-Ala, 1-Np-Ala, and N-Me-Trp were 32 μM, 30 μM, and 26 μM, respectively (Table 2.1). The increased EC_{50} is opposite to the prediction of the hydrogen-bond hypothesis. Thus, it appears that modulation of hydrogen-bonding ability does not explain the increase in EC_{50} in response to fluorination.

2.1.3 Position 90 in the 5-HT$_{3A}$R

An important question is whether the dramatic fluorination effect seen at position 183 in the 5-HT_{3A}R is unique to this site, as was observed for Trp α149 in the nAChR. In principle, the cation could interact simultaneously with several sides of the aromatic box. Based on sequence alignment and the AChBP structure, Trp 90— which aligns with Trp γ55/δ57— forms part of the binding site in the 5-HT_{3A}R. Thus, 4,5,6,7-F_4-Trp was incorporated at position 90. The EC_{50} value of this mutant was almost identical to wild type, 1.1 μM and 1.2 μM respectively, indicating that Trp 183 uniquely defines the cation-π binding site in the 5-HT_{3A}R (Table 2.1).

2.1.4 N-Me-5-HT and 5-HTQ at the 5-HT$_{3A}$R

Comparison of the fluorination plots for ACh and 5-HT shows that the slopes of the lines are quite different for the two agonists. The steeper slope seen for 5-HT indicates its ammonium center is more sensitive to electrostatic attenuation of the face of the tryptophan ring. Given the strong electrostatic component of the cation-π interaction, it is very likely this difference arises from the differing charge distributions between a

primary ammonium (5-HT) and a quaternary ammonium (ACh). To investigate this relationship further, we attempted to serially modulate the strength of the cation-π interaction by varying the degree of alkylation at the ammonium center.

Dose-response relations were recorded for the secondary serotonin analog, N-methyl-5-hydroxytryptamine (N-Me-5-HT) and the quaternary derivative, N,N,N-trimethyl-5-hydroxytryptamine (5-HTQ) with the fluoro-Trp series at position 183 (Figure 2.4b). The results for these experiments are presented in Table 2.1. Mono or tris methylation at the ammonium center of 5-HT has a minimal effect on EC_{50}; both agonists are comparable to the natural ligand, serotonin. At position 183 in the 5-HT_{3A}R— as with 5-HT itself— each additional fluorine substituent produces an increase in EC_{50}, indicating a significant cation-π interaction with the ammonium centers in both N-Me-5-HT and 5-HTQ (Figure 2.6).

Surprisingly, the expected trend for the substituted agonists (primary more sensitive than secondary, and secondary more sensitive than quaternary) is not seen. It is difficult to interpret these results, however, because in essence, these are double mutant studies with both the receptor and the agonist being simultaneously altered. It may be that though all three are potent agonists and bind to Trp 183 via a cation-π interaction, the binding mode for each is subtly different. Thus, the fluorination plots may be reporting on small differences in the binding distance and geometry between the ammonium center and aromatic face of the indole ring.

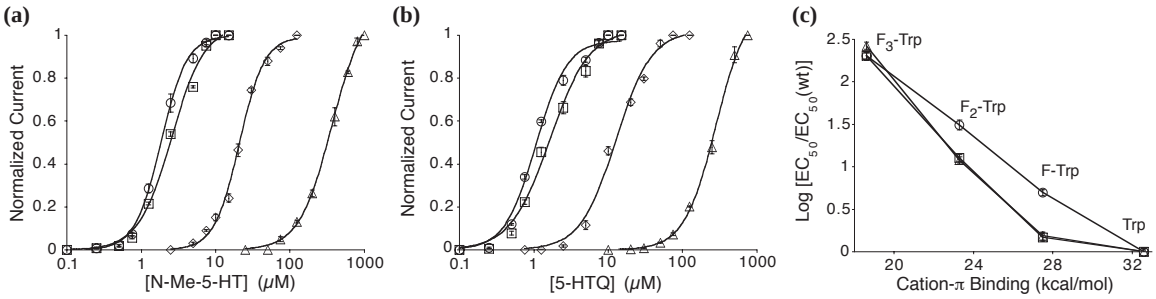

Figure 2.6. Electrophysiological analysis of 5-HT analogs. (a) N-Me-5-HT dose-response relations and fits to the Hill equation for 5-HT_{3A}R suppressed with Trp (*circles*), F–Trp (*squares*), F_2-Trp (*diamonds*), and F_3-Trp (*triangles*) at position 183. (b) 5-HTQ dose-response relations and fits to the Hill equation for 5-HT_{3A}R suppressed with Trp (*circles*), F–Trp (*squares*), F_2-Trp (*diamonds*), and F_3-Trp (*triangles*) at position 183 (c) Fluorination plot for 5-HT (*circles*) and N-Me-5-HT (*squares*) and 5-HTQ (*triangles*).

2.1.5 Effect of agonist alkylation state at the nAChR

As a complement to the studies of N-Me-5-HT and 5-HTQ at the 5-HT_{3A}R, Gabriel Brandt studied the behavior of the tertiary ACh analog, 2-dimethylaminoethyl acetate (noracetylcholine, or norACh) and the "simplified" quaternary ACh analog, tetramethylammonium (TMA) at the nAChR (Figure 2.4a). While TMA is a very low-potency agonist (Table 2.2), it does appear to experience a cation-π interaction with Trp α149 similar to that seen for ACh (Figure 2.7). Only data up to F_3-Trp are available because, as with other agonists studied, channel blockade by the agonist becomes a serious problem at the high concentrations necessary to activate the receptor with F_4-Trp at α149. However, it is clear that progressive fluorination leads to a steady increase in EC_{50} as seen with ACh.

The results for norACh highlight a significant difference between the 5-HT_{3A}R and the nAChR. While substantial variation in the alkylation state of 5-HT has no

significant effect on potency, simply removing one methyl group from the quaternary ammonium of ACh to produce norACh leads to vastly inferior potency. The EC_{50} for norACh is comparable to that of TMA. The fluorination data for norACh are not completely straightforward (Table 2.2). While monofluorination shows a 7-fold increase— comparable to ACh— di- and trifluorination show only modest increases and tetrafluorination leads to a *decrease* in EC_{50} (Figure 2.7).

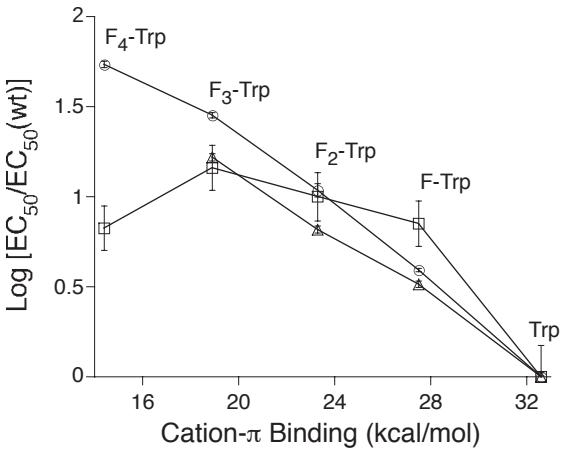

Figure 2.7. Fluorination plot for ACh (*circles*) and norACh (*squares*) and TMA (*triangles*).

2.1.6 Nicotine dose-response to F_n-Trp series at α149 in muscle nAChR

Nicotine is, of course, an important agonist of the nAChR, and all pharmacophore models for this drug and related compounds align the protonated pyrrolidine nitrogen with the quaternary ammonium of ACh.[25-29] To evaluate this model, we studied nicotine's potency with the series of fluorinated Trp derivatives at position α149 of the nAChR. The results are shown in Table 2.2 and Figure 2.8. Dose-response relations were collected for receptors with one (β subunit) or two (βγ subunits) L9'S mutations. The data for βL9'S receptors comes from Wenge Zhong, and Gabriel Brandt collected the

βγL9'S data. The results are similar in each case. If a single fluorine is added to the tryptophan ring by incorporating F-Trp at position α149, the EC_{50} increases almost three-fold, which is comparable to the four-fold increase observed with ACh. However, further fluorination does not lead to a significant further increase in EC_{50}. Figure 2.8c shows a fluorination plot for nAChR with a single L9'S mutation in the β subunit. Clearly, the progressive rise in EC_{50} seen with ACh and other agonists is not seen with nicotine.

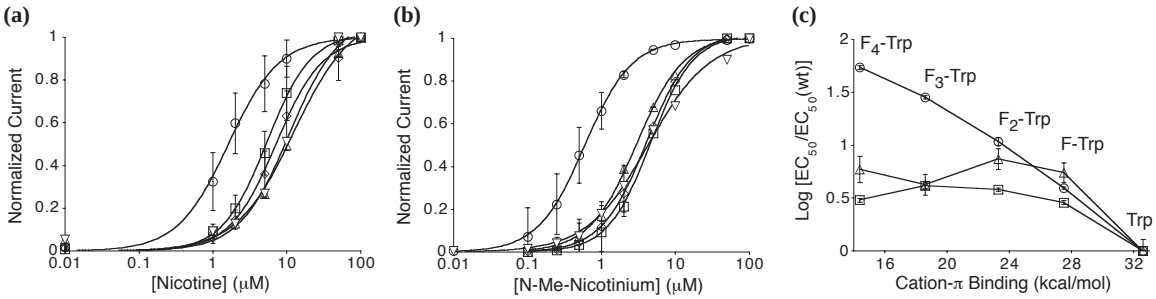

Figure 2.8. Electrophysiological analysis of nicotine and N-Me-nicotinium. (a) Nicotine dose-response relations and fits to the Hill equation for nAChR suppressed with Trp (*circles*), F–Trp (*squares*), F_2-Trp (*diamonds*), and F_3-Trp (*triangles*) at position 183. (b) N-Me-nicotinium dose-response relations and fits to the Hill equation for nAChR suppressed with Trp (*circles*), F–Trp (*squares*), F_2-Trp (*diamonds*), and F_3-Trp (*triangles*) at position 183 (c) Fluorination plot for ACh (*circles*) and nicotine (*squares*) and N-Me-nicotinium (*triangles*).

2.1.7 Nicotine dose-response to Trp analogs at γ55/δ57 in muscle nAChR

The lack of a strong response to fluorination at Trp α149 by nicotine indicates that it does not experience a significant cation-π interaction with this residue. This suggests the possibility that another aromatic residue in the binding site might form a cation-π interaction with nicotine. Based on the crystal structure of AChBP, an appealing candidate is Trp γ55/δ57, which is adjacent to Trp α149 in the binding site. We therefore evaluated the γ55/δ57 pair using, instead of fluorination, the alternative comparison of 5-CN-Trp vs. 5-Br-Trp. This nearly isosteric pair provides a useful qualitative indicator

of a cation-π interaction, since the cyano group is much more strongly deactivating than the bromo (Figure 2.3c). For example, at α149 with ACh as the agonist, the ratio of EC_{50} values for 5-CN-Trp/5-Br-Trp is 57.[8] As shown in Table 2.2, the ratio, 5-CN-Trp/5-Br-Trp is approximately 0.5 for nicotine at the γ55/δ57 position. This is not at all consistent with a cation-π interaction between nicotine and this tryptophan.

2.1.8 N-methyl-nicotinium dose-response to F_n-Trp series at nAChR α149

Both ACh and TMA show a progressive increase in EC_{50} with fluorination while nicotine does not. This suggests that a quaternary ammonium ion may be essential to see this effect in nAChR binding. To test this possibility, Gabriel Brandt evaluated the quaternary analog, N-methyl-nicotinium in the βγ L9'S nAChR. As shown in Table 2.2, the EC_{50} for N-methyl-nicotinium at wild-type receptors is similar to that of nicotine. In addition, N-methyl-nicotinium behaves quite similarly to nicotine in the fluorination plot. Thus, the unusual behavior of nicotine is not due to the lack of a quaternary ammonium group (Figure 2.8).

Table 2.2. Dose-response data for nAChR and unnatural amino acids

	Residue	EC_{50}±SEM (μM)	Hill±SEM
	W149		
Ach[a]	Trp	1.2 ± 0.0	ND[b]
β L9'S	F-Trp	4.7 ± 0.1	ND
	F_2-Trp	13 ± 1	ND
	F_3-Trp	34 ± 1	ND
	F_4-Trp	65 ± 3	ND
TMA	Trp	48 ± 2	ND
β,δ L9'S	F-Trp	155 ± 4	ND
	F_2-Trp	313 ± 8	ND
	F_3-Trp	789 ± 23	ND
norACh	Trp	23 ± 6	2.62 ± 1.00
β,γ L9'S	F-Trp	161 ± 9	1.92 ± 0.26
	F_2-Trp	225 ± 28	1.62 ± 0.04
	F_3-Trp	327 ± 18	1.62 ± 0.03
	F_4-Trp	152 ± 4	1.53 ± 0.03
Nicotine	Trp	45 ± 1	ND
β L9'S	F-Trp	130 ± 5	ND
	F_2-Trp	172 ± 6	ND
	F_3-Trp	188 ± 11	ND
	F_4-Trp	136 ± 5	ND
Nicotine	Trp	1.3 ± 0.3	2.92 ± 1.47
β,γ L9'S	F-Trp	4.2 ± 0.7	1.57 ± 0.09
	F_2-Trp	5.4 ± 0.5	1.53 ± 0.08
	F_3-Trp	12 ± 1	1.13 ± 0.07
	F_4-Trp	11 ± 1	1.28 ± 0.07
MeNicotinium	Trp	0.8 ± 0.1	1.34 ± 0.07
β,γ L9'S	F-Trp	4.2 ± 0.4	1.44 ± 0.08
	F_2-Trp	5.7 ± 0.7	1.42 ± 0.09
	F_3-Trp	3.3 ± 0.4	1.33 ± 0.07
	F_4-Trp	4.6 ± 1.0	1.05 ± 0.13
	Wγ55/δ57		
Nico	CN-Trp	1.4 ± 0.2	ND
α_2 L9'S	Br-Trp	3.0 ± 0.4	ND

[a] data from reference #7, Zhong et al. ,*PNAS* **1998**, 95, 12088.
[b] ND = no data

2.1.9 Studies of agonist efficacy

The EC_{50} for a receptor is a composite measurement comprising multiple elementary steps. Even in the simplest two-state model of channel opening, agonist binding to the closed channel is followed by a conformational change to an open channel state. Since the dose-response measurement does not distinguish between these two steps, experiments were undertaken to determine whether binding or channel gating accounted for the observed alterations in EC_{50} in response to increasing Trp fluorination. The efficacy of a compound on a ligand-gated ion channel is reflected in the maximal current passed at saturating agonist concentration under given electrophysiological conditions.[17, 30] Relative efficacies of all drugs were determined in ND96 medium in oocytes clamped at a membrane potential of -80 mV at a concentration five times the EC_{50} of the compound, and were determined for the various agonists at α149 suppressed receptors in nAChR and 183 suppressed receptors in 5-HT_{3A}R. The relative efficacy of each agonist was calculated as the ratio of I_{max} for the agonist to I_{max} for ACh or 5-HT.

For the 5-HT_3R and nAChR agonists considered here, there were no large statistical differences in efficacy among them (Table 2.3), nor was the relative efficacy ever observed to differ in receptors containing fluorinated Trp analogs. The process of channel gating is a complicated one and is postulated to involve numerous elementary steps for the nAChR. Thus, it is overly simplistic to conclude from these efficacy experiments that the effects observed are due exclusively to binding.[31] However, the fact that all compounds tested exhibit similar ability to initiate the conformational changes

associated with channel opening suggests the large effects that we see on potency most likely arise from effects on agonist binding.

Table 2.3 Efficacy values for the 5–HT_{3A}R and nAChR agonists

	Residue	Efficacy±SEM (%)[a]
	nAChR W149	
norACh	Trp	81.8 ± 6.1
β,γ L9'S	F-Trp	96.0 ± 3.3
	F_2-Trp	69.2 ± 31
	F_3-Trp	40.4 ± 11
TMA	Trp	97.5 ± 5.1
β,γ L9'S	F-Trp	62.1 ± 38
	F_2-Trp	94.4 ± 4.7
	F_3-Trp	95.2 ± 3.3
Nicotine	Trp	88.9 ± 7.5
β,γ L9'S	F-Trp	81.8 ± 11
	F_2-Trp	82.8 ± 12
	F_3-Trp	67.7 ± 13
MeNicotinium	Trp	86.4 ± 7.5
β,γ L9'S	F-Trp	83.8 ± 9.8
	F_2-Trp	87.9 ± 2.8
	F_3-Trp	79.3 ± 11
	5-HT_{3A}R W183	
N-Me-5-HT	Trp	70.7 ± 1.6
	F-Trp	78.5 ± 3.3
	F_2-Trp	70.3 ± 2.5
	F_3-Trp	71.8 ± 3.4
5-HTQ	Trp	75.0 ± 1.7
	F-Trp	70.0 ± 7.1
	F_2-Trp	70.3 ± 11
	F_3-Trp	91.8 ± 4.3

a efficacy is reported as the relative percentage of I_{max} for a given agonist to I_{max} of ACh or 5-HT

2.3 Discussion

The agonist response of a ligand-gated ion channel testifies to the organizing power of weak, non-covalent interactions. As the neurotransmitter approaches the much larger receptor, it must not be lured in by sites whose charge, shape, and hydrophobicity resemble the intended binding site. Instead, the molecule diffuses within the synaptic cleft and is drawn exactly to the appropriate location to trigger channel opening. In the case of the nicotinic acetylcholine receptor, we have previously proposed a unique role for Trp149 in the α subunit in the binding of the natural agonist, acetylcholine.[8] Based on subtle alterations of the electrostatic surface of the side chain at this position, it was concluded that this site participates in a strong cation-π interaction with the quaternary ammonium center of ACh. More recent structural work from other labs on AChBP has confirmed this conclusion.[2] The work presented here extends this technique to the serotonin receptor, 5-HT_{3A}R. In addition, the experimental scope is expanded at both the nAChR and 5-HT_{3A}R to consider in greater detail the nature of the interaction between agonist and receptor. Homology between the 5-HT_{3A}R, the alpha subunit of the muscle nAChR, and AChBP is significant, with strong conservation of the tryptophan residues making up two sides of the ligand-binding site box. In addition, two of the three tyrosine residues seen in the nAChR and AChBP are aromatic amino acids in 5-HT_{3A}R (Figure 2.2).[32]

The introduction of a series of fluorinated Trp analogs at position 183 of the mouse 5-HT_{3A}R provides clear evidence for a cation-π interaction between this residue and serotonin, as suggested by earlier site-directed mutagenesis studies.[33] This interaction appears to be unique to Trp183. Substitution of the fluorinated Trp series at

Trp 90— also in the binding site region— causes no significant effects. We thus conclude that both the nAChR and the 5-HT_{3A}R make use of a single potent cation-π interaction in recognizing the ammonium centers of their respective agonists.

Interestingly, the slope of the plot relating EC_{50} to calculated cation-π binding energy (the fluorination plot) is visibly different for ACh binding to nAChR than serotonin binding to the 5-HT_{3A}R. Inspection of Figure 2.5c shows that the serotonin slope is markedly steeper. We interpret this to mean that the strength of the cation-π interaction between the agonist and the relevant tryptophan is greater when serotonin is the agonist than when ACh is the agonist. This result is consistent with expectations based on electrostatics.[34] As shown in Figure 2.4, the smaller, primary ammonium center of serotonin presents a more focused positive charge than the quaternary center of ACh. Given the strong electrostatic component of the cation-π interaction, smaller ions are expected to show a stronger interaction.

The data for ACh and serotonin also provide one way to address a long-standing issue in molecular recognition: what is the strength of a cation-π interaction? From Figure 2.3a, it may be observed that the surface of F_4-Trp is essentially electrostatically neutral. Thus, a comparison of F_4-Trp and Trp provides a measure of the *electrostatic component* of the cation-π interaction. The F_4-Trp/Trp ratio reflects the energy cost of removing the attractive electrostatics, but maintaining the residue as if the Trp were replaced by a hydrophobic residue of the same shape. This new residue maintains most van der Waals and dispersion interactions, but cannot experience a cation-π interaction. For ACh, the F_4-Trp/Trp ratio is 54. For serotonin, the F_4-Trp EC_{50} value is obtained by extrapolation of the line in Figure 2.5c which leads to a F_4-Trp/Trp ratio of 836. If these

are viewed as ratios of binding constants, then the implied energetics of a cation-π interaction are 2.4 kcal/mol and 4.0 kcal/mol, respectively for ACh and serotonin. These are consistent with other estimates of the magnitude of the cation-π interaction,[7] and further establish that this non-covalent binding force is comparable to, or stronger than, any other individual force considered in biological recognition.

In an effort to probe the molecular recognition properties of these receptors further, we studied the effects of varying the alkylation state of the cationic center of the agonist. In such studies, a clear distinction emerges between the 5-HT_{3A}R and the nAChR. At the serotonin receptor, the monoalkylated agonist, N-Me-5-HT and the quaternary agonist, 5-HTQ show essentially the same EC_{50} as the natural agonist 5-HT. This suggests that the 5-HT_{3A}R agonist binding site is fairly tolerant, accommodating the much bulkier 5-HTQ with no loss in potency. These two unnatural agonists respond to fluorination much like the natural agonist, serotonin, although the perfect linear trend of Figure 2.5c is not reproduced. We hesitate to provide an extensive interpretation of this subtle distinction in which multiple variables, including both the agonist and the protein, are being changed. However, it is clear that a strong cation-π interaction to Trp 183 is involved with all of these agonists.

The nAChR behaves quite differently from the 5-HT_{3A}R in this regard. First, the change from ACh to norACh leads to a very large increase in EC_{50}. Simply removing one methyl group from ACh produces a very low-potency agonist. In fact, norACh is comparable in potency to tetramethylammonium (TMA), which lacks several moieties of the ACh molecule. Interestingly, the quaternary TMA— although a very low-potency agonist— does show a fluorination trend that is similar to that of ACh (Figure 2.7). The

norACh fluorination trend is less well-behaved with a large increase for F-Trp, followed by minimal further effects for F_2-Trp and F_3-Trp, which are then followed by a downturn at F_4-Trp (Figure 2.7). While this suggests some kind of cation-π interaction for the norACh agonist, more subtle factors may also be operative for this low-potency, non-native agonist. Clearly, the nAChR is much more sensitive to alterations in the region of Trp α149 than the 5-HT_{3A}R is to comparable changes with the aligned Trp 183.

This leaves the case of nicotine— an obviously important agonist of the nAChR. Before discussing the results, a few general comments are in order. The receptor studied here is the muscle-type receptor— the isoform found at the neuromuscular junction in the peripheral nervous system. Nicotine is a full agonist at this receptor, but as shown in Table 2.2, nicotine is not an especially potent agonist at the muscle receptor. The behavioral and addictive effects of nicotine arise exclusively from effects on the *neuronal* nAChRs.[35-38] These receptors are expressed widely in the central nervous system.[39, 40] While the overall architecture of neuronal nAChR is no doubt the same as the muscle type described here, the neuronal receptors are comprised of different combinations of α and β (non-α) subunits. There are many variants of each subunit, but they are highly homologous to the muscle subunits, and all the residues discussed here are conserved in the neuronal receptors. At present, at least 10 α and 4 β forms are known, termed $\alpha_{1\text{-}10}$ and $\beta_{1\text{-}4}$ (α_1 and β_1 are the muscle forms; all the rest are neuronal). Nicotine addiction is thought to depend partially on receptors formed from α_4 and β_2 subunits (stoichiometry unknown) and perhaps receptors involving α_7.[37, 38, 41, 42] While we believe our findings are clearly relevant to the pharmacology of nicotine, it must be remembered that subtle variations could arise in comparable studies of the neuronal receptors.

The fluorination plot for nicotine is shown in Figure 2.8b. In light of our findings for ACh versus norACh, we also studied N-Me-nicotinium in which the pyrrolidine nitrogen has been quaternarized. Interestingly, these two nicotinoid agonists are similar, both in potency and in their fluorination plots. The nicotine fluorination plot has the shallowest slope of any agonist examined at either the nAChR or the 5-HT_{3A}R. After a relatively small jump in EC_{50} for F-Trp, only very small changes in EC_{50} are seen upon further fluorination of Trp α149. This is strong evidence that nicotine does not make a strong cation-π interaction with Trp α149 of the muscle-type nAChR.

One possibility is that nicotine makes a cation-π interaction with one of the other aromatics that form the "aromatic box" of the nAChR binding site. A sensible candidate is γ55/δ57— the other conserved Trp in the agonist binding site. This residue has been implicated in nicotine binding by photoaffinity labeling studies from the Cohen group.[43, 44] As a probe of this site, we studied the pair 5-CN-Trp/5-Br-Trp. It has been previously shown that this nearly isosteric pair can provide a good qualitative indication of a cation-π interaction, since the cyano group is much more strongly deactivating than the bromo. The pair differ by a factor of 57 for ACh at Trp α149.[8] However, no significant effect is seen at γ55/δ57 with nicotine (or ACh) as the agonist, ruling out this site for a cation-π interaction with nicotine at the muscle receptor.

Subsequent to the completion of this work, several studies examining the anomalous binding properties of nicotine were reported. Taken together, these studies provide a more detailed portrait of nicotine binding to the nAChR. Modeling studies based on the structure of AChBP suggested a hydrogen bonding interaction from the N^+–H of nicotine to the backbone carbonyl of Trp α149.[45, 46] Amanda Cashin and E.

James Petersson, in a study combining both functional data from backbone ester mutations at Thr α150 and computational work, demonstrated that nicotine binding depends on a hydrogen bond with the backbone carbonyl of α149.[47] More recently Sixma and co-workers reported the crystal structure of AChBP in the presence of bound nicotine.[5] This structure verified that nicotine does not form a cation-π interaction with Trp α149, and that bound nicotine does indeed make a hydrogen bond with the backbone carbonyl of α149.

The conclusion that nicotine does not bind to the muscle nAChR via a cation-π interaction with tryptophan residues in the aromatic box has implications for existing pharmacophore models of the nAChR. All current pharmacophore models align the quaternary ammonium of ACh with the protonated tertiary amine of nicotine.[25-29] It seems an unavoidable conclusion that such a model requires a cation-π interaction between the cationic center of nicotine and Trp α149, but it is now clear that, at least in the muscle nAChR, such a cation-π interaction does not exist. The data with norACh suggest that the nAChR is quite sensitive to variations in agonist structure at the cationic center— much more so than the 5-HT_{3A}R. As nicotine analogs are assuming a greater prominence for drug leads in a variety of important diseases, some caution in applying the standard pharmacophore model seems to be in order.

2.4 Conclusions

Earlier work in the Dougherty group demonstrated that the nonsense suppression methodology provides a powerful tool for evaluating drug-receptor interactions. In particular, fluorination plots can clearly identify a specific cation-π interaction between an agonist and its receptor. Here, we build upon those findings in several ways.

A clear cation-π interaction between serotonin and Trp 183 of the 5-HT_{3A}R is established. A measure of the magnitude of the electrostatic component of the cation-π interaction is provided. We find it to be worth ~2 kcal/mol for ACh at the nAChR and ~4 kcal/mol for serotonin at the 5-HT_{3A}R. Studies of other agonists highlight the differences between the two homologous receptors: the nAChR and the 5-HT_{3A}R. The latter is relatively tolerant of changes at the cationic center and maintains a cation-π interaction, while the nAChR seems quite sensitive to changes in the nature of the cationic center of the agonist. Finally, studies of the binding of nicotine to the muscle nAChR suggest that present pharmacophore models require revision. Work on the neuronal nAChR will be required to further explore this issue.

2.5 Methods

2.5.1 Electrophysiology

Stage VI oocytes of *Xenopus laevis* were harvested according to approved procedures. Recordings were made 24 to 72 hours post-injection in standard two-electrode voltage clamp mode. Oocytes were superfused with calcium-free ND96 solution, as previously reported[8]. Nicotinic agonists were either synthesized as described earlier (N-methyl-nicotinium)[48], or purchased from Sigma/Adrich/RBI ([-]-nicotine tartrate) or Acros Organics (the tertiary ACh analog, 2-dimethyl aminoethyl acetate). Serotonin and its analogs were purchased from Sigma/Adrich/RBI. All drugs were prepared in sterile ddi water for dilution into calcium-free ND96. Dose-response data were obtained for a minimum of eight concentrations of agonists for a minimum of three

different cells. Curves were fit to the Hill equation to determine EC_{50} and Hill coefficient.

2.5.2 Unnatural amino acid suppression

Synthetic amino acids were conjugated to the dinucleotide dCA and ligated to truncated 74 nt tRNA as described.[9] Deprotection of charged tRNA was carried out by photolysis immediately prior to co-injection with mRNA in the manner described.[8, 49] Typically, 25 ng tRNA were injected per oocyte along with mRNA in a total volume of 50 nL per cell. mRNA was prepared by *in vitro* runoff transcription using the Ambion mMagic mMessage kit. Mutation to insert the *amber* stop codon at the site of interest was carried out by standard means and was verified by sequencing through both strands. For nAChR suppression, a total of 4.0 ng of mRNA was injected in the subunit ratio of 10:1:1:1 α:β:γ:δ. In many cases, one or more subunits contained a L9'S mutation, as discussed above. As reported previously, mouse muscle embryonic nAChR in the pAMV vector was used. For suppression in homomeric 5-HT_{3A}R, 5.0 ng of mRNA was injected. Mouse 5-HT_{3A}R was used in all cases, in the pAMV vector. Negative and positive controls for suppression were performed in the following way: as a negative control, truncated 74 nt tRNA or truncated tRNA ligated to dCA was co-injected with mRNA in the same manner as fully charged tRNA. At the positions studied here, no current was ever observed from these negative controls. The positive control involved wild-type recovery by co-injection with 74 nt tRNA ligated to dCA-Trp. In all cases, the dose-response was indistinguishable from injection of wild-type mRNA alone.

2.6 References

1. Armstrong, N.; Gouaux, E., Mechanisms for activation and antagonism of an AMPA-sensitive glutamate receptor: crystal structures of the GluR2 ligand binding core. *Neuron* **2000,** 28, (1), 165-81.
2. Brejc, K.; van Dijk, W. J.; Klaassen, R. V.; Schuurmans, M.; van Der Oost, J.; Smit, A. B.; Sixma, T. K., Crystal structure of an ACh-binding protein reveals the ligand-binding domain of nicotinic receptors. *Nature* **2001,** 411, (6835), 269-76.
3. Mayer, M. L.; Olson, R.; Gouaux, E., Mechanisms for ligand binding to GluR0 ion channels: crystal structures of the glutamate and serine complexes and a closed apo state. *J Mol Biol* **2001,** 311, (4), 815-36.
4. Miyazawa, A.; Fujiyoshi, Y.; Stowell, M.; Unwin, N., Nicotinic acetylcholine receptor at 4.6 A resolution: transverse tunnels in the channel wall. *J Mol Biol* **1999,** 288, (4), 765-86.
5. Celie, P. H. N.; van Rossum-Fikkert, S. E.; van Dijk, W. J.; Brejc, K.; Smit, A. B.; Sixma, T. K., Nicotine and carbamylcholine binding to nicotinic acetylcholine receptors as studied in AChBP crystal structures. *Neuron* **2004,** 41, (6), 907-914.
6. Dougherty, D. A., Cation-pi interactions in chemistry and biology: A new view of benzene, Phe, Tyr, and Trp. *Science* **1996,** 271, (5246), 163-168.
7. Ma, J. C.; Dougherty, D. A., The cation-pi interaction. *Chemical Reviews* **1997,** 97, (5), 1303-1324.
8. Zhong, W. G.; Gallivan, J. P.; Zhang, Y. N.; Li, L. T.; Lester, H. A.; Dougherty, D. A., From ab initio quantum mechanics to molecular neurobiology: A cation-pi binding site in the nicotinic receptor. *Proceedings of the National Academy of Sciences of the United States of America* **1998,** 95, (21), 12088-12093.
9. Nowak, M. W.; Gallivan, J. P.; Silverman, S. K.; Labarca, C. G.; Dougherty, D. A.; Lester, H. A., In vivo incorporation of unnatural amino acids into ion channels in Xenopus oocyte expression system. *Methods in Enzymology* **1998,** 293, 504-529.
10. Thorson, J. S.; Cornish, V. W.; J.E., B.; S.T., C.; Yano, T.; Schultz, P. G., A biosynthetic approach for the incorporation of unatural amino acids into proteins. *Topics in Current Chemistry* **1998,** 77, 43-73.
11. Gilmore, M. A.; Steward, L. E.; Chamberlin, A. R., Incorporation of noncoded amino acids by in vitro protein biosynthesis. *Topics in Current Chemistry* **1999,** 202, 77-99.
12. Sisido, M.; Hohsaka, T., Extension of protein functions by the incorporation of nonnatural amino acids. *Bulletin of the Chemical Society of Japan* **1999,** 72, (7), 1409-1425.
13. Mecozzi, S.; West, A. P.; Dougherty, D. A., Cation-pi interactions in simple aromatics: Electrostatics provide a predictive tool. *Journal of the American Chemical Society* **1996,** 118, (9), 2307-2308.
14. Mecozzi, S.; West, A. P.; Dougherty, D. A., Cation-pi interactions in aromatics of biological and medicinal interest: Electrostatic potential surfaces as a useful qualitative guide. *Proceedings of the National Academy of Sciences of the United States of America* **1996,** 93, (20), 10566-10571.

15. Labarca, C.; Nowak, M. W.; Zhang, H.; Tang, L.; Deshpande, P.; Lester, H. A., Channel gating governed symmetrically by conserved leucine residues in the M2 domain of nicotinic receptors. *Nature* **1995,** 376, (6540), 514-6.
16. Kearney, P. C.; Nowak, M. W.; Zhong, W.; Silverman, S. K.; Lester, H. A.; Dougherty, D. A., Dose-response relations for unnatural amino acids at the agonist binding site of the nicotinic acetylcholine receptor: tests with novel side chains and with several agonists. *Mol Pharmacol* **1996,** 50, (5), 1401-12.
17. Kenakin, T., Efficacy in drug receptor theory: outdated concept or under-valued tool? *Trends Pharmacol Sci* **1999,** 20, (10), 400-5.
18. Maricq, A. V.; Peterson, A. S.; Brake, A. J.; Myers, R. M.; Julius, D., Primary structure and functional expression of the 5HT3 receptor, a serotonin-gated ion channel. *Science* **1991,** 254, (5030), 432-7.
19. Davies, P. A.; Pistis, M.; Hanna, M. C.; Peters, J. A.; Lambert, J. J.; Hales, T. G.; Kirkness, E. F., The 5-HT3B subunit is a major determinant of serotonin-receptor function. *Nature* **1999,** 397, (6717), 359-63.
20. Brady, C. A.; Stanford, I. M.; Ali, I.; Lin, L.; Williams, J. M.; Dubin, A. E.; Hope, A. G.; Barnes, N. M., Pharmacological comparison of human homomeric 5-HT3A receptors versus heteromeric 5-HT3A/3B receptors. *Neuropharmacology* **2001,** 41, (2), 282-4.
21. Bhattacharya, A.; Dang, H.; Zhu, Q. M.; Schnegelsberg, B.; Rozengurt, N.; Cain, G.; Prantil, R.; Vorp, D. A.; Guy, N.; Julius, D.; Ford, A.; Lester, H. A.; Cockayne, D. A., Uropathic observations in mice expressing a constitutively active point mutation in the 5-HT3A receptor subunit. *Journal of Neuroscience* **2004,** 24, (24), 5537-5548.
22. Dang, H.; England, P. M.; Farivar, S. S.; Dougherty, D. A.; Lester, H. A., Probing the role of a conserved M1 proline residue in 5-hydroxytryptamine(3) receptor gating. *Molecular Pharmacology* **2000,** 57, (6), 1114-1122.
23. Abraham, M. H.; Grellier, P. L.; Prior, D. V.; Duce, P. P.; Morris, J. J.; Taylor, P. J., Hydrogen-Bonding .7. A Scale of Solute Hydrogen-Bond Acidity Based on Log K-Values for Complexation in Tetrachloromethane. *Journal of the Chemical Society-Perkin Transactions 2* **1989**, (6), 699-711.
24. Smart, B. E., Fluorine substituent effects (on bioactivity). *Journal of Fluorine Chemistry* **2001,** 109, (1), 3-11.
25. Tonder, J. E.; Olesen, P. H., Agonists at the alpha4beta2 nicotinic acetylcholine receptors: structure-activity relationships and molecular modelling. *Curr Med Chem* **2001,** 8, (6), 651-74.
26. Schmitt, J. D., Exploring the nature of molecular recognition in nicotinic acetylcholine receptors. *Curr Med Chem* **2000,** 7, (8), 749-800.
27. Tonder, J. E.; Hansen, J. B.; Begtrup, M.; Pettersson, I.; Rimvall, K.; Christensen, B.; Ehrbar, U.; Olesen, P. H., Improving the nicotinic pharmacophore with a series of (Isoxazole)methylene-1-azacyclic compounds: synthesis, structure-activity relationship, and molecular modeling. *J Med Chem* **1999,** 42, (24), 4970-80.
28. Sheridan, R. P.; Nilakantan, R.; Dixon, J. S.; Venkataraghavan, R., The ensemble approach to distance geometry: application to the nicotinic pharmacophore. *J Med Chem* **1986,** 29, (6), 899-906.
29. Curtis, L.; Chiodini, F.; Spang, J. E.; Bertrand, S.; Patt, J. T.; Westera, G.; Bertrand, D., A new look at the neuronal nicotinic acetylcholine receptor pharmacophore. *Eur J Pharmacol* **2000,** 393, (1-3), 155-63.

30. Kenakin, T., Inverse, protean, and ligand-selective agonism: matters of receptor conformation. *Faseb J* **2001,** 15, (3), 598-611.
31. Colquhoun, D., Binding, gating, affinity and efficacy: the interpretation of structure-activity relationships for agonists and of the effects of mutating receptors. *Br J Pharmacol* **1998,** 125, (5), 924-47.
32. Boess, F. G.; Steward, L. J.; Steele, J. A.; Liu, D.; Reid, J.; Glencorse, T. A.; Martin, I. L., Analysis of the ligand binding site of the 5-HT3 receptor using site directed mutagenesis: importance of glutamate 106. *Neuropharmacology* **1997,** 36, (4-5), 637-47.
33. Spier, A. D.; Lummis, S. C., The role of tryptophan residues in the 5-Hydroxytryptamine(3) receptor ligand binding domain. *J Biol Chem* **2000,** 275, (8), 5620-5.
34. Schmitt, J. D.; Sharples, C. G.; Caldwell, W. S., Molecular recognition in nicotinic acetylcholine receptors: the importance of pi-cation interactions. *J Med Chem* **1999,** 42, (16), 3066-74.
35. Benowitz, N. L., Pharmacology of nicotine: addiction and therapeutics. *Annu Rev Pharmacol Toxicol* **1996,** 36, 597-613.
36. Dani, J. A.; Heinemann, S., Molecular and cellular aspects of nicotine abuse. *Neuron* **1996,** 16, (5), 905-8.
37. Picciotto, M. R.; Zoli, M.; Rimondini, R.; Lena, C.; Marubio, L. M.; Pich, E. M.; Fuxe, K.; Changeux, J. P., Acetylcholine receptors containing the beta2 subunit are involved in the reinforcing properties of nicotine. *Nature* **1998,** 391, (6663), 173-7.
38. Tapper, A. R.; McKinney, S. L.; Nashmi, R.; Schwarz, J.; Deshpande, P.; Labarca, C.; Whiteaker, P.; Marks, M. J.; Collins, A. C.; Lester, H. A., Nicotine activation of alpha 4*receptors: Sufficient for reward, tolerance, and sensitization. *Science* **2004,** 306, (5698), 1029-1032.
39. McGehee, D. S.; Role, L. W., Physiological diversity of nicotinic acetylcholine receptors expressed by vertebrate neurons. *Annu Rev Physiol* **1995,** 57, 521-46.
40. Jones, S.; Sudweeks, S.; Yakel, J. L., Nicotinic receptors in the brain: correlating physiology with function. *Trends Neurosci* **1999,** 22, (12), 555-61.
41. Lena, C.; Changeux, J. P., Pathological mutations of nicotinic receptors and nicotine-based therapies for brain disorders. *Curr Opin Neurobiol* **1997,** 7, (5), 674-82.
42. Marubio, L. M.; del Mar Arroyo-Jimenez, M.; Cordero-Erausquin, M.; Lena, C.; Le Novere, N.; de Kerchove d'Exaerde, A.; Huchet, M.; Damaj, M. I.; Changeux, J. P., Reduced antinociception in mice lacking neuronal nicotinic receptor subunits. *Nature* **1999,** 398, (6730), 805-10.
43. Xie, Y.; Cohen, J. B., Contributions of Torpedo nicotinic acetylcholine receptor gamma Trp-55 and delta Trp-57 to agonist and competitive antagonist function. *J Biol Chem* **2001,** 276, (4), 2417-26.
44. Chiara, D. C.; Middleton, R. E.; Cohen, J. B., Identification of tryptophan 55 as the primary site of [3H]nicotine photoincorporation in the gamma-subunit of the Torpedo nicotinic acetylcholine receptor. *FEBS Lett* **1998,** 423, (2), 223-6.
45. Schapira, M.; Abagyan, R.; Totrov, M., Structural model of nicotinic acetylcholine receptor isotypes bound to acetylcholine and nicotine. *BMC Struct. Biol.* **2002,** 2, (1), 1.
46. Le Novere, N.; Grutter, T.; Changeux, J. P., Models of the extracellular domain of the nicotinic receptors and of agonist- and Ca2+-binding sites. *Proc. Natl. Acad. Sci. USA* **2002,** 99, (5), 3210-3215.

47. Cashin, A. L., Petersson, E.J., Lester, H.A., and Dougherty, D.A., *Journal of the American Chemical Society* **2004,** in press.
48. Seeman, J. I.; Whidby, J. F., The iodomethylation of nicotine. An unusual example of competitive nitrogen alkylation. *J Org Chem* **1976,** 41, (24), 3824-6.
49. Li, L. T.; Zhong, W. G.; Zacharias, N.; Gibbs, C.; Lester, H. A.; Dougherty, D. A., The tethered agonist approach to mapping ion channel proteins toward a structural model for the agonist binding site of the nicotinic acetylcholine receptor. *Chemistry & Biology* **2001,** 8, (1), 47-58.

Chapter 3. Structure-function studies of tyrosines in the ligand-binding pocket of the 5-HT_3R

3.1 Introduction

The determination of the structure of the ACh binding protein (AChBP) which is homologous to the extracellular domain of the nACh receptor (nAChR) has had a significant impact on the study of ligand-gated ion channels (LGIC).[1] As the first high-resolution portrait of the extracellular domain of these proteins, it has provided crucial structural information for structure-function studies. In addition, lower resolution images from cryo-electron microscopy (cryo-EM) have contributed to our understanding of the global structure of these receptors.[2-6] Insights from both the AChBP and cryo-EM structures have led to a model of channel opening in which agonist binding induces a rotation of the extracellular domains. This is then thought to be transduced via the M2–M3 loop to M2, the pore-lining domain. The subsequent rotation of M2 removes the hydrophobic residues lining the channel and allows the passage of ions.[2] Although this is a plausible model, more experimental data are required both to substantiate it and to determine the molecular details of these processes.

One area where the AChBP structure has proven particularly valuable is in the generation of homology-based models. Homology models based on AChBP have been constructed for the nACh, $GABA_A$, and 5-HT_3 receptors.[7-10] The homology model of the 5-HT_3R reveals a ligand-binding pocket containing a large proportion of aromatic residues.[8] Two of these residues are tryptophans, one of which (Trp 183) forms a cation-π interaction with agonist.[11] There is also a phenylalanine (Phe 226), but most of

the aromatic character is provided by tyrosines (Tyr 141, Tyr 143, Tyr 153, and Tyr 234). The agonist-binding site in LGICs is composed of several non-contiguous loops (loops A-E). Tyrosines 141, 143, and 153 are located in loop E which is contributed to the binding site by the minus-side subunit (or in nAChR terms, the non-alpha subunit). This loop is not highly conserved in other members of the Cys-loop LGIC family. Tyr 234 is in loop C which is contributed by the plus-side subunit (or alpha-subunit in nAChR), and is universally conserved in the Cys-loop superfamily. Previous data have shown the importance of these residues in the binding and/or function of the 5-HT_3R, but it has not been possible to define their exact roles.[12, 13]

The work presented in this chapter combines conventional mutagenesis and nonsense suppression methodology to examine the functional roles of these binding-site tyrosines in the 5-HT_3R. This work represents a collaboration with the Sarah Lummis group of Cambridge University, and in particular Kerry Price, who performed all of the conventional mutagenesis experiments and binding studies. In addition she supplied significant contributions and effort to the nonsense suppression studies. It should also be noted that all of the modeling work considered here was generated by our Cambridge colleagues.

Using nonsense suppression, a series of tyrosine analogs was introduced at each tyrosine site (Figure 3.1).[14, 15] The tyrosine analogs were selected based on rational perturbations of tyrosine's physico-chemical properties. The precision afforded by unnatural amino acids provided key information for delineating the functional role of these tyrosines. Assimilating these data with the homology model of the 5-HT_3R binding site into which 5-HT has been computationally docked allowed us to confirm the

orientation of 5-HT in the agonist binding pocket and to determine several non-covalent interactions that are important for receptor binding and/or gating. This information was used to generate a possible mechanism by which agonist binding could trigger a series of conformational changes near the binding site that may initiate the gating process.

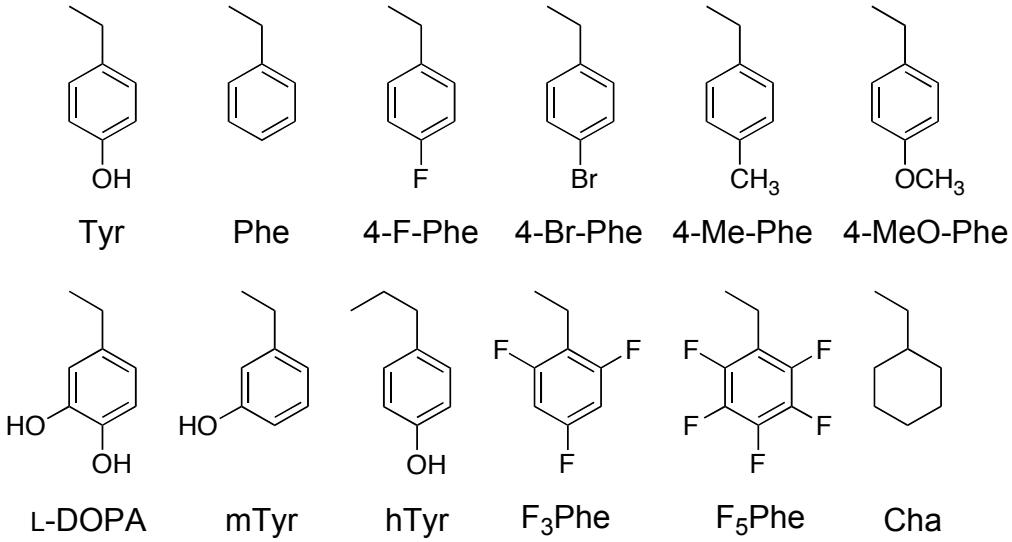

Figure 3.1. Structures of the side chains incorporated by nonsense suppression

3.2 Results

3.2.1 Nonsense suppression control experiments

3.2.1.1 Rescue of wild type through reintroduction of tyrosine

As an initial test of the viability of nonsense suppression at these sites, tyrosine was incorporated via acylated tRNA at each of the four positions (141, 143, 153, and 234). For the nonsense suppression methodology to give reliable results, the EC_{50} values and Hill coefficients for activation by 5-HT must replicate those of the wild-type (non-suppressed) 5-HT_{3A}R, heterologously expressed in *Xenopus* oocytes.

All mutant mRNAs, when co-injected into *Xenopus* oocytes with tRNA-Tyr, produced functional receptors that responded to application of 5-HT with an inward current that desensitized in response to maintained 5-HT. The results shown in Tables 3.1 and 3.2 establish that the EC_{50} values and Hill coefficients obtained from 141-Tyr, 143-Tyr, 153-Tyr, and 234-Tyr and wild type receptors were indeed similar to each other. This indicates that the wild-type phenotype was successfully "rescued" by the delivery of tRNA-Tyr molecules.

3.2.1.2 Validation of the pGEMHE vector

One novel feature of these studies was the use of the pGEMHE vector.[16] Traditionally we have almost exclusively relied on the pAMV vector for nonsense suppression. This vector produces reliable expression and results, but is not the most amenable vector for subcloning, in that the start codon of the open-reading frame must be placed adjacent to the AMV sequence. This requirement limits the possible restriction enzymes for subcloning. The pGEMHE vector is a high expression oocyte vector and does not have such stringent subcloning requirements.

Suppression experiments using pGEMHE showed that maximal 5-HT-induced currents (I_{max}) were typically 0.8–2 μA at a holding potential of -60mV (Figure 3.2). This suggests that the pGEMHE vector can yield levels of full-length, correctly folded protein at least as high as the original pAMV vector.[15] The efficiency of nonsense suppression has been estimated at ~10 percent[14], and comparison of I_{max} values for the wild-type $5\text{-}HT_{3A}$ receptor expressed in oocytes using pGEMHE to rescued TAG mutant receptors suggests a similar efficiency here.

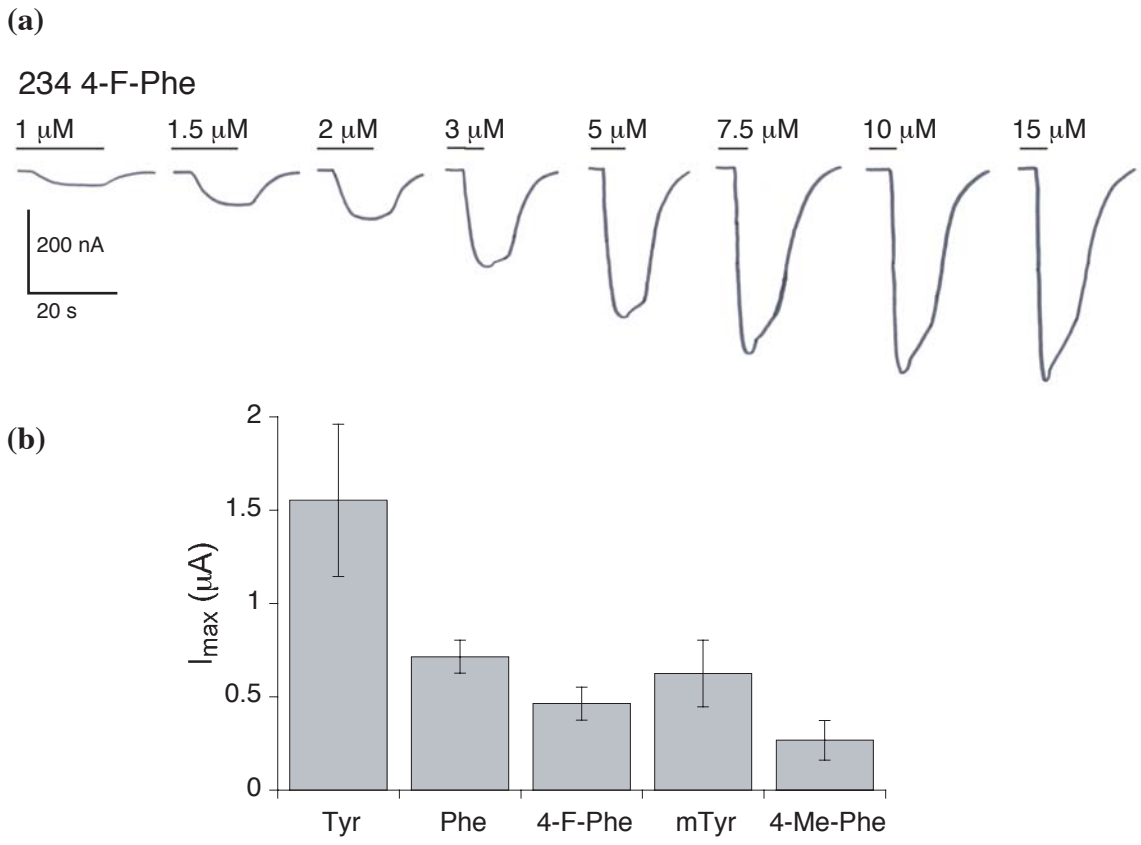

Figure 3.2. (a) Representative voltage-clamp current traces for oocytes expressing suppressed 5-HT_{3A}R. Bars represent application of 5-HT. (b) Representaive maximal currents (I_{max}) for suppression experiments using the pGEMHE vector, obtained from 5-HT_{3A}R suppressed at postion 234.

3.1.1.3 Testing read-through

No currents in response to application of high concentrations of 5-HT (1mM) were detected from oocytes injected with mRNA alone or with mRNA and tRNA not ligated to dCA-aa (THG73 74-mer tRNA). It therefore appears that transcripts, which have been truncated by the inclusion of a stop codon at the position of the mutated tyrosine residue, cannot produce functional receptors. This is to be expected because these truncated receptors would contain none of the transmembrane regions required for ion channel activity. We can also conclude that any amino acid that is incorporated into

these four sites of the mutant receptor is specifically introduced by the injected tRNA-aa and not by the endogenous tRNA population of the oocyte. Finally, the lack of response from oocytes injected with mRNA and unacylated tRNA shows that there is no detectable reacylation of tRNA by endogenous synthetases.

3.1.2 Incorporation of unnatural amino acids

A subset of the unnatural amino acids shown in Figure 1 was selected for testing at each of the mutant positions. These compounds were previously incorporated into the nAChR and are therefore compatible with the oocyte expression system.[14, 15] In addition to the standard amino acids tyrosine and phenylalanine, the amino acids tested include: 3-hydroxyphenylalanine (meta-tyrosine or mTyr), homotyrosine (hTyr), L-DOPA, 4-methylphenylalanine (4-Me-Phe), 4-fluoro-phenylalanine (4-F-Phe), 2,4,6-F_3-phenylalanine (F_3-Phe), 2,3,4,5,6-F_5-phenylalanine (F_5-Phe), 4-methoxyphenylalanine (4-MeO-Phe), and cyclohexylalanine (Cha).

Current traces from a typical dose-response experiment (4-F-Phe at position 234) are shown in Figure 3.2. Although there were changes in the EC_{50} values and Hill coefficients for some mutant receptors (see below), activation and desensitization kinetics were similar to wild type for all receptors incorporating unnatural amino acids that responded to 5-HT.

3.1.3 Tyr 141

Incorporation of Phe, mTyr, 4-F-Phe, 4-MeO-Phe, F_5-Phe, and Cha using nonsense suppression mutagenesis and substitution by the natural amino acids Ala, Ser, and Phe using standard mutagenesis techniques produced receptors that responded to

5-HT in a manner very similar to wild-type 5-HT_{3A}R (Figure 3.3, Table 3.1 and Table 3.3). These data therefore show that neither the aromatic nor the hydroxyl groups are important for agonist binding or receptor gating. However, this residue has been implicated in antagonist binding because changes in affinity of 5-HT_3R antagonists have been observed when this residue was substituted with a non-aromatic amino acid.[12, 13] Thus, Tyr141Ala receptors have decreased [^{3}H]granisetron, D-tubocurarine, and lerisetron binding affinity compared with wild-type receptors, whereas Tyr141Ser receptors do not bind [^{3}H]granisetron at all. The model of the 5-HT_3R binding site (Figure 3.5) [based on model 4 of reference #8] supports these data, because Tyr 141 could contact these larger antagonists, but is not close enough to be in direct contact with a bound 5-HT molecule.[8]

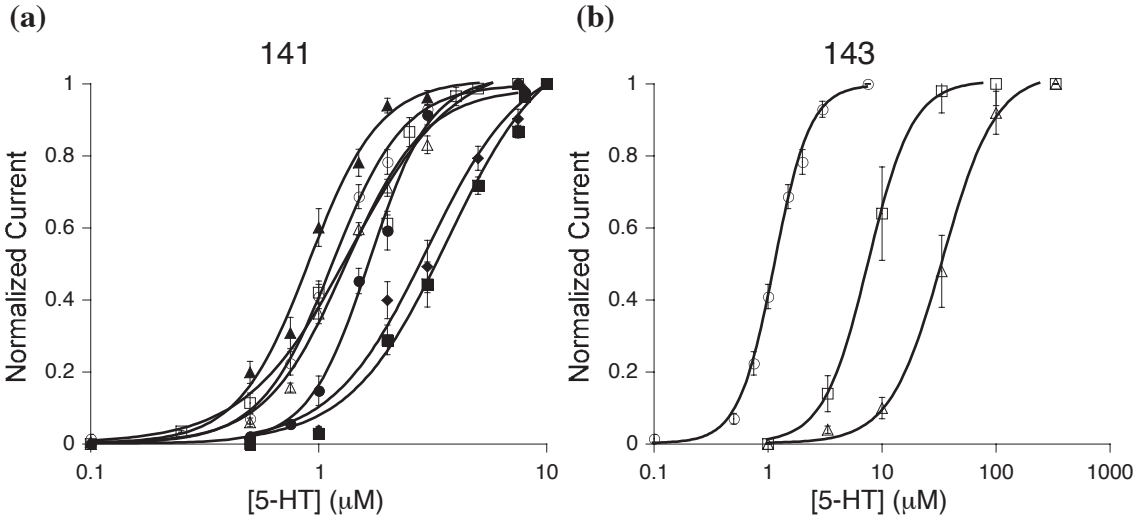

Figure 3.3. Dose-response relations for 5-HT_{3A}R nonsense suppression experiments. (a) Suppression at position 141: Tyr (*open circles*), mTyr (*filled circles*), 4-Me-Phe (*filled squares*), Phe (*filled triangles*), 4-F-Phe (*open triangles*), F_5Phe (*open squares*), and Cha (*filled diamonds*). (b) Suppression at position 143: Tyr (*open circles*), hTyr (*open triangles*), and DOPA (*open squares*).

In previous studies, Tyr141Ala and Tyr141Ser receptors did not function when expressed in human embryonic kidney 293 cells.[12, 13] However, our data show they have

similar characteristics to wild-type receptors when expressed in oocytes. Oocytes are generally more tolerant than mammalian cells to expression of ion channel proteins, which may require longer periods to fold correctly, the difference perhaps arising from the fact that oocytes are incubated at lower temperatures which would favor complex multisubunit assemblies.[17] These data therefore suggest a role for this residue in correct receptor folding and/or assembly, perhaps locally in the binding-site region.

3.1.4 Tyr 143

Data from Tyr 143 mutant receptors suggest that an aromatic ring with a hydroxyl group at the 4 position is essential for efficient receptor function. DOPA, which has these groups, was the only substitution at 143 that produced receptors with less than a 10-fold increase in EC_{50}. Incorporation of even subtle changes such as 4-F-Phe, 4-MeO-Phe, and mTyr resulted in receptors that did not respond to 5-HT (Table 3.1). DOPA also has a hydroxyl at the 3 position, and the increase in EC_{50} observed with this compound (approximately sixfold) suggests that bulk here is not desirable. An increased chain length or removal of the hydroxyl, however, is more deleterious. Phe and hTyr caused 30- to 40-fold increases in EC_{50}. Removal of the aromatic group and/or further displacement of the hydroxyl group as in replacement with Ala or Ser resulted in even more severe changes: 100-fold EC_{50} increases. In addition, changes in apparent activation and desensitization rates (10–90% rise times were twofold to fourfold slower than wild-type receptors) (Table 3.3), and little or no desensitization were observed. These data demonstrate the importance of both the aromatic and the hydroxyl group of Tyr 143, and in particular, suggest that the hydroxyl forms a hydrogen bond that is essential for efficient receptor gating.

To confirm the presence of such a bond would require x-ray crystal structural data which unfortunately, is not available. However, mutagenesis data alone can provide strong evidence, particularly when there is some supporting structural data such as a homology model.[18] Indeed, the unnatural amino acid methodology employed here is a much more powerful probe for this type of bond than conventional mutagenesis because not only can we introduce subtle changes that minimally perturb the global protein structure, but also design the amino acid to determine whether the residue acts as a hydrogen bond donor or acceptor. Thus, using conventional mutagenesis, we can remove the hydroxyl at position 143 (in Phe), but not replace it. Ser is unsatisfactory as a replacement because hydrogen bonds depend critically on the distance between donor and acceptor atoms, and the hydroxyls of Ser and Tyr are in quite distinct locations. Unnatural amino acid substitution can surmount this problem; DOPA has a similarly placed hydroxyl to Tyr, whereas 4-MeO-Phe places an oxygen atom in the same location, and the hydroxyl of hTyr is only subtly displaced from that of Tyr. Data from these substitutions support the proposal of a hydrogen bond at Tyr 143 and indeed, further suggest that the hydroxyl here acts as a hydrogen bond donor.

The model of 5-HT docked into the 5-HT_{3A}R extracellular domain (Figure 3.5) shows that the hydroxyl of Tyr 143 has the potential to hydrogen bond with one of a number of residues on the opposite side of the binding pocket. These are the hydroxyl or the ring of Tyr 234 and the carbonyl oxygen of Trp 183 or Leu 184, all of which are 3Å away. The fact that 4-Me-Phe could substitute satisfactorily for Tyr 234 suggests that there is no such bond between the hydroxyls of Tyr 143 and Tyr 234, but as yet, we cannot exclude any of the other possibilities. Of course, the accuracy of the inter-residue

distances must be viewed with caution both because of the problems inherent with using a model based on a homologous structure, and because in the docking procedure, the protein side chains remain rigid, which is certainly not the case in the functioning receptor. Nevertheless, the modeling data suggest that the most probable hydrogen bonding partner of Tyr 143 is the backbone carbonyl of Trp 183— an interaction that has also been previously suggested.[19]

The presence of either an aromatic or a hydroxyl at position 143, however, is not essential for antagonist interactions: alanine, serine, and phenylalanine mutants of Tyr 143 bound [^{3}H]granisetron with an affinity similar to wild-type receptors (Table 3.3).[12, 13] Competitive antagonists such as granisetron bind in the binding pocket, but cannot trigger the conversion to the open state. These data, combined with the modeling data, thus suggest that neither an aromatic group nor a hydrogen bond is required for ligand binding, but both are essential for efficient receptor gating.

3.1.5 Tyr 153

Large increases in EC_{50} values, modifications in receptor kinetics, and changes in [^{3}H]granisetron binding affinity (Figure 3.4, Table 3.2 and Table 3.3) in mutant receptors suggest that Tyr 153 plays a role in both binding and gating of the receptor. The data show that both an aromatic ring and a hydroxyl group in the 4 position are required for correct receptor function. Removing (Ala, Ser) or drastically perturbing (F_5Phe) the aromatic ring resulted in 100-fold increases in EC_{50},. Deleting the tyrosine hydroxyl group (Phe) or replacing it (4-F-Phe or 4-Me-Phe) led to ~20-fold increases in EC_{50}, and relocating it (mTyr and Ser) resulted in 100-fold EC_{50} increases. However, 4-MeO-Phe increased EC_{50} only sixfold, indicating that the importance of the hydroxyl is via its

oxygen atom. These data strongly indicate the presence of a hydrogen bond with the hydroxyl of Tyr153 functioning as a hydrogen bond acceptor.

Table 3.1 Dose-response data for suppression at positions 141 and 143

Residue	141		143	
	EC_{50}±SEM (μM)	**Hill±SEM**	**EC_{50}±SEM (μM)**	**Hill±SEM**
Tyr	1.16 ± 0.04	2.76 ± 0.20	1.15 ± 0.03	2.98 ± 0.19
Phe	0.92 ± 0.06	2.80 ± 0.44	78.6 ± 2.86	2.73 ± 0.21
4-MeO-Phe	3.36 ± 0.14	2.17 ± 0.16	NR	NR
4-F-Phe	1.32 ± 0.05	2.47 ± 0.17	NR	NR
F_5-Phe	1.38 ± 0.08	1.89 ± 0.17	NA	NA
Cha	3.14 ± 0.40	1.92 ± 0.21	NA	NA
mTyr	1.69 ± 0.06	3.24 ± 0.29	NR	NR
hTyr	NA	NA	33.24 ± 2.60	1.80 ± 0.22
DOPA	NA	NA	7.16 ± 0.90	2.34 ± 0.54

NA = not attempted, NR = no response to concentrations up to 1 mM 5-HT

Table 3.2 Dose-response data for suppression at positions 153 and 234

Residue	153		234	
	EC_{50}±SEM (μM)	**Hill±SEM**	**EC_{50}±SEM (μM)**	**Hill±SEM**
Tyr	1.15 ± 0.04	2.78 ± 0.20	1.24 ± 0.05	2.89 ± 0.28
Phe	22.5 ± 0.43	2.60 ± 0.11	10.22 ± 0.80	1.92 ± 0.26
4-MeO-Phe	6.65 ± 0.27	1.98 ± 0.12	NA	NA
4-F-Phe	19.7 ± 1.22	1.82 ± 0.14	4.11 ± 0.20	2.36 ± 0.19
4-Br-Phe	NA	NA	1.78 ± 0.08	2.79 ± 0.32
4-Me-Phe	18.2 ± 0.48	2.48 ± 0.11	1.13 ± 0.05	2.49 ± 0.22
F_3-Phe	NA	NA	NR	NR
F_5-Phe	(>500)		NR	NR
Cha	NA	NA	NR	NR
mTyr	(>500)		7.42 ± 0.32	2.83 ± 0.32

NA = not attempted, NR = no response to concentrations up to 1 mM 5-HT

In the homology model, this hydroxyl is located such that it could participate in a hydrogen bond interaction, either with the 5-HT indole nitrogen (2.9 Å away) or with Arg 92 (3.1 Å). Arg 92— like Tyr 153— is located on the subunit "inner loop," which is

proposed to move relative to the "outer loop" after receptor activation.[3] Because the relative movement of the two residues during channel opening would therefore be negligible, it is unlikely that removing a hydrogen bond here would result in the changes that we observed. It therefore seems plausible that Tyr 153 hydrogen bonds to 5-HT.

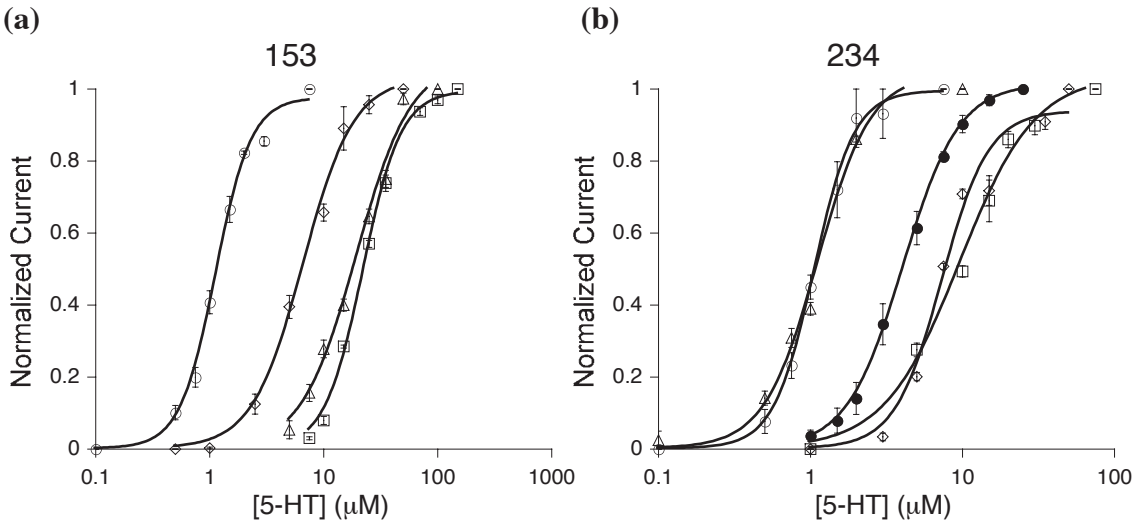

Figure 3.4. Dose-response relations for 5-HT_{3A}R nonsense suppression experiments. (a) Suppression at position 153: Tyr (*open circles*), Phe (*open squares*), 4-F-Phe (*open triangles*), and 4-MeO-Phe (*open diamonds*). (b) Suppression at position 234: Tyr (*open circles*), mTyr (*open diamonds*), Phe (*open squares*). 4-F-Phe (*filled circles*), and 4-Me-Phe (*open triangles*).

3.1.6 Tyr 234

Replacement of tyrosine at this position with Phe, 4-F-Phe, mTyr, and 4-Me-Phe produced receptors for which EC_{50} values for 5-HT activation were either unchanged or increased only 10-fold compared with wild-type receptors (Figure 3.4, Table 3.2). Thus, the hydroxyl group of Tyr 234 is not essential for correct receptor function. Indeed, the equivalent residue here in the guinea pig 5-HT_3R is Phe.[20] The electrostatic potential of the aromatic group here, however, does seem important. Replacement with Cha, Ala or Ser resulted in nonfunctional receptors. In many ways Cha is an ideal mutation for

examining the importance of aromatic character. It is nearly isosteric with Phe and maintains very similar shape and hydrophobicity, but cannot participate in any of the special aromatic interactions (cation-π, CH-π, or aromatic-aromatic). Thus, its non-viability at this site does suggest a role for the aromatic character of Tyr.

The potential importance of the aromatic group is supported by the results with 4-F-Phe and F_5-Phe. Here, a single fluorine substituent (4-F-Phe) caused a small increase in EC_{50}, and multiple fluorine substituents (F_5-Phe) resulted in nonfunctional receptors. Substitution of the aromatic group with electron-withdrawing groups pulls electron density away from the face of the aromatic ring, thereby disrupting the special aromatic interactions listed above. The data, however, are not consistent with a cation-π interaction at 234. Phe— which displays a similar affinity as Tyr in binding cations— leads to an eightfold increase in EC_{50}, but 4-F-Phe and 4-Br-Phe— both of which would almost equally weaken any cation-π interaction, lead to roughly 1.5- and 3-fold increases, respectively in EC_{50}. These results are not consistent with a cation-π interaction at 234, which is interesting because in the model (Figure 3.5), this residue has the potential to interact with the primary ammonium of 5-HT. Thus, these results provide experimental feedback for improving the homology model.

The pattern of EC_{50} values for unnatural amino acid substitution at 234 is consistent with bulk at the 4 position of the aromatic ring being required for correct receptor function. Those residues with a substituent at the 4 position (4-Me-Phe, 4-Br-Phe, and 4-F-Phe) give lower EC_{50} values than those without (Phe, mTyr). Such a finding was reported for the aligning residue (Tyr198) in the nAChR[21], where a larger number of unnatural residues were tested. The size of this substituent also appeared to be

important, with larger substituents not being tolerated and smaller ones also being less favored, suggesting a steric role.

Table 3.3 Conventional mutagenesis studies: dose-response data, [^{3}H]granisetron binding affinities, and 10-90% rise times for current onset

Residue	EC_{50}±SEM (μM)	Hill±SEM	K_d (nM)	Rise time (s)
Wild type (Y)	1.34 ± 0.12	2.38 ± 0.23	0.32 ± 0.035	2.1 ± 0.3
141				
Ala	2.73 ± 0.15	2.68 ± 0.4	8.97 ± 2.44	2.4 ± 0.2
Ser	4.7 ± 0.38	2.02 ± 0.31	NB	2.4 ± 0.3
Phe	ND	ND	0.98 ± 0.15	ND
143				
Ala	354 ± 29.0	2.62 ± 0.53	1.2 ± 0.24	7.9 ± 0.5
Ser	472 ± 47.9	2.68 ± 0.62	1.1 ± 0.23	8.4 ± 0.8
Phe	78.6 ± 2.86	2.73 ± 0.21	0.53 ± 0.10	4.5 ±1.0
153				
Ala	120 ± 9.43	2.43 ± 0.38	3.62 ± 1.75	8.3 ± 0.7
Ser	84.1 ± 5.60	2.54 ± 0.37	NB	8.1 ± 0.4
Phe	ND	ND	0.53 ± 0.10	ND

ND = No data, NB = No binding

3.1.7 A new model of the 5-HT binding pocket

The new data strongly support previous suggestions by the Lummis group arising from their modeling studies that the correct orientation of 5-HT in the binding pocket is with the ammonium group located between Trp 183 and Tyr 234. In addition, the data are consistent with hydrogen bonds between Tyr 143 and Trp 183, and Tyr 153 and 5-HT (Figure 3.5). The Lummis group also created a new "closed state" model based on the structural work by Unwin and coworkers.[3] Unwin's data indicate differences in the binding pocket between the closed state of the nAChR and AChBP (which is considered to be closer to the open or desensitized state). In the closed state model, Tyr 143 and 153 are 3 Å closer to the center of the pocket, and clashes between these residues and 5-HT

indicate that binding of this agonist in the orientation supported by the experimental data is not possible (Figure 3.6). Antagonist binding, however, would not be affected. Thus, if we assume that similar movements in the binding pocket occur in the nACh and 5-HT_3 receptors, and that the new model provides a reasonable approximation of the closed state of the receptor, then Tyrs 143 and 153 would need to be displaced to allow 5-HT to dock into the binding site (Figure 3.6).

3.3 Discussion

The *in vivo* nonsense suppression method of unnatural amino acid incorporation is a powerful tool for the investigation of receptor structure-function relationships. Using a selection of tyrosine analogs, we show that tyrosines located in or close to the receptor binding pocket each play a different role in receptor function and do not simply provide a featureless extended aromatic environment. Tyr 141 does not appear to be a critical site, as the various mutations introduced here had little effect. Tyr 143 and Tyr 153, however, are important sites for receptor function, and the results for substitution at these sites indicate that the hydroxyls of these tyrosines form functionally necessary hydrogen bonds. At Tyr 234 we find that both the aromatic group and an appropriately sized substituent at the 4 position of the ring are important. These data, combined with previous work from the Dougherty group elucidating the cation-π interaction between Trp 183 and the ammonium group of 5-HT[11], have provided insight into the correct orientation of 5-HT in a homology model of the 5-HT_3R binding site. In addition, findings from the present study, along with a new closed state model of the 5-HT_3R, suggest a possible series of bond rearrangements in the binding site that are required for

gating, and thus may represent early conformational changes that lead to channel opening.

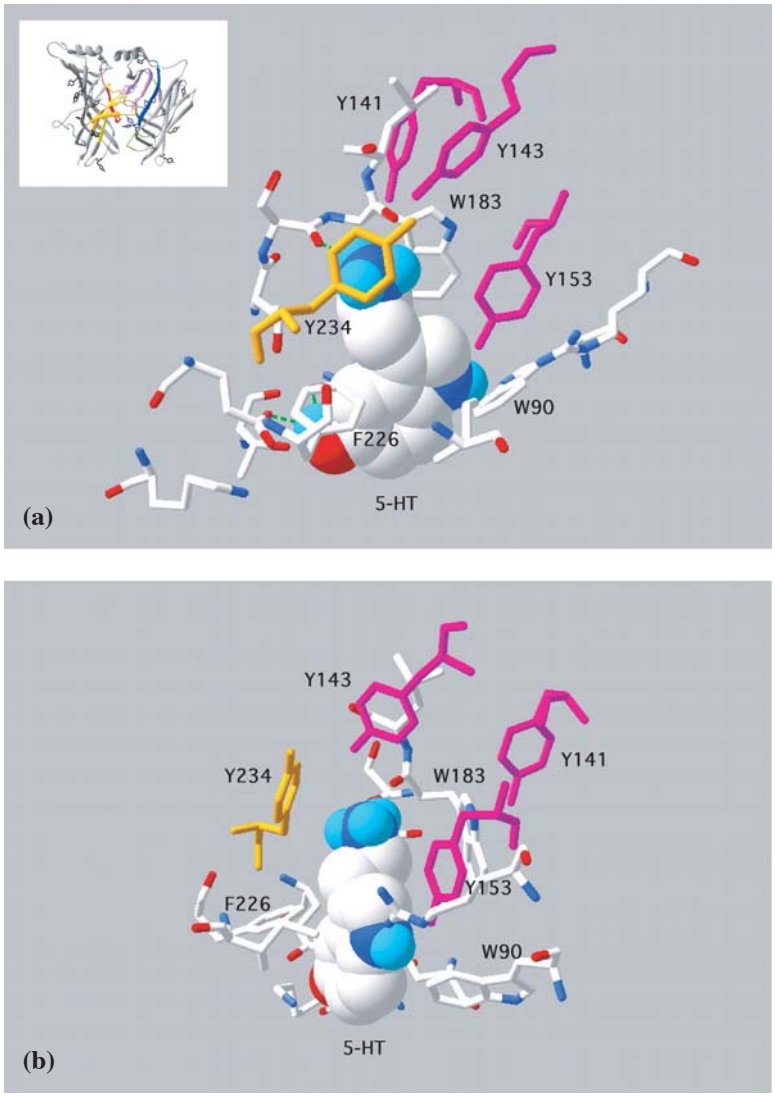

Figure 3.5. Model showing two views of 5-HT docked into the 5-HT3A receptor binding site. This is based on model 4 of reference #8 (Reeves et al. (2003)). Tyrosine residues considered here are shown in purple for loop E (141, 143, 153) and orange for loop C (234,). Docked 5-HT is shown in CPK, with the primary ammonium group sandwiched between Trp183 where there is a cation- interaction and Tyr234. The indole nitrogen abuts the Tyr153 side chain. Other binding site residues are labeled.

3.1.1 Roles of 5-HT$_3$R binding-site tyrosine residues

Tyr 141 does not play a critical role in 5-HT$_3$R agonist binding or gating, but it may be involved in antagonist binding and receptor assembly. The recent structure of AChBP bound to agonists shows that the residue equivalent to Tyr141 (Leu 102) hydrogen bonds to nicotine via a water molecule.[22] In the homology model of the 5-HT$_3$R, Tyr 141 does not contact 5-HT (and indeed in AChBP, residue Leu 102 does not contact carbachol), but this does not preclude from it interacting with larger antagonists and/or to another residue in the binding pocket, perhaps during subunit folding to assist its correct formation.

Tyr 143 is a sensitive residue in that it can only be replaced by a limited number of alternative amino acids to form functional receptors. Data from these mutant receptors (no change in [^{3}H]granisetron binding affinity and a large change in EC$_{50}$) combined with the modeling data (no interaction with 5-HT) strongly suggest that Tyr 143 forms a hydrogen bond between two regions of the receptor that is essential for receptor gating. The modeling data further suggest that this bond may be between the hydroxyl group and the backbone carbonyl group of Trp 183, which has been previously suggested by Maksay et al.[19] Previous data have also shown the importance of this residue in 5-HT$_3$R function[13], and the equivalent residue in AChBP (Arg 104) has been shown to make contact with carbachol.[22]

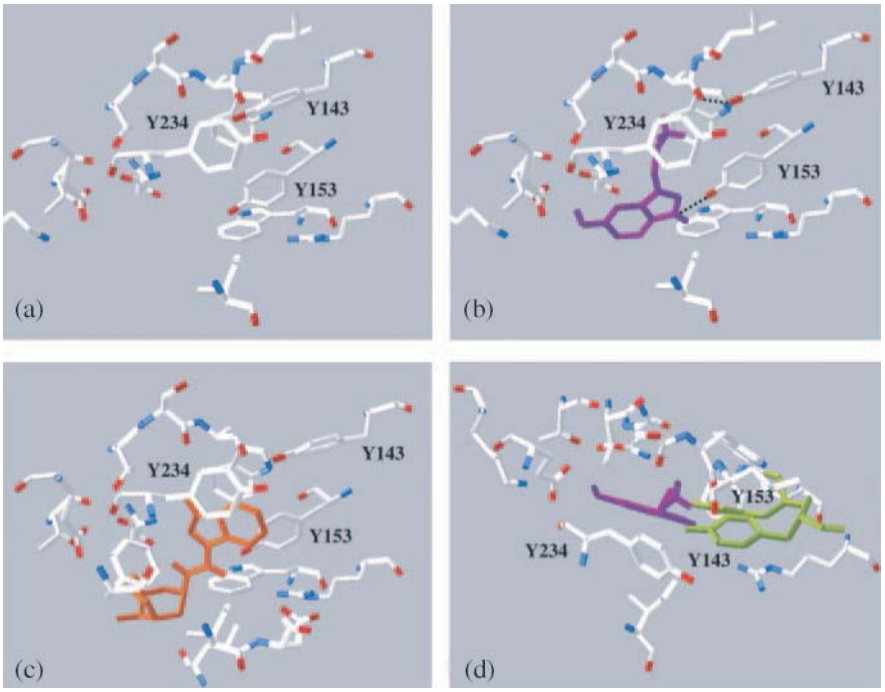

Figure 3.6. (a) Model of the 5-HT_3R binding site in the closed state; Tyr 143 and Tyr 153 are 3 Å closer to the center of the pocket than in the open state model. (b) Model of the 5-HT_3R binding site in the open state with 5-HT (purple) docked, showing potential new hydrogen bonds formed by Tyr143 and Tyr153. (c) Model of the 5-HT_3R binding site in the open state with granisetron (orange). Granisetron, however, is most likely to bind to the closed state and, thus, there may be some inaccuracies in this model. Nevertheless, granisetron in this orientation would fit into the closed state model, where it would be within 3Å of Tyr 153 but further from Tyr 143. (d) Rotated model *a* with 5-HT (purple) docked in the same position as in *b*. Steric interference with Tyr 143 and Tyr153 (both green) would not allow 5-HT to be docked in this position.

The data also strongly suggest that Tyr 153 forms a hydrogen bond, and that this bond plays a role in both binding and gating. The equivalent residue in AChBP (Met 114) makes contact with both carbachol and nicotine[22], and data from other studies also suggest that it is involved in gating. Tyr153Ala mutant receptors display unusual response and desensitization kinetics[13], and mutation of the aligning residue in the $GABA_A$ receptor α-subunit (Thr 142) resulted in the antagonist flumazenil acting as a partial agonist.[23] Interestingly, the equivalent residue in the 5-HT_{3B} subunit is histidine.[24]

Thus, heteromeric (A plus B) receptors would also have a residue with the potential to hydrogen bond in the binding site at this position.

Thus, our data show that the hydrogen bonds formed by Tyr 143 and Tyr 153 are critical for correct receptor function, suggesting these bonds play an important role in the conformational change leading to gating. This could be because they stabilize the bound state of the receptor and/or provide the energy required for protein rearrangement.

An aromatic residue at position 234 is essential for 5-HT_3R function. Indeed, conservation of an aromatic residue at the aligning position among all 5-HT_3R subunits— and in fact all Cys-loop receptors— indicates the importance of this aromatic group which appears to play a vital role as part of the "aromatic box" proposed to be critical for agonist binding in all members of this LGIC family.[25] However, a substituent at the 4 position appears to be important solely for gating because antagonist binding is unaffected by removal of the Tyr 234 hydroxyl, and the docking data suggest that there is no interaction between this group and 5-HT.[8] The effect is steric because hydroxyl and bromine which have similar sizes yield optimum function, whereas smaller substituents such as fluorine and hydrogen are less effective.

3.1.2 A model for initiating gating

The differences observed between AChBP x-ray crystal data and nAChR cryo-electron microscopy data suggest that AChBP better represents the open rather than the closed state of the receptor.[3] Thus, the docking of 5-HT into the homology model of the 5-HT_3R binding site as shown in Figure 3.5 is likely to be broadly accurate, whereas removal of 5-HT from this structure would not be a good representation of the closed state. Data from Unwin and coworkers show that in this region, the residues

equivalent to Tyr 143 and Tyr 153 are closer to the residues equivalent to Trp 183 and Tyr 234 in the unbound (closed state) nAChR compared with AChBP (open-like state).[3] These changes in distance are likely to be only a few ångstroms, because the binding site is close to the point around which the inner and outer loops of the subunit pivot. Shown in Figure 3.6 is a homology model of the 5-HT_3R binding site in the closed state based on Unwin's data. Here, both Tyr 143 and Tyr 153 are 3 Å closer to the center of the binding pocket. We propose that 5-HT entering the pocket forms a cation-π interaction with Trp 183 and in so doing, displaces Tyr 143. The hydroxyl of Tyr 234 ensures that Tyr 143 moves toward and subsequently, hydrogen bonds with the backbone carbonyl of Trp 183 and not with another E loop residue, as might be the case if formation of the alternative rotamer was not prevented by the 234 hydroxyl group. Tyr 153 is also relocated as 5-HT enters the pocket, assisted by the hydrogen bond it forms with the indole amine on 5-HT. These two residues (Tyr 143 and Tyr 153) are located on separate β-sheets linked by a turn and therefore, their combined movement could provide considerable torsional force. Combined with energy provided by the formation of hydrogen and other bonds, this could initiate the twist that triggers the conformational change.

Some support for this hypothesis comes from docking studies with the 5-HT_3R antagonist granisetron, which when bound does not induce the conformational changes associated with receptor gating. A recent report by Maksay and coworkers suggests that granisetron docked into a homology model of the 5-HT_3R binding site does not approach Tyr 143, but does come relatively close to Tyr 153 and interacts strongly with the aromatic group of Tyr 234.[19] Docking studies performed by the Lummis group (unpublished observations) similarly reveal potential interactions of granisetron with

Tyr 234 and Tyr 153, but not with Tyr 143. One orientation of granisetron that was observed, and is similar to that reported by Maksay and coworkers is shown in Figure 3.5. Granisetron in this orientation would also fit comfortably into the closed state model, and indeed, it may hydrogen bond with the hydroxyl of Tyr 153 (3 Å distant) in this model.

Additional support comes from reports of movement in the nAChR binding site[2, 3, 26] and in the $GABA_A$ receptor[27], which is likely to be similar in all Cys-loop receptors. However this has not yet been confirmed as no ligand–free atomic resolution structure of AChBP has yet been resolved.

3.4 Conclusion

In summary, the data obtained from introducing subtle changes to tyrosine residues in the 5-HT_3R binding site— combined with those obtained from models of the binding pocket— have shown distinct roles of each of these residues in the binding site. Combining these data with those from a model of the binding pocket has allowed us to generate a hypothesis of the mechanism that triggers the conformational change leading to channel opening. The data therefore show the power of unnatural amino acid mutagenesis in providing high-precision information that is highly complementary to modeling efforts. In addition, given the structural and functional similarity of ligand-gated ion channels, we believe the proposed mechanism of conformation change (agonist-stimulated movement of the binding loops combined with the formation of novel hydrogen bonds) will be broadly similar in all members of the family.

3.5 Methods

3.5.1 Mutagenesis and preparation of cRNA and Oocytes

Mutant 5-HT_{3A}R subunits were developed using the eukaryotic expression vector, pcDNA 3.1 (InVitrogen, Abingdon, U.K.), containing the complete coding sequence for the 5-$HT_{3A(B)}$ subunit from NIE-115 cells as previously described.[28] Mutagenesis reactions were performed using the Kunkel method[29] and confirmed by DNA sequencing. Wild type (WT) and mutant receptor subunit coding sequences were then subcloned into pGEMHE plasmid.[16] This was linearized with Nhe1 (New England Biolabs) and cRNA synthesized using T7 mMESSAGE mMACHINE kit (Ambion). Oocytes from *Xenopus laevis* were prepared and maintained as described previously.[11]

3.5.2 Synthesis of tRNA and dCA-amino acids

Unnatural amino acids were chemically synthesized as nitroveratryloxycarbonyl (NVOC) protected cyanomethyl esters and coupled to the dinucleotide dCA, which was then enzymatically ligated to 74-mer THG73 $tRNA_{CUA}$ as detailed previously.[30] Immediately prior to co-injection with mRNA, tRNA-aa was deprotected by photolysis.[31] Typically, 5 ng mRNA and 25 ng tRNA-aa were injected into Stage V-VI oocytes in a total volume of 50 nl. For control experiments, mRNA was injected 1) in the absence of tRNA and 2) with the THG73 74-mer tRNA. Experiments were preformed 18-36 h post injection.

3.5.3 Characterization of mutant receptors

5-HT-induced currents were recorded from individual oocytes using two-electrode voltage clamp with either a GeneClamp 500 amplifier or an OpusXpress system

(Axon Instruments, Inc., Union City, CA). All experiments were performed at 22-25° C. Serotonin (creatinine sulphate complex, Sigma) was stored as 25 mM aliquots at -80°C, diluted in calcium-free ND96, and delivered to cells via computer-controlled perfusion systems. Glass microelectrodes were backfilled with 3 M KCl and had a resistance of approximately 1 MΩ. The holding potential was -60 mV unless otherwise specified. To determine EC_{50}s, 5-HT concentration-response data were fitted to the Hill equation, $I = (I_{max}[A]^n)/(EC_{50}^n + [A]^n)$, where I_{max} is the maximal peak current, [*A*] is the concentration of agonist, and n is the Hill coefficient.

3.6 References

1. Brejc, K.; van Dijk, W. J.; Klaassen, R. V.; Schuurmans, M.; van der Oost, J.; Smit, A. B.; Sixma, T. K., Crystal structure of an ACh-binding protein reveals the ligand-binding domain of nicotinic receptors. *Nature* 2001, 411, (6835), 269-276.
2. Miyazawa, A.; Fujiyoshi, Y.; Unwin, N., Structure and gating mechanism of the acetylcholine receptor pore. *Nature* 2003, 423, (6943), 949-955.
3. Unwin, N.; Miyazawa, A.; Li, J.; Fujiyoshi, Y., Activation of the nicotinic acetylcholine receptor involves a switch in conformation of the a subunits. *Journal of Molecular Biology* 2002, 319, (5), 1165-1176.
4. Unwin, N., Structure and action of the nicotinic acetylcholine receptor explored by electron microscopy. *Febs Letters* 2003, 555, (1), 91-95.
5. Unwin, N., The Croonian Lecture 2000. Nicotinic acetylcholine receptor and the structural basis of fast synaptic transmission. *Philosophical Transactions of the Royal Society of London Series B-Biological Sciences* 2000, 355, (1404), 1813-1829.
6. Miyazawa, A.; Fujiyoshi, Y.; Stowell, M.; Unwin, N., Nicotinic acetylcholine receptor at 4.6 angstrom resolution: Transverse tunnels in the channel wall. *Journal of Molecular Biology* 1999, 288, (4), 765-786.
7. Le Novere, N.; Grutter, T.; Changeux, J. P., Models of the extracellular domain of the nicotinic receptors and of agonist- and Ca2+-binding sites. *Proceedings of the National Academy of Sciences of the United States of America* 2002, 99, (5), 3210-3215.
8. Reeves, D. C.; Sayed, M. R. F.; Chau, P. L.; Price, K. L.; Lummis, S. C. R., Prediction of 5-HT3 receptor agonist-binding residues using homology modeling. *Biophysical Journal* 2003, 84, (4), 2338-2344.
9. Schapira, M.; Abagyan, R.; Totrov, M., Structural model of nicotinic acetylcholine receptor isotypes bound to acetylcholine and nicotine. *BMC Struct. Biol.* 2002, 2, (1), 1.
10. Cromer, B. A.; Morton, C. J.; Parker, M. W., Anxiety over GABA(A) receptor structure relieved by AChBP. *Trends in Biochemical Sciences* 2002, 27, (6), 280-287.
11. Beene, D. L.; Brandt, G. S.; Zhong, W. G.; Zacharias, N. M.; Lester, H. A.; Dougherty, D. A., Cation-pi interactions in ligand recognition by serotonergic (5-HT3A) and nicotinic acetylcholine receptors: The anomalous binding properties of nicotine. *Biochemistry* 2002, 41, (32), 10262-10269.
12. Price, K. L.; Lummis, S. C. R., The role of tyrosine residues in the extracellular domain of the 5-hydroxytryptamine(3) receptor. *Journal of Biological Chemistry* 2004, 279, (22), 23294-23301.

13. Venkataraman P, V. S., Joshi Pr, Muthalagi M, Schulte MK, Identification of critical residues in Loop E in the 5-HT_{3AS}R binding site. *BMC Biochem* 2002, 3, (15).
14. Nowak, M. W.; Kearney, P. C.; Sampson, J. R.; Saks, M. E.; Labarca, C. G.; Silverman, S. K.; Zhong, W.; Thorson, J.; Abelson, J. N.; Davidson, N.; Schultz, P. G.; Dougherty, D. A.; Lester, H. A., Nicotinic Receptor-Binding Site Probed with Unnatural Amino-Acid-Incorporation in Intact-Cells. *Science* 1995, 268, (5209), 439-442.
15. Nowak, M. W.; Gallivan, J. P.; Silverman, S. K.; Labarca, C. G.; Dougherty, D. A.; Lester, H. A., In vivo incorporation of unnatural amino acids into ion channels in Xenopus oocyte expression system. In *Ion Channels, Pt B*, 1998; 293, 504-529.
16. Liman, E. R.; Tytgat, J.; Hess, P., Subunit Stoichiometry of a Mammalian K+ Channel Determined by Construction of Multimeric Cdnas. *Neuron* 1992, 9, (5), 861-871.
17. Denning, G. M.; Anderson, M. P.; Amara, J. F.; Marshall, J.; Smith, A. E.; Welsh, M. J., Processing of Mutant Cystic-Fibrosis Transmembrane Conductance Regulator Is Temperature-Sensitive. *Nature* 1992, 358, (6389), 761-764.
18. Grutter, T.; de Carvalho, L. P.; Le Novere, N.; Corringer, P. J.; Edelstein, S.; Changeux, J. P., An H-bond between two residues from different loops of the acetylcholine binding site contributes to the activation mechanism of nicotinic receptors. *Embo Journal* 2003, 22, (9), 1990-2003.
19. Maksay, G.; Bikadi, Z.; Simonyi, M., Binding interactions of antagonists with 5-hydroxytryptamine(3A) receptor models. *Journal of Receptors and Signal Transduction* 2003, 23, (2-3), 255-270.
20. Lankiewicz, S.; Lobitz, N.; Wetzel, C. H. R.; Rupprecht, R.; Gisselmann, G.; Hatt, H., Molecular cloning, functional expression, and pharmacological characterization of 5-hydroxytryptamine(3) receptor cDNA and its splice variants from guinea pig. *Molecular Pharmacology* 1998, 53, (2), 202-212.
21. Kearney, P. C.; Nowak, M. W.; Zhong, W.; Silverman, S. K.; Lester, H. A.; Dougherty, D. A., Agonist binding site of the nicotinic acetylcholine receptor: Tests with novel side chains and with several agonists. *Molecular Pharmacology* 1996, 50, (5), 1401-1412.
22. Celie, P. H. N.; van Rossum-Fikkert, S. E.; van Dijk, W. J.; Brejc, K.; Smit, A. B.; Sixma, T. K., Nicotine and carbamylcholine binding to nicotinic acetylcholine receptors as studied in AChBP crystal structures. *Neuron* 2004, 41, (6), 907-914.
23. Mihic, S. J.; Whiting, P. J.; Klein, R. L.; Wafford, K. A.; Harris, R. A., A Single Amino-Acid of the Human Gamma-Aminobutyric-Acid Type-a Receptor Gamma(2) Subunit Determines Benzodiazepine Efficacy. *Journal of Biological Chemistry* 1994, 269, (52), 32768-32773.
24. Hanna, M. C.; Davies, P. A.; Hales, T. G.; Kirkness, E. F., Evidence for expression of heteromeric serotonin 5-HT3 receptors in rodents. *Journal of Neurochemistry* 2000, 75, (1), 240-247.
25. Mu, T. W.; Lester, H. A.; Dougherty, D. A., Different binding orientations for the same agonist at homologous receptors: A lock and key or a simple wedge? *Journal of the American Chemical Society* 2003, 125, (23), 6850-6851.
26. Chakrapani, S.; Bailey, T. D.; Auerbach, A., Gating dynamics of the acetylcholine receptor extracellular domain. *Journal of General Physiology* 2004, 123, (4), 341-356.
27. Wagner, D. A.; Czajkowski, C., Structure and dynamics of the GABA binding pocket: A narrowing cleft that constricts during activation. *Journal of Neuroscience* 2001, 21, (1), 67-74.
28. Hargreaves, A. C.; Gunthorpe, M. J.; Taylor, C. W.; Lummis, S. C. R., Direct inhibition of 5-hydroxytryptamine(3) receptors by antagonists of L-type Ca2+ channels. *Molecular Pharmacology* 1996, 50, (5), 1284-1294.
29. Kunkel, T. A., Rapid and Efficient Site-Specific Mutagenesis without Phenotypic Selection. *Proceedings of the National Academy of Sciences of the United States of America* 1985, 82, (2), 488-492.
30. Nowak, M. W.; Gallivan, J. P.; Silverman, S. K.; Labarca, C. G.; Dougherty, D. A.; Lester, H. A., In vivo incorporation of unnatural amino acids into ion channels in Xenopus oocyte expression system. *Methods Enzymol* 1998, 293, 504-29.
31. Kearney, P. C.; Nowak, M. W.; Zhong, W.; Silverman, S. K.; Lester, H. A.; Dougherty, D. A., Dose-response relations for unnatural amino acids at the agonist binding site of the nicotinic acetylcholine receptor: tests with novel side chains and with several agonists. *Mol Pharmacol* 1996, 50, (5), 1401-12.

Chapter 4. Conserved prolines in the M2-M3 loop

4.1 Introduction

Ligand-gated ion channels (LGIC) are highly dynamic proteins, undergoing multiple conformational transitions among various states. Their primary function is to transduce a chemical signal— binding of a small molecule— into an electrical signal— ion flux across the cell membrane. They accomplish this feat through a global reorganization of their quaternary structure. Agonist binding to these proteins initiates a series of conformational changes resulting in the opening of an ion permeant channel across the cell membrane. This process, linking agonist binding to the open conductance state of the receptor, is termed gating.[1-3] From a molecular perspective, this represents a fairly amazing process. The agonist-binding site and channel gate are separated by almost 50 Å and nearly 100 amino acids of the protein's primary sequence. Thus, the number of steric and noncovalent interactions driving this conformational transition is significantly greater than that traditionally considered in the conformational analysis of organic molecules. Although advances in areas such as molecular dynamics have certainly broadened the theoretical framework necessary for conformational analysis on this scale, molecular details of the gating process still remain poorly understood.

Study of the gating process in LGICs has lacked an essential ingredient: structural information. This has made it difficult to relate functional changes observed in structure-function studies to specific structural transitions associated with the gating process. However, with recent publications of the AChBP crystal structures[4, 5] and Nigel Unwin's structure of the transmembrane domains derived from 4 Å cryo-electron micrographs

(cryo-EM) of the *Torpedo* nAChR,[6] we may finally have sufficient structural information to elucidate some of the molecular events of the gating mechanism.

Presumably, local conformational changes at the binding site (arising from agonist binding) initiate the gating mechanism. It is believed that rather than communicating these changes sequentially through the primary sequence of the protein, intermediate functional domains link binding site changes to the receptor gate.[7] Evidence from several studies highlights the possibility that the functional interface between the extracellular and transmembrane domains is formed by interacting loops contributed by each domain. Both biophysical studies and structural data point to two loops: the Cys loop and β1-β2 loop in the extracellular domain as important components of the gating pathway.[6, 8] In a recent study where chimeric receptors were constructed by replacing the extracellular domain of the 5-HT_3R with the AChBP sequence, functional receptors were observed only in chimeras where both the Cys loop and the β1-β2 loop contained the 5-HT_3R amino acid sequence.[9] This work provides telling evidence that these loops may form functional domains, coupling conformational changes at the binding site to the channel gate.

Findings from several studies indicate that the Cys and β1-β2 loops convey structural changes in the extracellular domain to the channel gate through a direct interaction with the M2-M3 loop— a short loop that connects transmembrane domains M2 and M3 and projects above the extracellular membrane.[2, 6, 8-10] The M2-M3 loop is an appealing candidate because not only are there several studies supporting its involvement in the gating process (discussed below), but the channel gate lies in M2. Hence any movement of M2 would likely involve conformational changes in this loop. In the work

presented in this chapter, nonsense suppression methodology is used to investigate the functional role of two conserved prolines, 301 and 308, in the M2-M3 loop of the 5-HT_3R. This work has been a collaborative effort with the Sarah Lummis group at the University of Cambridge . Sarah Lummis performed all of the immunofluorescence work and contributed significant effort to the electrophysiology experiments.

4.2 Transmembrane domains and the M2-M3 loop

As detailed in chapter 1, LGICs are formed by five subunits arranged in a pentagonal array around a central pore. Each subunit has four transmembrane domains as identified by hydropathy analysis. The cryo-EM structure of the transmembrane region shows that each of these domains forms an α-helix spanning the bilayer[6] (Figure 4.1). The M2 domain of each subunit lines the channel lumen with the side chains of Leu 9' and Val 13' in M2 (the convention for numbering residues in M2 starts with 1' at the N-terminal or cytoplasmic side), forming the channel gate. These are thought to present a hydrophobic barrier preventing the flow of ions.[11] The overall structure detailed by the cryo-EM images is supported by much of the previous biochemical and electrophysiological work. Indeed, several earlier studies proposed an α-helical structure for M2[12, 13], and Leu 9' has long been thought to form the channel gate.[14, 15] In addition, several novel features predicted by the structure have also been suggested by earlier work. In Unwin's structure, the M2 helix extends two turns above the membrane. Results from $GABA_A$ studies using the substituted cystine accessibility method (SCAM) showed a modification pattern consistent with an extended helix.[16] The structure also shows a water-filled crevice between M2 and M3 which previously had been suggested.[17]

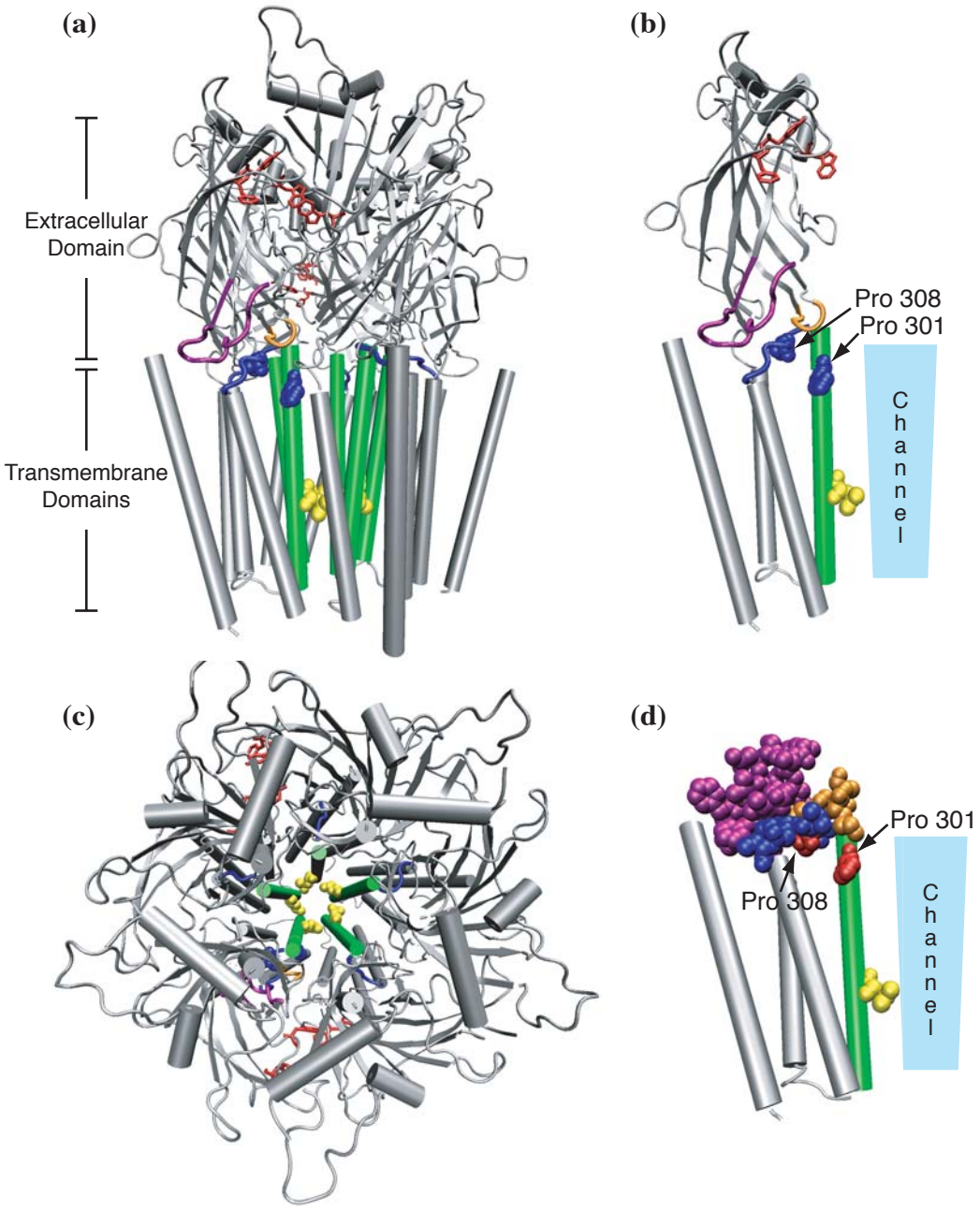

Figure 4.1. Several views of the 5-HT_3R as predicted by homology modeling. Highlighted features: binding site (red), Cys loop (purple), β1-β2 loop (orange), M2 (green), M2-M3 loop (blue), Leu 9' (yellow) and prolines 301 and 308 (blue CPK in *a-c* and red CPK in *d*). (a) Side view of entire receptor showing general arrangement of extracellular and transmembrane domains. (b) Single subunit showing Pro 301 and 308, and transmembrane topology. (c) Top view looking down the pore from the extracellular side. The cluster of residues (Leu 9') forms the channel gate. (d) Transmembrane domains, Cys loop and β1-β2 loop of a single subunit showing relative location of the loop structures.

Based on the cryo-EM data Unwin has proposed a model for the gating mechanism in nAChR (and by extension all LGIC).[6] The model posits that ligand binding induces a 15° rotation of the α subunits, which in turn, causes the tip of the β1-β2 loop— Val 44 specifically— to contact the M2-M3 loop (docking into the hydrophobic pocket formed by Ser 269-Pro 272 of the M2-M3 loop). The torsional force provided by this contact pivots the M2-M3 loop, thereby rotating M2 and gating the receptor. Although this seems to be a plausible model for the gating process, as yet, there is still a lack of experimental evidence to substantiate it. Several of the details, however, are supported by previous findings.

In the model, the M2-M3 loop plays a prominent role in the gating process. It not only serves as the direct link communicating conformational changes in the extracellular domain to the channel gate, but also functions as a pivot point for the gating movement of M2. The M2-M3 loop has long been speculated to be part of the gating pathway. Mutagenesis studies in the GlyR and nAChR showed that mutations in this loop could decouple agonist binding and channel gating.[18-22] More detailed single-channel studies in the nAChR demonstrated that mutations in the M2-M3 loop affect the gating equilibrium and do not change the binding equilibrium.[23] These studies also showed that the effects of mutations in the loop were dependent on their position in the primary sequence of the loop with one mutation increasing the gating rate and a similar substitution at the adjacent residue decreasing the rate. SCAM studies in both the GlyR and $GABA_A$ have shown the M2-M3 loop becomes more water accessible during channel gating, indicating that it undergoes a conformational change during the process.[16, 24]

A recent study in $GABA_A$ points to a direct interaction between the M2-M3 loop and the Cys loop during the gating process.[8] This study swapped charged residues between the Cys and M2-M3 loops to show that an electrostatic interaction between a Lys in the M2-M3 loop and a conserved Asp in the Cys loop is formed during gating. Interestingly, this Lys is not conserved in either the nAChR or 5-HT_3R, and similar studies in the GlyR did not show the same interaction[10]— raising the possibility that there may be subtle variations in the gating mechanism for each of the Cys-loop receptors. Unwin's model emphasizes an interaction between the β1-β2 loop and M2-M3. It is very likely that M2-M3 interacts with both of these extracellular loops. Inspection of the structure in Figure 4.1d shows that the Cys and β1-β2 loops bracket M2-M3, and the chimeric studies point to a need for both loops in coupling agonist binding and channel gating. Thus, while the exact role the M2-M3 loop plays is not clear, the cumulative evidence strongly supports it being functionally important in the gating pathway.

4.3 Potential dynamic role of proline

One interesting feature of the M2-M3 loop in the 5-HT_3R is the presence of two proline residues (Figure 4.2). Pro 301 is conserved in all Cys-loop receptors and is located roughly two helical turns below the C-terminal end of M2 (Figure 4.1). Pro 308 is conserved in all of the cation-selective receptors (nAChR and 5-HT_3R) and is located two residues after the C-terminal end of the extended M2 helix (Figure 4.1). This proline aligns with Pro 272 in the nAChR, which in Unwin's model forms part of the hydrophobic pocket into which the β1- β2 loop docks. Proline has several special features (discussed below) that make it an intriguing consideration in terms of the gating process.

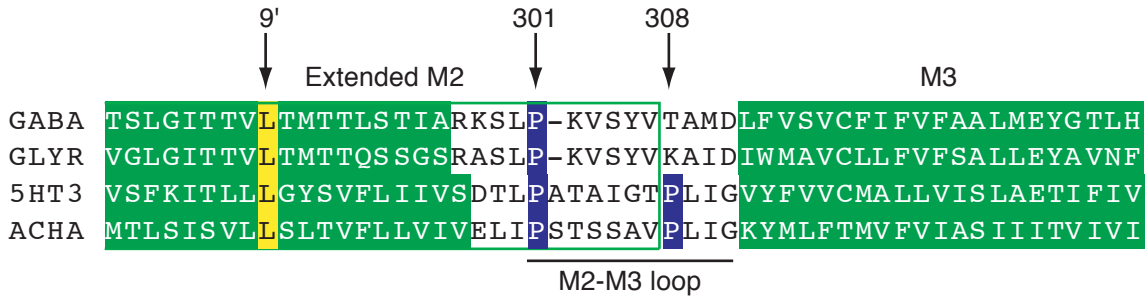

Figure 4.2. Sequence alignment of the murine sequences for α_1 $GABA_A$, α_1 GlyR, 5-HT_{3A}R, and α_1 nAChR. Pro 301, Pro 308, and secondary structural domains are indicated. The M2 helix as identified by hydropathy analysis is shown in green, and the extended helix as predicted in the cryo-EM structure is designated by the green box. Pro 301 is conserved in all Cys loop receptors, Pro 308 is conserved in the cation-selective receptors.

Proline is unique among the 20 standard amino acids in that its side chain is covalently bonded to the α-amino group. This cyclic structure severely limits the main chain conformations proline can adopt. In terms of the backbone dihedral angles, ϕ and ψ, proline is the most conformationally restricted amino acid. The cyclic structure fixes the ϕ dihedral at -65°±25° and leaves the ψ dihedral hindered with two local minima near –55° and 145°, though surveys of the protein databank show that ψ values around 80° are also common.[25, 26] Another consequence of the cyclic structure is that the secondary peptide bond formed with the nitrogen of proline lacks a hydrogen, resulting in the loss of a hydrogen-bond donor at prolyl backbone sites. Due to its conformational limitations and the absence of an amide hydrogen, proline is rarely found in periodic secondary structure such as β-sheets or α-helices.[25, 26] In fact, in globular proteins, proline is considered the classic helix-breaker.

Interestingly proline is found with anomalous frequency in the putative helices of integral membrane receptors and transport proteins.[27] The reasons for this are not yet clear, but it has lead to wide speculation that proline is important in the structure and

function of these proteins.[28-30] The potential importance of proline is evidenced by the recent observation that mutations of proline have one of the highest phenotypic propensities in the analysis of TM sequences from the Human Gene Mutation Database.[31] As a result of its lacking a hydrogen-bond donor and the local steric restrictions it presents, proline, when found in helices imparts a 25º kink to the helix trajectory.[32, 33] From a structural standpoint, modeling studies have shown that this kink can serve to stabilize transmembrane helix bundles by increasing the van der Waals contact between the helices.[34] It is also hypothesized that a proline kink may serve a dynamic role because it removes at least one hydrogen-bonding pair (between the NH of proline at *i* and the carbonyl O at *i-4*) and often leads to loss of a second pair (the NH of *i+1* and the carbonyl O of *i-3*).[28, 29] This allows the two ends of the helix to pivot independently. Thus, the proline kink could function as a hinge point in the conformational changes of ion channel function.

Another interesting feature that has generated much speculation about proline is it is the only standard amino acid for which the *cis* peptide bond is energetically accessible[30] (Figure 4.3). Surveys of the protein data bank show that roughly 5-6% of all prolines are in the *cis* conformation, as opposed to the other amino acids for which less than 1% are *cis*.[35, 36] Proline's ability to adopt the *cis* conformation arises largely due to destabilization of the *trans* conformation from steric conflicts between C_δ of proline and C_β of the preceding residue. From a structural standpoint, *cis* proline is found in several types of β-turns, where the protein chain direction is reversed over a short distance.[26, 37] This characteristic of proline may also play a dynamic role in that *cis*/*trans* isomerization of prolyl peptide bonds may function as a conformational switch.[38] Recently, several

cis/*trans* proline switches have been elucidated in globular proteins, most notably the tyrosine kinase Itk where isomerization shuttles the protein between different active states.[39-41]

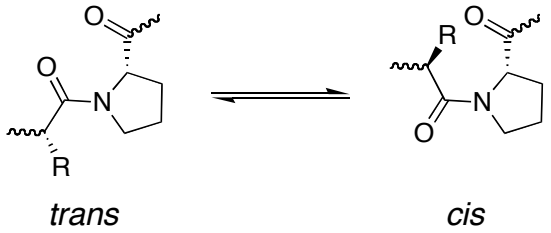

Figure 4.3. Schematic of *trans* and *cis* conformations of the prolyl peptide bond.

It has long been speculated that *cis*/*trans* isomerization of prolyl peptide bonds could be involved in the gating pathway of ion channels.[27, 30] Indirect evidence has come from studies on gap junction proteins[42], but to date, there is no clear experimental evidence supporting this hypothesis. However, given the anomalous frequency of proline in transmembrane helices and the recent demonstrations of proline switches, this still remains an attractive hypothesis. Another potential way in which proline could facilitate the conformational changes associated with ion channel gating is in shuttling between favored states at the hindered ψ angle. NMR studies on model peptides corresponding to the second intracellular loop of the vasopressin receptor (a GPCR) have demonstrated a conformationally heterogeneous proline, where the ψ angle flipped between two stable conformations.[43] This proline is conserved throughout the GPCR family and is believed to be important for coupling to G proteins. Thus, this may represent a general motif where proline functions as a conformational switch without *cis*/*trans* isomerization.

4.4 Experimental design

A series of proline analogs was selected to evaluate the functional role of Pro 301 and Pro 308 in the 5-HT_3R (Figure 4.4). The analogs were chosen to assay specific features of proline's structure and function, and many of the analogs have been previously studied in model peptides, providing some quantitative background data for interpreting our results.[44-50] In addition some of the analogs have been used in previous nonsense suppression studies to evaluate a conserved proline in the M1 domain of the nAChR and 5-HT_3R.[51, 52]

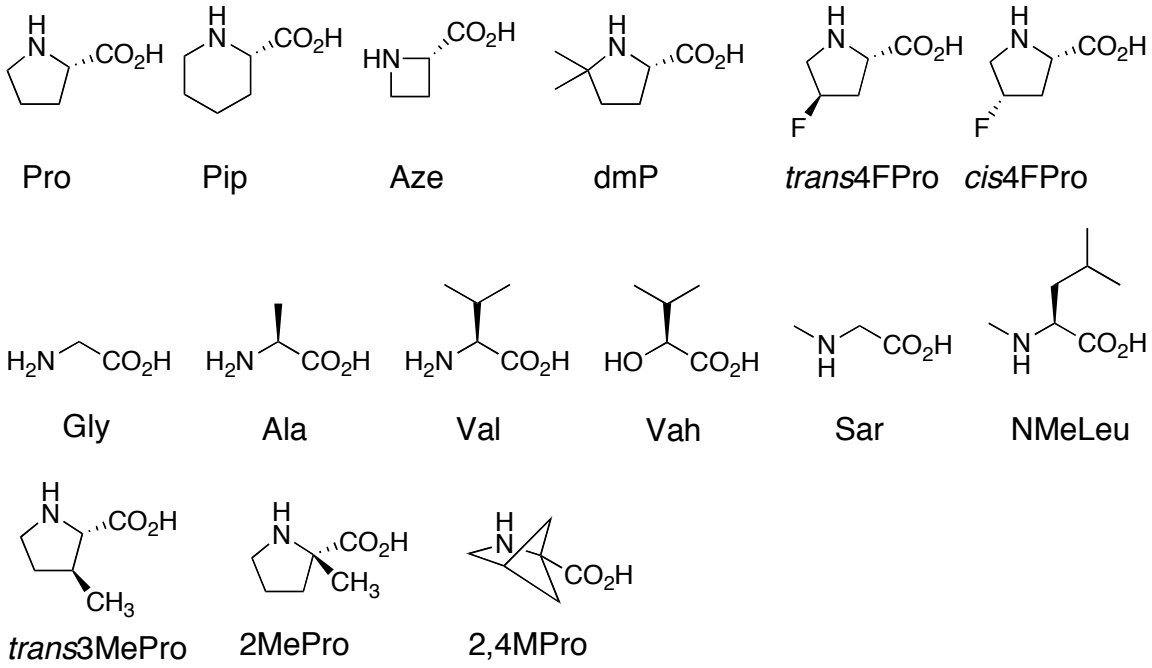

Figure 4.4. Structures of the amino acids used to probe Pro 308 and Pro 301.

In many ways, proline is an ideal target residue for structure-function studies with unnatural amino acids, as it has several features that can be readily tested with minor perturbations. Ring size and the attendant flexibility can be tested with the 4- and 6-membered ring analogs, Aze and Pip, respectively. The ring of proline displays two

stable conformations: endo pucker and exo pucker (discussed below). This feature of proline can be tested with the fluoro-prolines, which each prefer a different puckered conformation.[47, 53] The hydrogen bonding properties can be examined using backbone ester substitutions with hydroxy acids or N-methyl amino acids.[51] The latter can also be used to assay the potential role of the secondary prolyl amide. In addition N-methyl amino acids mirror many of the conformational features of proline, but lack the rigid ring structure. Finally the potential of *cis*/*trans* isomerization can be readily tested using analogs of proline that are selective for a particular conformation (*cis*-selective: Aze, Pip, and dmP[46, 48]; *trans*-selective: *trans*-3-Me-Pro, 2-Me-Pro, and 2,4-methano-Pro[44, 49, 54]).

4.5 Results

4.5.1 General experimental details

Both unnatural and natural amino acids were incorporated into positions 301 and 308 of the 5-HT_3R using *in vivo* nonsense suppression methods, and mutant receptors were evaluated electrophysiologically[55]. The whole-cell currents induced by the application of 5-HT were measured by two-electrode voltage clamp techniques. Non-functional receptors were assayed for surface expression using immunofluorescent imaging. The functional effects arising from the introduced mutations were determined from the dose-response relations and the macroscopic rate constants for receptor activation and deactivation. Macroscopic rate constants were determined from the single-exponential fits of the whole-cell current traces using *pCLAMP 9.0* analysis software. In all experiments, the 5-HT_{3A}R homomer was used.

4.5.2 Control experiments for 301 and 308

Initial experiments at both 301 and 308 focused on several important controls: ensuring no protein was produced through any read-through of the UAG-containing mRNA, and recovery of the wild type receptor through nonsense suppression. Injection of either of mRNA with the UAG stop codon at 301 or 308 resulted in no 5-HT induced currents. In addition, injection of UAG-containing mRNA and uncharged tRNA produced no 5-HT induced currents at either site. Both of these controls indicate that in the absence of charged tRNA functional receptors are not produced by read-through of the UAG-containing mRNA. Injection of UAG-modified mRNA with aminoacyl tRNA-Pro into oocytes resulted in receptors with functional properties similar to wild type, EC_{50}s of ~1.2 μM and Hill coefficients of ~2 (Table 4.1 and 4.2).

4.1.3 Electrophysiology results for substitution at 308

4.1.3.1 Dose-response data

In all, 15 different residues were attempted at position 308. Interestingly, nine of these did not produce functional receptors (see Table 4.1), indicating this is a fairly stringent position. All mutations that produced functional receptors were close analogs of proline and maintained a cyclic structure. The dose-response data show that with the exception of dmP, the functional mutations lead to only modest changes in EC_{50} (Figure 4.5 and Table 4.1). The two ring-size analogs, Aze and Pip, lead to 3- and 1.7-fold reductions in EC_{50}, respectively, whereas the two fluoro-prolines, *cis*-4-F-Pro and *trans*-4-F-Pro, produced EC_{50}s very near wild type. In the case of dmP, however, a 23-fold reduction in EC_{50} was observed. This finding is suggestive of the possibility that

a *cis*-proline is functionally important at position 308, as model peptide studies have shown dmP to prefer the *cis*-amide isomer by ~1.1 kcal/mol relative to *trans*.[48] It is also possible that given the increased sterics of dmP, this residue alters the conformation of the M2-M3 loop, biasing it towards the open state conformation.

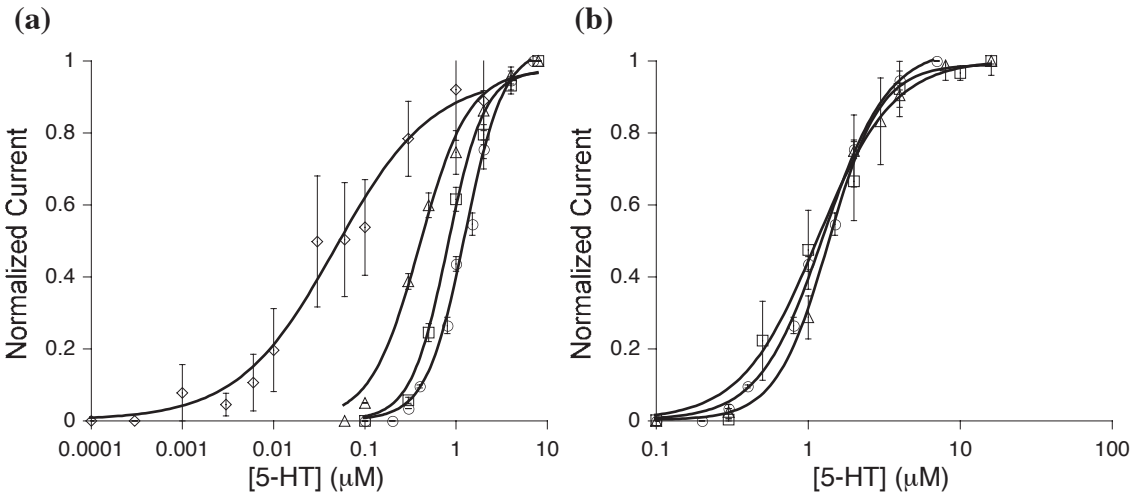

Figure 4.5. Dose-response relations for Pro 308 mutants. (a) Pro (*circles*), Aze (*triangles*), Pip (*squares*), and dmP (*diamonds*). (b) Pro (*circles*), *cis*-4-F-Pro (*squares*), and *trans*-4-F-Pro (*triangles*).

Further analysis of the dose-response data shows a strong correlation between the EC_{50} for the mutant receptors and the *cis* preference of the proline analogs (Table 4.2). Figure 4.6 shows a plot of $\Delta\Delta G$ EC_{50} (mutant – wt) versus $\Delta\Delta G$ for the cis preference of the analogs relative to proline. The linear correlation seen for the plotted values provides additional evidence that a *cis* proline at 308 may be functionally important in the gating mechanism.

Several underlying assumptions in this plot, however, should be noted. The quantity EC_{50} is not a true equilibrium constant. It is a composite of equilibria for both binding and gating. Our assumption, however, is that changes in EC_{50} with these mutants

reflect changes in the gating equilibrium and do not affect binding. Support for this assumption comes from single-channel studies which demonstrated that mutations in this region of the nAChR solely affected gating.[23] Furthermore, position 308 is ~30 Å from the binding site, and thus, mutations here are not likely to affect agonist binding. The $\Delta\Delta G$ values for the *cis* preference of the analogs come from several literature studies and were determined for small model peptides.[46-48] It is known that many factors including both the local protein sequence and longer-range interactions can affect the *cis* preference of proline.[36, 37, 56] We assume, however, that these factors will be similar for all the analogs considered, and thus, the trend in *cis* preference for the analogs will not be overly distorted from that seen in the model studies. Finally, this plot, although spanning two orders of magnitude in EC_{50}, shows that the data is clustered into two regions. The plot requires an intermediate data point between Aze and dmP, as linear fits of data clustered into two regions can be misleading.

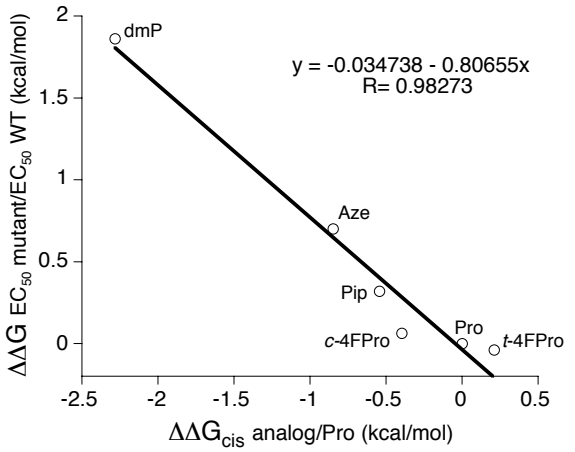

Figure 4.6. Plot of ΔΔG EC_{50} for the Pro 308 mutants versus ΔΔG for the *cis* preference of the analogs relative to proline. Equation for the linear fit and R value are shown at the top.

Table 4.1 Dose-response data and macroscopic rates for the Pro 308 mutants

Residue	EC_{50}±SEM (μM)	Hill±SEM	Act. rate±SEM (s^{-1})	Deact. Rate±SEM (s^{-1})
Pro	1.29 ± 0.07	2.04 ± 0.18	2.85 ± 0.91	0.03 ± 0.01
Aze	0.42 ± 0.03	1.56 ± 0.19	0.48 ± 0.06	0.02 ± 0.01
Pip	0.75 ± 0.06	2.16 ± 0.28	8.61 ± 0.27	0.29 ± 0.03
*cis*4FPro	1.16 ± 0.12	1.74 ± 0.27	5.95 ± 0.75	ND
*trans*4FPro	1.38 ± 0.06	2.53 ± 0.23	7.22 ± 0.34	ND
dmP	0.055 ± 0.01	0.77 ± 0.1	2.93 ± 0.69	ND
Ala	NR	NR		
Gly	NR	NR		
Val	NR	NR		
Vah	NR	NR		
Sar	NR	NR		
NMeLeu	NR	NR		
*trans*3MePro	NR	NR		
2,4MPro	NR	NR		
2MePro	NR	NR		

ND = not attempted, NR = no response to concentrations up to 1 mM 5-HT

Table 4.2. Thermodynamic data for proline analogs

Residue	*%cis*	K_{cis}	ΔG_{cis} (kcal/mol)	$\Delta\Delta G_{cis}$[a] (kcal/mol)
Reference 47				
Pro	17	0.20	0.96	0.0
*trans*4FPro	12	0.14	1.17	0.21
*cis*4FPro	28	0.39	0.55	-0.40
Reference 46				
Pro	6	0.06	1.67	0.0
Pip	13	0.15	1.13	-0.54
Aze	20	0.25	0.82	-0.85
Reference 48				
Pro	13	0.15	1.13	0.0
dmP	87.5	7.0	-1.15	-2.28

[a] ΔΔGcis for analog/proline

4.1.1.2 Incorporation of dmP at 308 shows blockable leak currents

Experimental support for the conclusion that the dmP 308 mutant stabilizes the open channel conformation of the M2-M3 loop comes from the observation that oocytes expressing dmP-containing receptors showed a continual increase in leak current following initial receptor activation (Figure 4.7). This leak was almost completely reversible by the open-channel blocker TMB-8, indicating the leak current was associated with receptor activation and not with any oocyte specific process. This finding suggests that upon activation dmP locks the channel in the open state. Furthermore, the lowered EC_{50} and blockable leak current seen with the dmP mutant indicate that Pro 308 undergoes a conformational change associated with the gating pathway.

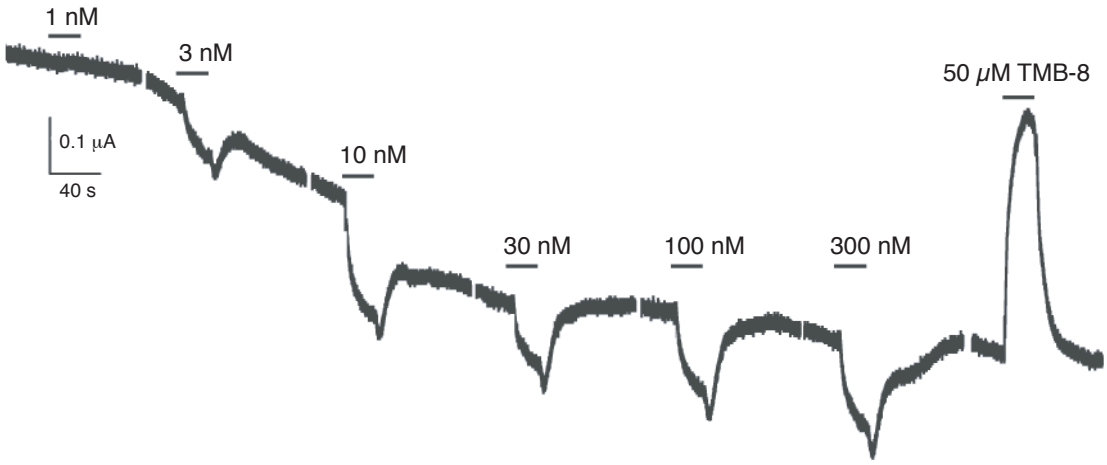

Figure 4.7. Current traces for dmP at position 308, showing the TMB-8 blockable leak currents seen after receptor activation by 5-HT. Bars represent 5-HT application.

4.1.1.3 Macroscopic rates

An interesting feature of these studies is that all functional mutants at 308 lead to changes in the macroscopic rates of activation and desensitization (Table 4.1). Figure 4.8 shows representative traces illustrating the altered rates. The fluoro-prolines and dmP lead to ~2-fold increases in the macroscopic activation rates. Pip lead to 3- and 8-fold increases in the rates of activation and deactivation, respectively. Aze was the only mutation to show decreased rates, producing a 6- and 1.7-fold decrease in activation and deactivation, respectively.

The rates for Aze, Pro and Pip match the trend in ring size with the 4-membered ring (Aze) slower than the 5 (Pro) and 5-membered ring slower than the 6 (Pip). It is possible that this trend in rates reflects differences in either ring flexibility or ring conformation among these residues. The potential importance of the ring conformation is supported by the changes seen with the fluoro-prolines, as *cis*-4-F-Pro favors an endo ring pucker and *trans*-4-F-Pro favors an exo ring pucker (Figure 4.9).[47, 53, 57, 58] (The

proline ring exhibits two preferred ring conformations or puckers: endo where C_γ is flipped *cis* to the carboxy group and exo where C_γ is flipped *trans* to the carboxy group). Thus, small changes in the ring conformation may cause subtle differences in the gating pathway.

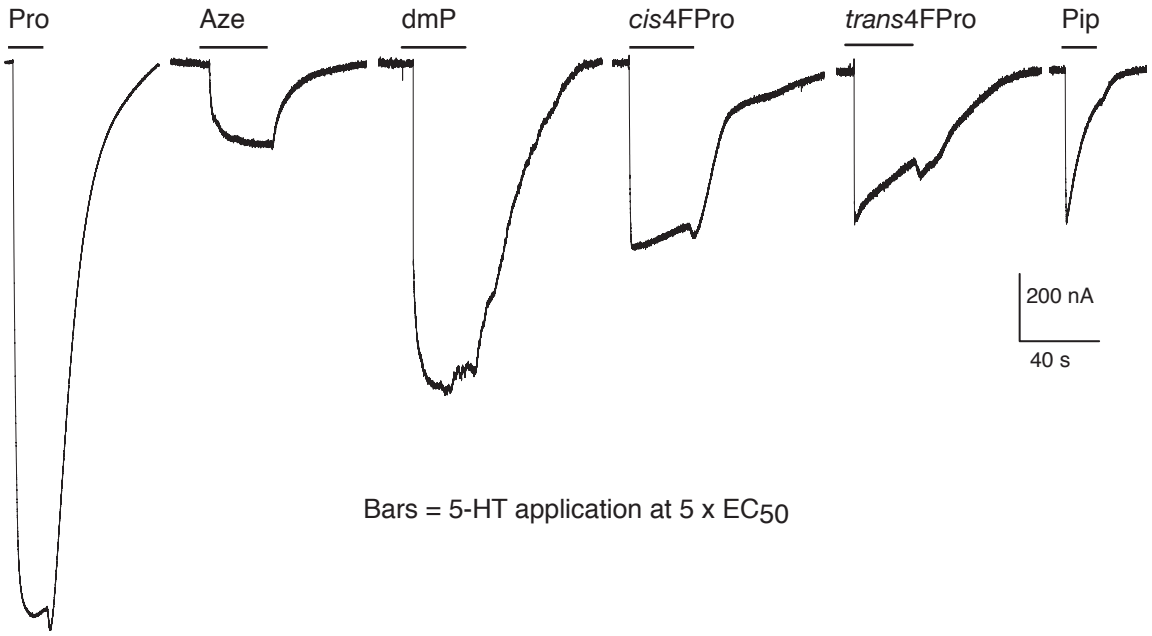

Figure 4.8. Current traces showing the altered rates of activation and deactivation for the 308 mutants. Bars represent application of 5-HT at 5 times EC_{50} of the respective mutant.

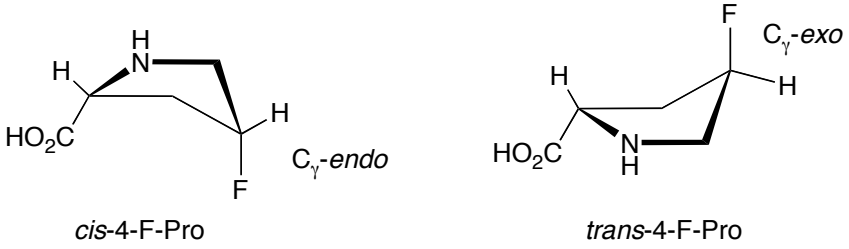

Figure 4.9. Schematic showing the two stable ring conformations (endo and exo) in proline and the preferred ring conformation for the 4-fluoro prolines.

4.1.4 Surface expression of nonfunctional mutants at 308

In order to rule out the possibility that the nonfunctional mutants arose from injection of hydrolyzed aminoacyl-tRNA, all tRNAs were analyzed by MALDI-TOF mass spec to ensure that the aminoacyl linkage was still intact.[59] In addition, all the attempted residues have successfully been incorporated into other sites in either the 5-HT_3R or nAChR using nonsense suppression.[51, 52] Thus, it seems very doubtful that the lack of functional receptors was caused by any incompatibilities with the ribosome or translation machinery.

The cell-surface expression of the non-functional mutants was examined by immunofluorescence to determine if these mutations had impaired receptor assembly and processing, or if they produced surfaced expressed but silent receptors. This work was performed by Sarah Lummis. Oocytes expressing the mutant receptors were fixed in 4 % paraformaldehyde, placed in glycerol and strored at –80º C. After thawing, oocytes were labeled with the primary antibody pAB120, washed, and then labeled with the secondary antibody, Cy5-conjugated anti-rabbit IgG.[60] Immunofluorescence was observed with a Nikon optiphot or a confocal (BioRad-MRC600) microscope.

All of the nonfunctional mutants showed surface labeling, indicating that these mutations had lead to silent receptors (Figure 4.10). The fact that the natural amino acids Gly, Ala, and Val produced surface expressed but silent receptors supports the idea that this position requires a conformationally restricted residue. However, even the N-methyl amino acids Sar and N-Me-Leu were silent, and as these residues replicate some of the conformational restrictions imposed by proline but lack the ring, clearly the more rigid ring structure is important. The fact that both the N-methyl residues and Vah were silent

rules out the possibility that the unique hydrogen bonding characteristics of Pro 308 are important. This latter possibility was found to be the case in earlier studies of a conserved proline in M1 of both the nAChR and 5-HT_3R.[51, 52] These studies found that replacement of this proline with a hydroxy acid produced functional receptors with wild type characteristics.

Not all of the ring-containing residues produced functional receptors. 2-Me-Pro, *trans*-3-Me-Pro and 2,4-methano-Pro were all silent. This suggests that the rigid ring structure is not sufficient to produce functional receptors. Both 2-Me-Pro and 2,4-methano-Pro are highly selective for the *trans* amide bond, lending further support to the possibility of a functionally important *cis* peptide bond at position 308.[49, 54] *Trans*-3-Me-Pro, on the other hand, is a fairly close analog of proline and studies have shown that it closely mirrors proline's *cis* preference.[49] One difference for *trans*-3-Me-Pro is that it has a higher barrier to *cis*/*trans* isomerization.[26, 44] This supports the conclusion that *cis*/*trans* isomerization at Pro 308 is mechanistically important in the gating pathway. Additionally, the reason for the higher barrier in *trans*-3-Me-Pro is believed to arise from its inability to form a hydrogen bond between the prolyl N and the NH at position *i+1*. This hydrogen bond has been shown to catalyze isomerization of prolyl-peptide bonds, increasing the isomerization rate 260-fold in model studies.[61, 62] One of the concerns for suggesting *cis*/*trans* isomerization at Pro 308 is that this isomerization may proceed at too slow a rate to be functionally viable in receptor gating, as the latter process occurs on the μs to ms timescale and isomerization is more often on the *seconds* timescale. Thus, the results with *trans*-3-Me-Pro point to the possibility that the formation of this hydrogen bond may catalyze the isomerization at Pro 308. It should also be noted that many

researchers have hypothesized that long-range protein interactions could increase the isomerization rate of proline, to make it a viable conformational switch in fast-acting processes.[30, 56]

Aside from the trends in *cis* and *trans* preference, the immunofluorescence findings show that incorporation of proline analogs substituted at the 2 or 3 position results in receptors where agonist binding and channel gating have been decoupled. A possible explanation is that steric bulk on this side of the proline ring may disrupt the proper orientation of the M2-M3 loop. Alternatively, bulk on this side of the ring may interfere with specific interactions of the proline ring, possibly even with interactions between Pro 308 and one of the extracellular loops. This latter speculation could fit with Unwin's model in that steric bulk at the 2 or 3 position of the proline ring may prevent docking of the β1- β2 loop into the hydrophobic pocket of the M2-M3 loop.

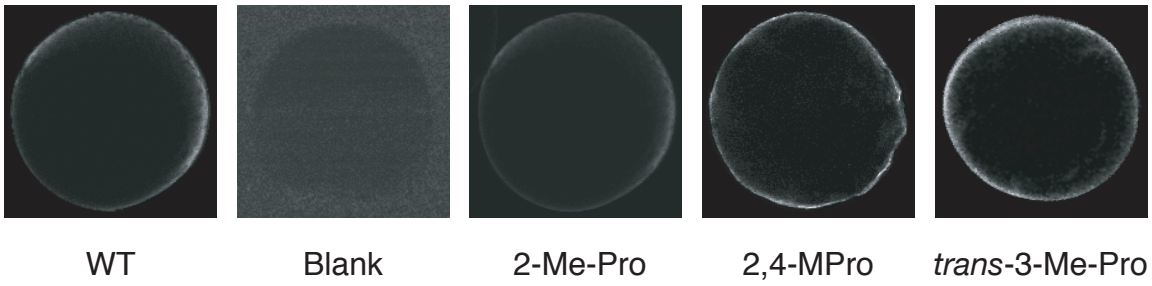

Figure 4.10. Immunofluorescent images of the nonfunctional 308 mutants. Visible labeling of mutants expressing *trans*-selective proline analogs demonstrates these receptors are expressed at the cell surface.

4.1.5 Poor expression of dmP and Aze at 308

A final observation to note in the studies of Pro 308 is that both dmP and Aze displayed very inconsistent expression. In all, approximately 200 oocytes from 10 different batches were tried for each of the residues. For dmP, expression was seen in

only 9 oocytes and with Aze, 13 oocytes showed expression. Several avenues were taken to increase the expression in these two mutants: incubation at different temperatures, expression with the 5-HT_{3B} subunit, and double injection. None, however, lead to any increase in expression.

Both of these unnaturals present steric and conformational demands. In dmP significant steric bulk has been introduced adjacent to the nitrogen. This may interfere with the efficiency of the peptidyl-transfer reaction during translation. In Aze, the conformational restrictions imposed by the 4-membered ring may interfere with processing and assembly. This latter concern could also be a problem with dmP mutants. It is known that the folding of the 5-HT_3R is dependent on the activity of the proline-peptidyl isomerase cyclophilin A (CypA).[63] It is plausible that dmP and Aze are inefficient substrates for CypA, which would certainly lead to a reduction in the expression for both mutants. In addition, studies of the cystic fibrosis transmembrane receptor have shown that mutations of proline residues embedded in transmembrane regions can have a deleterious effect on the kinetics and robustness of folding.[33]

4.1.6 Substitution at 301

In all, 13 different amino acids were incorporated at position 301, and much like with 308, only six produced functional receptors (see Table 4.3). In contrast to the substitution pattern at 308, however, residues not maintaining a cyclic structure produced functional receptors at 301. The dose-response data show that none of the functional mutations lead to large changes in EC_{50}. (Figure 4.11 and Table 4.3) Substitution by Val resulted in a 3-fold decrease in EC_{50}. The fact, that this standard residue which has a hydrogen at the amide position and shows a strong preference for the *trans*-amide

produced functional receptors with only a modest shift in EC_{50} indicates that neither the special hydrogen-bonding properties of proline nor a *cis*-proline are important at this site. Incorporation of Vah, dmP, and Pip at 301 lead to roughly 2-fold increases in EC_{50}, and incorporation of Aze lead to a 2-fold decrease in EC_{50}. Thus, aside from the Val mutations, the dose-response data do not point to any special features of this site.

All functional mutations, however, did lead to increases in the macroscopic rates of activation and deactivation (Figure 4.12 and Table 4.3). Val, Aze and Pip resulted in 3- to 4-fold increases in the activation rates and 9- to 14-fold increases in deactivation rates. More dramatic rate increases were seen with dmP and Vah. The former lead to 22- and 68-fold increases in activation and deactivation, respectively, and the latter lead to 25- and 85-fold increases in activation and deactivation, respectively. The only obvious parallels between the two residues is that relative to proline and the other mutations, both dmP and Vah have lower barriers for amide bond isomerization. The results for Val, however, make this a doubtful scenario. Thus, position 301 does seem to be tuned for the presence of proline, as all mutations were either non-functional or lead to rate increases. Given that the cryo-EM structure of the transmembrane domains shows a kink in the helix at Pro 265 (the homolog of 301), it seems possible that this proline may establish the proper orientation of the M2 helix. Thus, the changes we observe in the rates may reflect alterations in the M2 helix kink and/or orientation.

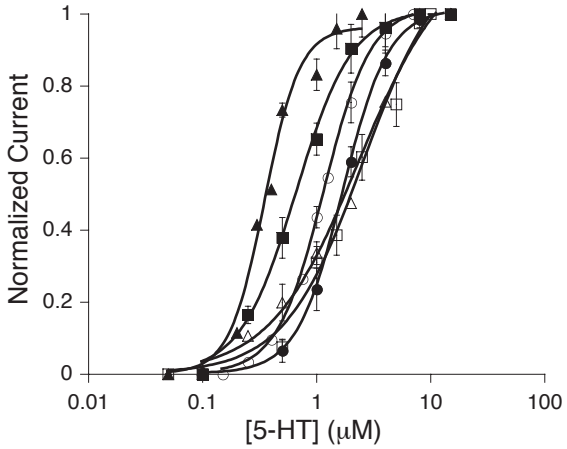

Figure 4.11. Dose-response relations for Pro 301 mutants. Pro (*open circles*), Aze (*filled squares*), Pip (*filled circles*), dmP (*open triangles*), Val (*filled triangles*), and Vah (*open squares*).

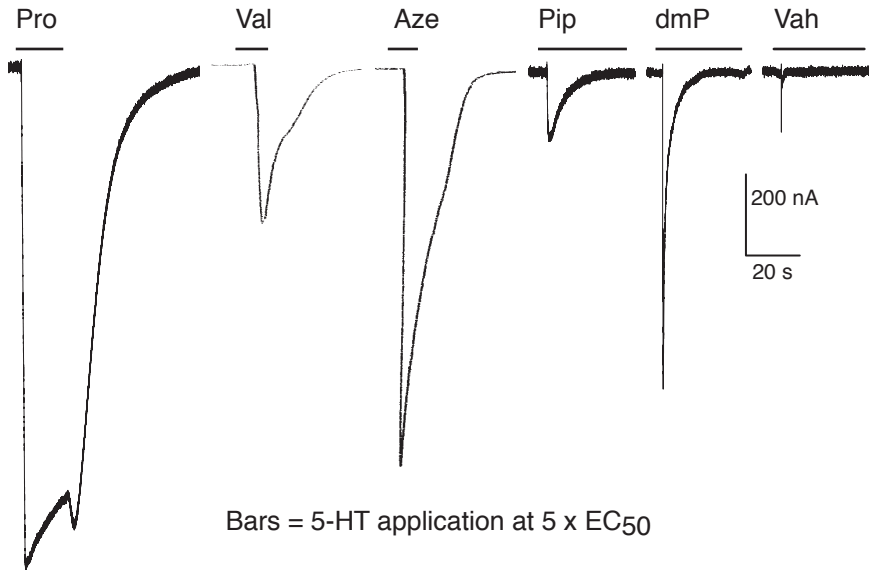

Figure 4.12. Current traces showing the altered rates of activation and deactivation for the 301 mutants. Bars represent application of 5-HT at 5 times EC_{50} of the respective mutant.

Table 4.3 Dose-response data and macroscopic rates for the Pro 301 mutants

Residue	EC_{50}±SEM (μM)	Hill±SEM	Act. rate±SEM (s^{-1})	Deact. Rate±SEM (s^{-1})
Pro	1.18 ± 0.02	2.12 ± 0.08	2.85 ± 0.91	0.02 ± 0.0005
Aze	0.68 ± 0.03	1.77 ± 0.11	10.75 ± 2.64	0.16 ± 0.021
Pip	1.73 ± 0.02	2.16 ± 0.04	12.45 ± 2.94	0.25 ± 0.026
Val	0.36 ± 0.02	2.82 ± 0.47	9.62 ± 2.07	0.13 ± 0.022
Vah	2.6 ± 0.62	1.27 ± 0.22	71.11 ± 5.66	1.46 ± 0.013
dmP	2.37 ± 0.54	1.12 ± 0.17	64.44 ± 4.48	1.15 ± 0.101
Ala	NR	NR		
Gly	NR	NR		
Sar	NR	NR		
NMeLeu	NR	NR		
*trans*3MePro	NR	NR		
2,4MPro	NR	NR		
2MePro	NR	NR		

NR = no response to concentrations up to 1 mM 5-HT

4.6 Discussion

Agonist binding in ligand-gated ion channels initiates a series of conformational changes that ultimately lead to opening of an ion permeant channel across the cell membrane. The molecular details linking binding to the channel gate some 50 Å away remain largely unknown. From a chemical standpoint, this is an intriguing consideration: how does the noncovalent binding of a small molecule induce a dramatic structural change in a multisubunit ~300 kDa protein?

Previous work has indicated a potentially prominent role for the M2-M3 loop in the gating pathway. This small loop connects the channel-lining domain (M2) with the M3 domain, and is an appealing candidate because of its location at the interface between the binding and transmembrane domains (Figure 4.1). To investigate the functional role of the M2-M3 loop, we have probed two conserved prolines in this domain using unnatural amino acids. Our findings indicate Pro 301 and Pro 308 are functionally important in the

gating pathway, and in particular the results at Pro 308 lend experimental support for a recently proposed gating model

Based on cryo-EM data from the nAChR, the model posits that binding of agonist induces a 15° rotation of the extracellular domains.[6] This rotation leads to contact between the β1-β2 loop of the extracellular domain and the M2-M3 loop. Specifically, Val 44 docks into a hydrophobic pocket formed by Ser269-Pro 272. This then provides the torsional force for movement of the M2 domain and gating of the channel. In the model, the M2-M3 loop not only acts as the mechanical receiver of conformational changes in the extracellular domain, but also serves as the hinge for the gating movement of M2. Pro 308 in the 5-HT_3R aligns with Pro 272 of the nAChR. This residue is conserved amongst the cation-selective members of the Cys-loop family. Our data support a conformational change at Pro 308 during the gating process that is consistent with this domain functioning as a hinge.

The data show that Pro 308 is a highly stringent site that requires a rigid ring structure for proper receptor function. Substitution by Ala, Gly, Sar, Val, Vah or N-Me-Leu resulted in receptors that were expressed at the cell surface, but did not respond to agonist, indicating these mutations decoupled agonist binding and channel gating. A rigid ring structure, however, is not sufficient. Substitution by *trans*-3-Me-Pro, 2-Me-Pro, or 2,4MPro also leads to surfaced-expressed, yet nonfunctional receptors (Figure 4.10). This group of mutations shares a common characteristic in that they disfavor the *cis*-amide isomer. In model peptide studies, 2-Me-Pro and 2,4-methano-Pro showed no detectable *cis* isomer, and *trans*-3-Me-Pro has a higher barrier to

isomerization relative to proline.[44, 49, 54] These results suggest the possibility that a *cis*-peptide bond is functionally important at Pro 308.

This conclusion is supported by the dose-response data, where incorporation of the *cis*-selective proline analog, dmP leads to a significant decrease in EC_{50}. Furthermore a plot of $\Delta\Delta G$ EC_{50} for the various mutants versus the $\Delta\Delta G$ values for the *cis* preference of the analogs relative to proline shows a linear correlation (Figure 4.6). The correlation between EC_{50} and *cis* preference is seen for over two-orders of magnitude change in EC_{50} and almost a 2.5 kcal difference in *cis* preference. This is fairly compelling evidence for a functionally important *cis*-proline at 308.

It is also possible that given the increased steric bulk of dmP, this residue is altering the conformation of the M2-M3 loop in a way that biases the receptor towards the open state. The functional role of Pro 308, however, does appear to be dynamic, as activation of the dmP mutants lead to an increase in the standing current that was blockable by TMB-8 (Figure 4.7). This standing current was seen only after initial activation of the mutant receptors and grew progressively larger after each application of 5-HT. This seems to indicate that once open the dmP mutant is slow to deactivate (i.e. transiting to either the desensitized or closed state). This result suggests that the gating process involves a conformational change at Pro 308. A consistent interpretation of this finding combined with the immunofluorescence and dose-response data is that in the resting closed state, Pro 308 is in the *trans*-conformation and during gating, it isomerizes to the *cis*-conformation (Figure 4.13). It is also possible that the functional changes we see with the 308 mutants reflect a gating specific heterogeneity in the conformation of Pro 308 that does not involve *cis*/*trans* isomerization. Pro 308 may function as a

conformational switch converting between two stable orientations of ψ. Our findings, however, do support a dynamic role for Pro 308 in the gating pathway.

The results at Pro 301 are also suggestive of a role in the gating pathway. Here, however, we did not see large changes in EC_{50}, but changes in the macroscopic rates. This site is not as stringent as Pro 308 and the data do not suggest any obvious trend, as both cyclic proline analogs, natural amino acids and the hydroxy acid Vah lead to functional receptors. The rate changes however suggest that indeed, the mutations were affecting the gating pathway, possibly by changing the orientation or kink angle of the M2 helix.

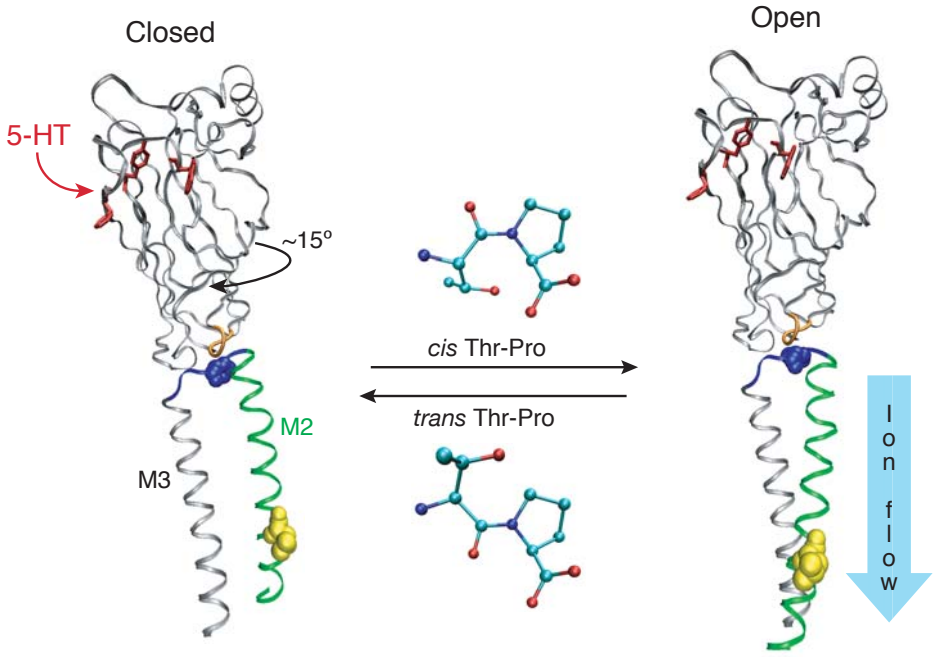

Figure 4.13. Cartoon of a single 5-HT_3R subunit depicting how *trans* to *cis* isomerization could function as a hinge for movement of M2 (green) during gating. The general gating mechanism is based on Unwin's proposed model, where agonist binding (red) induces a rotation of the extracellular domains. This brings the β1-β2 loop (orange) into contact with the M2-M3 loop (blue) causing the latter loop to pivot. Here the pivot is depicted as *trans* to *cis* isomerization of Pro 308 (blue CPK). The hinge movement in the M2-M3 loop allows rotation of M2 and gates the channel. Leu 9', the gate, is shown in yellow CPK. The open structure on the right was generated by manually converting Pro 308 to the *cis* conformation.

4.7 Future directions

In conclusion, our findings support a functional role for both Pro 301 and Pro 308 in the gating process of the 5-HT_3R. The results at Pro 308 in particular suggest this site functions as a conformational switch during gating, which is consistent with Unwin's prediction that the M2-M3 loop serves as a hinge during the gating process. Several possibilities, however, could be pursued to strengthen this conclusion. First, the plot of $\Delta\Delta G$ EC_{50} versus $\Delta\Delta G$ *cis* preference requires an intermediate data point between dmP and Aze. Experiments by Lori Lee with *cis*-5-*tBu*-Pro are currently underway to remedy this concern. Second, if Pro 308 does indeed function as a conformational switch (either through *cis*/*trans* isomerization or converting between stable ψ conformations) this is likely to be a mechanism that is at least conserved in the nAChR, which also has a proline at this site. Thus, repeating these studies in the nAChR is a necessary validation of our conclusions. And third, for both the 301 and 308 studies the nAChR offers the possibility to combine unnatural mutagenesis with single–channel experiments. This would allow better resolution of the mutational effects, and could provide telling information on how these mutations perturb the gating mechanism.

4.8 Methods

4.8.1 Synthesis of dCA-NVOC-5,5-dimethylproline

Synthesis of NVOC-DL-5,5-dimethylproline was adapted from the procedure of Magaard and coworkers[64] (Scheme 4.1).

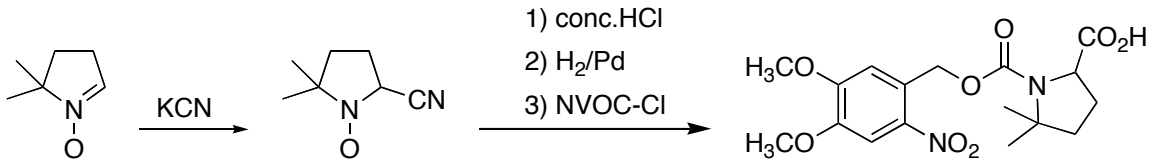

Scheme 4.1 Adapted synthesis of NVOC-DL-5,5-dimethylproline.

4.8.1.1 1-Hydroxy-2-cyano-5,5-dimethylpyrrolidine

KCN (1.15 g, 17.6 mmol) was dissolved in 2.5 mL of water and cooled to –10° C. To this was added 5,5-dimethyl-1-pyrroline N-oxide (1 g, 8.8 mmol) in 2.5 mL of water. 2 N HCl (25 mL) was added dropwise over one hour, then stirred at 0° C for 3 hours and at room temperature overnight. The pH was adjusted to 11 with 6 N KOH and the solution was extracted with diethyl ether. The ether extracts were dried over $MgSO_4$ and rotary evaporated to yield 0.92 g (75% yield) of a white powder. ^{1}H NMR (300 MHz, $CDCl_3$) δ = 1.06 (6H, s), 1.67-1.84 (2H, m), 1.99-2.28 (2H, m), 3.92 (1H, t), 6.25 (1H, s). ^{13}C NMR (75 MHz, $CDCl_3$) δ = 19.4, 34.4, 54.8, 64.4, 120.5. MS Calcd for $C_7H_{11}N_2O$ 139.18. Found: (ESI^+) 141.0 $[M+H^+]^+$.

4.1.1.2 NVOC-DL-5,5-dimethylproline

1-Hydroxy-2-cyano-5,5-dimethylpyrrolidine (400 mg, 2.8 mmol) was hydrolyzed in conc. HCl (1.6 mL) at 50° C for 5 hours and evaporated to a white solid. After evaporating from water two times to remove traces of HCl, the residue was dissolved in 20 mL of methanol/water 1:1 and hydrogenated over 10% Pd/C (120 mg) at 1 atm for 4 hours. The reaction was filtered through celite to remove the catalyst and the solvent was removed by rotary evaporation. The product was then dissolved in 25 mL of water/dioxane 1:1 and Na_2CO_3 (742 mg, 7 mmol) was added. A solution of NVOC-Cl (1.1 g, 3.9 mmol) in 25 mL water/dioxane was added dropwise and the mixture was

allowed to stir. After two hours, 50 mL of CH_2Cl_2 was added followed by 1 M (aq) $KHSO_4$ (25 mL). The aqueous layer was extracted three times with 25 mL CH_2Cl_2. The organic extracts were combined, dried over $MgSO_4$, and the solvent was removed by rotary evaporation. The crude product was purified by flash chromatography (silica, 50:50 hexane/ethyl acetate w/ 1% acetic acid) to give a bright orange solid (210 mg, 20% yield). ^{1}H NMR (300 MHz, $CDCl_3$) δ = 1.40 (3H, s), 1.56 (3H, s), 1.79-2.08 (3H, m), 2.08-2.32 (1H, m), 3.91 (3H, s), 3.94 (3H, s), 4.50-4.56 (1H, m), 5.45 (2H, dd), 6.94 (1H, s), 7.65 (1H, s). ^{13}C NMR (75 MHz, $CDCl_3$) δ = 25.3, 26.3,26.6, 39.5, 56.3, 56.5, 60.8, 61.8, 64.1, 107.9, 109.2, 128.2, 140.4, 147.7, 153.8, 155.1, 178.1. MS Calcd for $C_{17}H_{22}N_2O_8$ 382.37. Found: (ESI$^-$) 381.2 $[M-H]^-$.

4.1.1.3 NVOC-DL-5,5-dimethylproline cyanomethyl ester

Under positive argon pressure, a dried flask was charged with a solution of NVOC-5,5-dimethylproline (75 mg, 0.19 mmol) dissolved in 3 mL of dry DMF. Triethylamine (66 μL, 0.48 mmol) and $ClCH_2CN$ (3 mL, 47 mmol) were added; the reaction was run under a continuous stream of argon. After six hours, the volatiles were removed *in vacuo* and the crude product was purified by flash chromatography (silica, 3/1/hexane/ethyl acetate) to give an orange oil (0.63 mg, 80% yield). ^{1}H NMR (300 MHz, $CDCl_3$) δ = 1.41 (3H, s), 1.57 (3H, s), 1.85-2.04 (3H, m), 2.22-2.38 (1H, m), 3.94 (3H, s) 4.0 (3H, s), 4.54-4.58 (1H, m), 4.76 (2H, q), 5.51 (2H, dd), 6.93 (1H, s), 7.69 (1H, s). ^{13}C NMR (75 MHz, $CDCl_3$) δ = 25.4, 26.4, 27.1, 39.4, 48.9, 56.4, 56.5, 60.5, 61.8, 64.2, 108.2, 109.9, 114.0, 128.3, 139.4, 148.0, 152.3, 153.8, 171.3. MS Calcd for $C_{19}H_{23}N_3O_8$ 421.4. Found: (ESI$^+$) 422.0 $[M+H^+]^+$.

4.1.1.4 dCA-NVOC-DL-5,5-dimethylproline

To a dry flask was added NVOC-5,5-dimethylproline cyanomethyl ester (25 mg, 0.06 mmol), dCA (20 mg), and 0.8 mL of dry DMF, and the reaction was stirred under argon. The reaction was monitored by reverse-phase HPLC. After four hours, the reaction was purified by semi-preparative reverse phase (C_{18}) HPLC. The appropriate fractions were combined and lyophilized. The white powder was dissolved in 10 mM acetic acid and lyophilized. This step was repeated to yield a white fluffy powder (3.3 mg). MS Calcd for $C_{36}H_{45}N_{10}O_{21}P_2$ 1016.75. Found: (ESI^+) 1017.8 $[M+H^+]^+$.

4.1.2 Mutagenesis and preparation of cRNA and Oocytes

Mutant 5-HT_{3A} receptor subunits were developed using the eukaryotic expression vector pcDNA 3.1 (InVitrogen, Abingdon, U.K.) containing the complete coding sequence for the 5-$HT_{3A(b)}$ subunit from NIE-115 cells as previously described.[65] Mutagenesis reactions were performed using the Kunkel method[66], and confirmed by DNA sequencing. Wild type and mutant receptor subunit coding sequences were then subcloned into pGEMHE plasmid.[67] This was linearized with Nhe1 (New England Biolabs) and cRNA synthesized using T7 mMESSAGE mMACHINE kit (Ambion). Oocytes from Xenopus laevis were prepared and maintained according to standard laboratory protocol.

4.1.3 Synthesis of tRNA and dCA-amino acids

Unnatural amino acids were chemically synthesized as nitroveratryloxycarbonyl (NVOC) protected cyanomethyl esters and coupled to the dinucleotide dCA, which was then enzymatically ligated to 74-mer THG73 $tRNA_{CUA}$ as detailed previously [68].

Immediately prior to co-injection with mRNA, tRNA-aa was deprotected by photolysis [69]. Typically, 5 ng mRNA and 25 ng tRNA-aa were injected into Stage V-VI oocytes in a total volume of 50 nl. For control experiments, mRNA was injected 1) in the absence of tRNA and 2) with the THG73 74-mer tRNA. Electrophysiological experiments were performed 18 to 36 hours post injection.

4.1.4 Characterization of mutant receptors

5-HT-induced currents were recorded from individual oocytes using two-electrode voltage clamp with either a GeneClamp 500 amplifier or an OpusXpress system (Axon Instruments, Inc., Union City, CA). All experiments were performed at 22-25º C. Serotonin (creatinine sulphate complex, Sigma) was stored as 25 mM aliquots at –80°C, diluted in calcium-free ND96, and delivered to cells via computer-controlled perfusion systems. Glass microelectrodes were backfilled with 3 M KCl and had a resistance of approximately 1 MΩ. The holding potential was –60 mV unless otherwise specified. To determine EC_{50}s, 5-HT concentration-response data were fitted to the Hill equation, $I = (I_{max}[A]^n)/(EC_{50}{}^n + [A]^n)$,where I_{max} is the maximal peak current, [*A*] is the concentration of agonist, and n is the Hill coefficient.

4.9 References

1. Lummis, S. C. R., The transmembrane domain of the 5-HT3 receptor: its role in selectivity and gating. *Biochemical Society Transactions* **2004,** 32, 535-539.
2. Absalom, N. L.; Lewis, T. M.; Schofield, P. R., Mechanisms of channel gating of the ligand-gated ion channel superfamily inferred from protein structure. *Experimental Physiology* **2004,** 89, (2), 145-153.
3. Lester, H. A.; Dibas, M. I.; Dahan, D. S.; Leite, J. F.; Dougherty, D. A., Cys-loop receptors: new twists and turns. *Trends in Neurosciences* **2004,** 27, (6), 329-336.
4. Brejc, K.; van Dijk, W. J.; Klaassen, R. V.; Schuurmans, M.; van der Oost, J.; Smit, A. B.; Sixma, T. K., Crystal structure of an ACh-binding protein reveals the ligand-binding domain of nicotinic receptors. *Nature* **2001,** 411, (6835), 269-276.
5. Celie, P. H. N.; van Rossum-Fikkert, S. E.; van Dijk, W. J.; Brejc, K.; Smit, A. B.; Sixma, T. K., Nicotine and carbamylcholine binding to nicotinic acetylcholine receptors as studied in AChBP crystal structures. *Neuron* **2004,** 41, (6), 907-914.

6. Miyazawa, A.; Fujiyoshi, Y.; Unwin, N., Structure and gating mechanism of the acetylcholine receptor pore. *Nature* **2003,** 423, (6943), 949-955.
7. Dougherty, D. A.; Lester, H. A., Neurobiology - Snails, synapses and smokers. *Nature* **2001,** 411, (6835), 252-254.
8. Kash, T. L.; Jenkins, A.; Kelley, J. C.; Trudell, J. R.; Harrison, N. L., Coupling of agonist binding to channel gating in the GABA(A) receptor. *Nature* **2003,** 421, (6920), 272-275.
9. Bouzat, C.; Gumilar, F.; Spitzmaul, G.; Wang, H. L.; Rayes, D.; Hansen, S. B.; Taylor, P.; Sine, S. M., Coupling of agonist binding to channel gating in an ACh-binding protein linked to an ion channel. *Nature* **2004,** 430, (7002), 896-900.
10. Absalom, N. L.; Lewis, T. M.; Kaplan, W.; Pierce, K. D.; Schofield, P. R., Role of charged residues in coupling ligand binding and channel activation in the extracellular domain of the glycine receptor. *Journal of Biological Chemistry* **2003,** 278, (50), 50151-50157.
11. Beckstein, O., Tai, K., and Sansom, M.P., Not Ions Alone: Barriers to Ion Permeation in Nanopores and Channels. *Journal of the American Chemical Society* **2004,** 126, (45), 14695-14696.
12. Reeves, D. C.; Goren, E. N.; Akabas, M. H.; Lummis, S. C. R., Structural and electrostatic properties of the 5-HT3 receptor pore revealed by substituted cysteine accessibility mutagenesis. *Journal of Biological Chemistry* **2001,** 276, (45), 42035-42042.
13. Akabas, M. H.; Kaufmann, C.; Archdeacon, P.; Karlin, A., Identification of Acetylcholine-Receptor Channel-Lining Residues in the Entire M2 Segment of the Alpha-Subunit. *Neuron* **1994,** 13, (4), 919-927.
14. Unwin, N., Nicotinic Acetylcholine-Receptor at 9-Angstrom Resolution. *Journal of Molecular Biology* **1993,** 229, (4), 1101-1124.
15. Labarca, C.; Nowak, M. W.; Zhang, H.; Tang, L.; Deshpande, P.; Lester, H. A., Channel gating governed symmetrically by conserved leucine residues in the M2 domain of nicotinic receptors. *Nature* **1995,** 376, (6540), 514-6.
16. Bera, A. K.; Chatav, M.; Akabas, M. H., GABA(A) receptor M2-M3 loop secondary structure and changes in accessibility during channel gating. *Journal of Biological Chemistry* **2002,** 277, (45), 43002-43010.
17. Wick, M. J.; Mihic, S. J.; Ueno, S.; Mascia, M. P.; Trudell, J. R.; Brozowski, S. J.; Ye, Q.; Harrison, N. L.; Harris, R. A., Mutations of gamma-aminobutyric acid and glycine receptors change alcohol cutoff: Evidence for an alcohol receptor? *Proceedings of the National Academy of Sciences of the United States of America* **1998,** 95, (11), 6504-6509.
18. Rovira, J. C.; Ballesta, J. J.; Vicente-Agullo, F.; Campos-Caro, A.; Criado, M.; Sala, F.; Sala, S., A residue in the middle of the M2-M3 loop of the beta(4) subunit specifically affects gating of neuronal nicotinic receptors. *Febs Letters* **1998,** 433, (1-2), 89-92.
19. Rovira, J. C.; Vicente-Agullo, F.; Campos-Caro, A.; Criado, M.; Sala, F.; Sala, S.; Ballesta, J. J., Gating of alpha(3)beta(4) neuronal nicotinic receptor can be controlled by the loop M2-M3 of both alpha(3) and beta(4) subunits. *Pflugers Archiv-European Journal of Physiology* **1999,** 439, (1-2), 86-92.
20. Lynch, J. W.; Rajendra, S.; Pierce, K. D.; Handford, C. A.; Barry, P. H.; Schofield, P. R., Identification of intracellular and extracellular domains mediating signal transduction in the inhibitory glycine receptor chloride channel. *Embo Journal* **1997,** 16, (1), 110-120.
21. Lynch, J. W.; Rajendra, S.; Barry, P. H.; Schofield, P. R., Mutations Affecting the Glycine Receptor Agonist Transduction Mechanism Convert the Competitive Antagonist, Picrotoxin, into an Allosteric Potentiator. *Journal of Biological Chemistry* **1995,** 270, (23), 13799-13806.
22. CamposCaro, A.; Sala, S.; Ballesta, J. J.; VicenteAgullo, F.; Criado, M.; Sala, F., A single residue in the M2-M3 loop is a major determinant of coupling between binding and gating in neuronal nicotinic receptors. *Proceedings of the National Academy of Sciences of the United States of America* **1996,** 93, (12), 6118-6123.
23. Grosman, C.; Salamone, F. N.; Sine, S. M.; Auerbach, A., The extracellular linker of muscle acetylcholine receptor channels is a gating control element. *Journal of General Physiology* **2000,** 116, (3), 327-339.
24. Lynch, J. W.; Han, N. L. R.; Haddrill, J.; Pierce, K. D.; Schofield, P. R., The surface accessibility of the glycine receptor M2-M3 loop is increased in the channel open state. *Journal of Neuroscience* **2001,** 21, (8), 2589-2599.
25. Macarthur, M. W.; Thornton, J. M., Influence of Proline Residues on Protein Conformation. *Journal of Molecular Biology* **1991,** 218, (2), 397-412.

26. Chakrabarti, P.; Pal, D., The interrelationships of side-chain and main-chain conformations in proteins. *Progress in Biophysics & Molecular Biology* **2001,** 76, (1-2), 1-102.
27. Brandl, C. J.; Deber, C. M., Hypothesis About the Function of Membrane-Buried Proline Residues in Transport Proteins. *Proceedings of the National Academy of Sciences of the United States of America* **1986,** 83, (4), 917-921.
28. Sansom, M. S. P.; Weinstein, H., Hinges, swivels and switches: the role of prolines in signalling via transmembrane alpha-helices. *Trends in Pharmacological Sciences* **2000,** 21, (11), 445-451.
29. Tieleman, D. P.; Shrivastava, I. H.; Ulmschneider, M. R.; Sansom, M. S. P., Proline-induced hinges in transmembrane helices: Possible roles in ion channel gating. *Proteins-Structure Function and Genetics* **2001,** 44, (2), 63-72.
30. Williams, K. A.; Deber, C. M., Proline Residues in Transmembrane Helices - Structural or Dynamic Role. *Biochemistry* **1991,** 30, (37), 8919-8923.
31. Partridge, A. W.; Therien, A. G.; Deber, C. M., Missense mutations in transmembrane domains of proteins: Phenotypic propensity of polar residues for human disease. *Proteins-Structure Function and Bioinformatics* **2004,** 54, (4), 648-656.
32. Sankararamakrishnan, R.; Vishveshwara, S., Geometry of Proline-Containing Alpha-Helices in Proteins. *International Journal of Peptide and Protein Research* **1992,** 39, (4), 356-363.
33. Senes, A.; Engel, D. E.; DeGrado, W. F., Folding of helical membrane proteins: the role of polar, GxxxG-like and proline motifs. *Current Opinion in Structural Biology* **2004,** 14, (4), 465-479.
34. Deber, C. M.; Glibowicka, M.; Woolley, G. A., Conformations of Proline Residues in Membrane Environments. *Biopolymers* **1990,** 29, (1), 149-157.
35. Deane, C. M.; Lummis, S. C. R., The role and predicted propensity of conserved proline residues in the 5-HT3 receptor. *Journal of Biological Chemistry* **2001,** 276, (41), 37962-37966.
36. Pal, D.; Chakrabarti, P., Cis peptide bonds in proteins: Residues involved, their conformations, interactions and locations. *Journal of Molecular Biology* **1999,** 294, (1), 271-288.
37. Bhattacharyya, R.; Chakrabarti, P., Stereospecific interactions of proline residues in protein structures and complexes. *Journal of Molecular Biology* **2003,** 331, (4), 925-940.
38. Andreotti, A. H., Native state proline isomerization: An intrinsic molecular switch. *Biochemistry* **2003,** 42, (32), 9515-9524.
39. Mallis, R. J.; Brazin, K. N.; Fulton, D. B.; Andreotti, A. H., Structural characterization of a proline-driven conformational switch within the Itk SH2 domain. *Nature Structural Biology* **2002,** 9, (12), 900-905.
40. Martin, A.; Schmid, F. X., A proline switch controls folding and domain interactions in the gene-3-protein of the filamentous phage fd. *Journal of Molecular Biology* **2003,** 331, (5), 1131-1140.
41. Gitti, R. K.; Lee, B. M.; Walker, J.; Summers, M. F.; Yoo, S.; Sundquist, W. I., Structure of the amino-terminal core domain of the HIV-1 capsid protein. *Science* **1996,** 273, (5272), 231-235.
42. Suchyna, T. M.; Xu, L. X.; Gao, F.; Fourtner, C. R.; Nicholson, B. J., Identification of a Proline Residue as a Transduction Element Involved in Voltage Gating of Gap-Junctions. *Nature* **1993,** 365, (6449), 847-849.
43. Demene, H.; Granier, S.; Muller, D.; Guillon, G.; Dufour, M. N.; Delsuc, M. A.; Hibert, M.; Pascal, R.; Mendre, C., Active peptidic mimics of the second intracellular loop of the V-1A vasopressin receptor are structurally related to the second intracellular rhodopsin loop: A combined H-1 NMR and biochemical study. *Biochemistry* **2003,** 42, (27), 8204-8213.
44. Beausoleil, E.; Sharma, R.; Michnick, S. W.; Lubell, W. D., Alkyl 3-position substituents retard the isomerization of prolyl and hydroxyprolyl amides in water. *Journal of Organic Chemistry* **1998,** 63, (19), 6572-6578.
45. Dugave, C.; Demange, L., Cis-trans isomerization of organic molecules and biomolecules: Implications and applications. *Chemical Reviews* **2003,** 103, (7), 2475-2532.
46. Kern, D.; Schutkowski, M.; Drakenberg, T., Rotational barriers of cis/trans isomerization of proline analogues and their catalysis by cyclophilin. *Journal of the American Chemical Society* **1997,** 119, (36), 8403-8408.
47. Renner, C.; Alefelder, S.; Bae, J. H.; Budisa, N.; Huber, R.; Moroder, L., Fluoroprolines as tools for protein design and engineering. *Angewandte Chemie-International Edition* **2001,** 40, (5), 923-925.
48. An, S. S. A.; Lester, C. C.; Peng, J. L.; Li, Y. J.; Rothwarf, D. M.; Welker, E.; Thannhauser, T. W.; Zhang, L. S.; Tam, J. P.; Scheraga, H. A., Retention of the cis proline conformation in tripeptide fragments of bovine pancreatic ribonuclease A containing a non-natural proline analogue, 5,5-dimethylproline. *Journal of the American Chemical Society* **1999,** 121, (49), 11558-11566.

49. Delaney, N. G.; Madison, V., Novel Conformational Distributions of Methylproline Peptides. *Journal of the American Chemical Society* **1982,** 104, (24), 6635-6641.
50. Hunston, R. N.; Gerothanassis, I. P.; Lauterwein, J., A Study of L-Proline, Sarcosine, and the Cis Trans Isomers of N-Acetyl-L-Proline and N-Acetylsarcosine in Aqueous and Organic Solution by O-17 Nmr. *Journal of the American Chemical Society* **1985,** 107, (9), 2654-2661.
51. Dang, H.; England, P. M.; Farivar, S. S.; Dougherty, D. A.; Lester, H. A., Probing the role of a conserved M1 proline residue in 5-hydroxytryptamine(3) receptor gating. *Molecular Pharmacology* **2000,** 57, (6), 1114-1122.
52. England, P. M.; Zhang, Y. N.; Dougherty, D. A.; Lester, H. A., Backbone mutations in transmembrane domains of a ligand-gated ion channel: Implications for the mechanism of gating. *Cell* **1999,** 96, (1), 89-98.
53. Improta, R.; Benzi, C.; Barone, V., Understanding the role of stereoelectronic effects in determining collagen stability. 1. A quantum mechanical study of proline, hydroxyproline, and fluoroproline dipeptide analogues in aqueous solution. *Journal of the American Chemical Society* **2001,** 123, (50), 12568-12577.
54. Matsui, S.; Srivastava, V. P.; Holt, E. M.; Taylor, E. W.; Stammer, C. H., Synthesis and Conformational-Analysis of L-Aspartylproline and L-Aspartyl-2,3-Methanoproline Propyl Esters. *International Journal of Peptide and Protein Research* **1991,** 37, (4), 306-314.
55. Nowak, M. W.; Gallivan, J. P.; Silverman, S. K.; Labarca, C. G.; Dougherty, D. A.; Lester, H. A., In vivo incorporation of unnatural amino acids into ion channels in Xenopus oocyte expression system. *Methods in Enzymology* **1998,** 293, 504-529.
56. Reimer, U.; Fischer, G., Local structural changes caused by peptidyl-prolyl cis/trans isomerization in the native state of proteins. *Biophysical Chemistry* **2002,** 96, (2-3), 203-212.
57. Milnerwhite, E. J.; Bell, L. H.; Maccallum, P. H., Pyrrolidine Ring Puckering in Cis and Trans-Proline Residues in Proteins and Polypeptides - Different Puckers Are Favored in Certain Situations. *Journal of Molecular Biology* **1992,** 228, (3), 725-734.
58. DeRider, M. L.; Wilkens, S. J.; Waddell, M. J.; Bretscher, L. E.; Weinhold, F.; Raines, R. T.; Markley, J. L., Collagen stability: Insights from NMR spectroscopic and hybrid density functional computational investigations of the effect of electronegative substituents on prolyl ring conformations. *Journal of the American Chemical Society* **2002,** 124, (11), 2497-2505.
59. Petersson, E. J.; Shahgholi, M.; Lester, H. A.; Dougherty, D. A., MALDI-TOF mass spectrometry methods for evaluation of in vitro aminoacyl tRNA production. *Rna-a Publication of the Rna Society* **2002,** 8, (4), 542-547.
60. Spier, A. D.; Wotherspoon, G.; Nayak, S. V.; Nichols, R. A.; Priestley, J. V.; Lummis, S. C. R., Antibodies against the extracellular domain of the 5-HT3 receptor label both native and recombinant receptors. *Molecular Brain Research* **1999,** 67, (2), 221-230.
61. Cox, C.; Lectka, T., Intramolecular catalysis of amide isomerization: Kinetic consequences of the 5-NH- -N-a hydrogen bond in prolyl peptides. *Journal of the American Chemical Society* **1998,** 120, (41), 10660-10668.
62. Rankin, K. N.; Boyd, R. J., A computational study of the isomerization of prolyl amides as catalyzed by intramolecular hydrogen bonding. *Journal of Physical Chemistry A* **2002,** 106, (46), 11168-11172.
63. Helekar, S. A.; Patrick, J., Peptidyl prolyl cis-trans isomerase activity of cyclophilin A in functional homo-oligomeric receptor expression. *Proceedings of the National Academy of Sciences of the United States of America* **1997,** 94, (10), 5432-5437.
64. Magaard, V. W.; Sanchez, R. M.; Bean, J. W.; Moore, M. L., A Convenient Synthesis of the Conformationally Constrained Amino-Acid 5,5-Dimethylproline. *Tetrahedron Letters* **1993,** 34, (3), 381-384.
65. Hargreaves, A. C.; Gunthorpe, M. J.; Taylor, C. W.; Lummis, S. C. R., Direct inhibition of 5-hydroxytryptamine(3) receptors by antagonists of L-type Ca2+ channels. *Molecular Pharmacology* **1996,** 50, (5), 1284-1294.
66. Kunkel, T. A., Rapid and Efficient Site-Specific Mutagenesis without Phenotypic Selection. *Proceedings of the National Academy of Sciences of the United States of America* **1985,** 82, (2), 488-492.
67. Liman, E. R.; Tytgat, J.; Hess, P., Subunit Stoichiometry of a Mammalian K+ Channel Determined by Construction of Multimeric Cdnas. *Neuron* **1992,** 9, (5), 861-871.
68. Nowak, M. W.; Gallivan, J. P.; Silverman, S. K.; Labarca, C. G.; Dougherty, D. A.; Lester, H. A., In vivo incorporation of unnatural amino acids into ion channels in Xenopus oocyte expression system. *Methods Enzymol* **1998,** 293, 504-29.

69. Kearney, P. C.; Nowak, M. W.; Zhong, W.; Silverman, S. K.; Lester, H. A.; Dougherty, D. A., Dose-response relations for unnatural amino acids at the agonist binding site of the nicotinic acetylcholine receptor: tests with novel side chains and with several agonists. *Mol Pharmacol* **1996,** 50, (5), 1401-12.

Chapter 5. Miscellaneous studies

5.1 Introduction

This chapter contains several miscellaneous studies. These studies represent work that is either in its initial stages or yielded not so interesting results. Two of the studies related in this chapter examine aromatic residues at the ligand-binding site in the Cys loop receptors. These studies were done in collaboration with the Sarah Lummis group at the University of Cambridge. The first study describes investigations of Tyr 198 in the gamma-amino butyric acid C receptor ($GABA_C$). This tyrosine aligns with Trp α149 in the nAChR, and the study of Tyr 198 represents ongoing efforts by our group to characterize the nature of the cation-π interaction in ligand recognition at Cys loop receptors. The second study examines Phe 226 in 5-HT_3R with a series of phenylalanine analogs. This residue aligns with Tyr 190 in the nAChR. This study completes the survey of the aromatic box in the 5-HT_3R. The final study considered in this chapter represents initial efforts to incorporate a backbone thioamide via nonsense suppression methods. This project is now in the capable hands of Lori Lee.

5.2 $GABA_C$ studies

5.2.1 Background

GABA is the main inhibitory neurotransmitter in the nervous system where its action is mediated by three classes of receptors: $GABA_A$, $GABA_B$, and $GABA_C$.[1-3] The $GABA_B$ receptor is a G-protein coupled receptor, while both $GABA_A$ and $GABA_C$ receptors belong to the Cys loop family of ligand-gated ion channels (LGIC). In contrast

to the nAChR and 5-HT_3R, these are anion-selective ion channels. The $GABA_A$ receptor is the major inhibitory LGIC in the peripheral and central nervous system.[1] The $GABA_C$ receptor is much less prominent and found primarily in the retina, with lower levels in the brain and spinal cord.[1, 4, 5] Three subunits for the $GABA_C$ receptor have thus far been identified (ρ1-ρ3). These can all form functional homomeric receptors, and the ρ1 and ρ2 subunits can coassemble to form heteromeric receptors. [2] The $GABA_C$ receptor displays a distinct physiology and pharmacology from that of $GABA_A$. $GABA_C$ has a higher sensitivity to GABA, does not desensitize, and is insensitive to benzodiazepines, barbiturates, and bicuculline.[6-10]

5.1.2 The ligand-binding site

Based on homology to the nAChR and AChBP, the ligand-binding site in the $GABA_C$ receptor is believed to be located at subunit interfaces with the primary ligand-binding determinants being contributed by residues in five noncontiguous loops, labeled A-E.[1, 3] As with other receptors in the Cys loop family, there is a predominance of aromatic residues at the $GABA_C$ binding site. The x-ray crystal structure of AChBP shows the configuration of these residues to be an 'aromatic box' (Figure 5.1a).[11] In $GABA_C$, four of the five aromatics that comprise the box are conserved (Figure 5.1b). Previous work by our group has demonstrated that the loop B tryptophans in the nAChR (Trp α149) and 5-HT_3R (Trp 183) bind the respective agonists of these receptors via a cation-π interaction.[12, 13] Interestingly, the aligning residue in $GABA_C$ is Tyr 198. In the MOD-1 receptor, another member of the Cys loop family— the loop B residue is also a tyrosine. Here, however, research from our group has demonstrated that the cation-π site is located in loop C at Trp 226.[14] Like the nAChR and 5-HT_3R, this loop C residue is a

tyrosine (Tyr 241) in $GABA_C$. In fact, all residues that form the aromatic box in $GABA_C$ are tyrosines (Figure 5.1b). While the indole ring of tryptophan exhibits the greatest affinity for cations among the standard aromatic residues, the phenolic side chain of tyrosine is also capable of forming strong cation-π interactions.

(a)

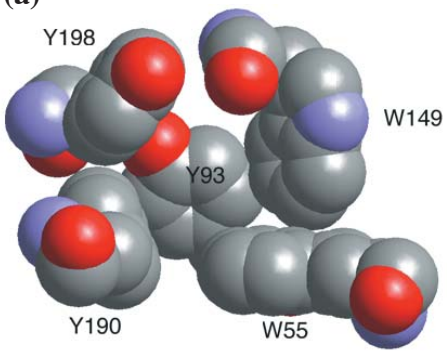

(b)

	Loop			
Receptor	**B**	**C1**	**C2**	**D**
nAChR	W149	Y190	Y198	W55
AChBP	W143	Y185	Y192	W53
5-HT_3R	W183	F226	Y234	W90
MOD-1	Y180	Y221	W226	F83
$GABA_C$	Y198	Y241	Y247	Y102

Figure 5.1. Residues at the ligand-binding site in Cys loop LGIC. (a) The aromatic box from the x-ray crystal structure of AChBP. Residue numbering is for muscle nAChR. (b) Alignment of conserved residues in the aromatic box contributed by loops B-D. Red residues represent cation-π binding sites.

In the work presented here a series of fluorinated phenylalanines (4-F-Phe, 3,5-F_2-Phe, 3,4,5-F_3-Phe) is incorporated at position 198 of $GABA_C$ to probe the possible role of this site in binding the ammonium center of GABA via a cation-π interaction (Figure 5.2). The cation-π interaction is a noncovalent binding interaction between the negative electrostatic potential on the face of an aromatic ring and a cation, and as such, is sensitive to perturbation of the ring's electrostatic potential.[15] Thus, the strength of the cation-π interaction can be serially modulated by progressive fluorination of the aromatic ring.

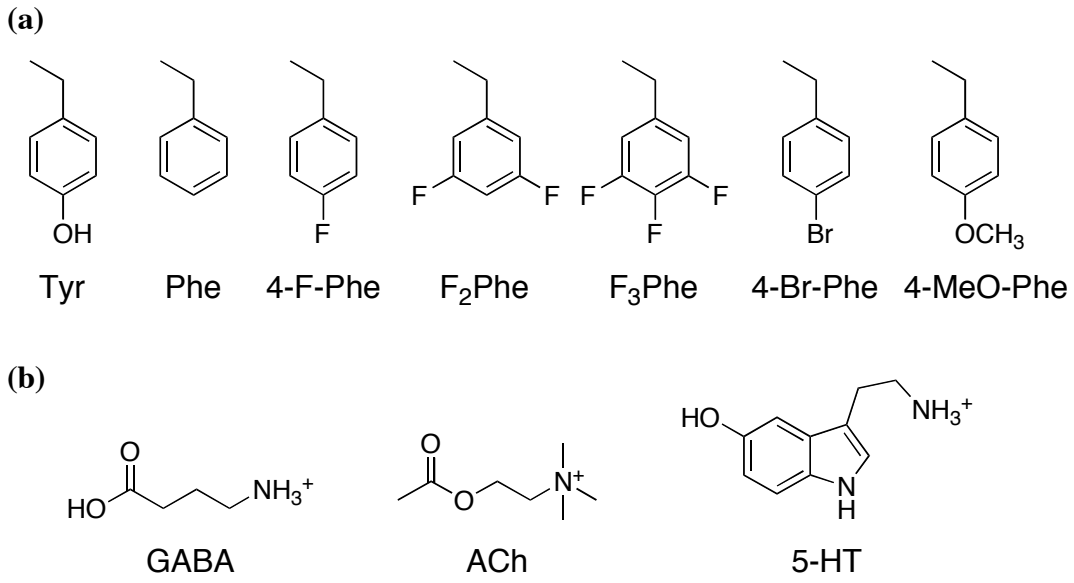

Figure 5.2. (a) Amino acids incorporated at Tyr 198 in $GABA_C$ using nonsense suppression methods. (b) Agonists discussed in the text.

5.1.3 Results and discussion

The unnatural and natural amino acids used in this study were incorporated at position 198 of $GABA_C$ using *in vivo* nonsense suppression methods.[16, 17] The specific $GABA_C$ subtype examined in these studies is the homomeric mouse receptor formed from ρ1 subunits. Initial studies focused on the important controls of nonsense suppression, ensuring no functional receptors are produced in the absence of charged aminoacyl tRNA and rescue of the wild type receptor by reintroduction of tyrosine. Oocytes injected with 198 UAG-containing mRNA only or with UAG-containing mRNA and uncharged tRNA did not show any inducible currents with application of 1 mM GABA, indicating that any readthrough of the mRNA does not produce functional receptors. Injection of oocytes with 198 UAG-containing mRNA and tRNA-Tyr produced receptors with wild type characteristics: EC_{50} values around 2.0 μM and Hill coefficients near 2.5 (Table 5.1).

Incorporation of Phe at 198 leads to a 6-fold increase in EC_{50} (Figure 5.3 and Table 5.1). This is similar to previously published work, where the Phe 198 Tyr mutation yielded an 11-fold increase in EC50.[6] The role of the hydroxyl oxygen was assessed using 4-MeO-Phe and 4-Br-Phe. The unnatural amino acid 4-MeO-Phe maintains an oxygen atom at the 4 position of the ring, which can act as a hydrogen-bond acceptor, but cannot function as a hydrogen bond donor. 4-Br-Phe was used as a measure of the steric requirements of this site. The bromo group is larger than a hydroxyl group, but roughly similar in size to the methoxy group. In addition, 4-Br-Phe and 4-F-Phe bind cations with comparable affinity. Incorporation of 4-MeO-Phe and 4-Br-Phe at 198 resulted in 3- and 4-fold increases in EC_{50}, respectively. Relative to Phe, these mutations show a partial rescue of wild type function, suggesting that both the size of the substituent and the presence of an oxygen at the 4 position of the ring are important.

Before discussing the results from incorporation of the fluorinated phenylalanine series, several important details should be noted. In studies examining tryptophan cation-π sites, the baseline for evaluating the functional effects produced by fluorination is the wild type receptor.[12-14] Tyrosine, however, contains an ionizable hydroxyl group. Fluorination of the phenol ring would lower the pKa of this group and could result in a phenolate anion at this position. Consequently, in considering tyrosine sites, it is necessary to use the fluorinated phenylalanine series which eliminates this complication. The baseline for evaluating the effects of fluorination in these studies, however, is the phenylalanine mutant, and not the wild type residue. This is a reasonable comparison, as phenylalanine and tyrosine bind cations with similar affinity, and any effects arising from

the absence of the hydroxyl group will likely be consistent across the series of phenylalanine derivatives.

Table 5.1. Dose-response data for suppression at 198 in $GABA_C$

Residue	Cation-π binding (kcal/mol)	EC_{50}±SEM (μM)	Hill±SEM
Tyr	26.9	2.1 ± 0.11	2.46 ± 0.25
Phe	27.1	14.0 ± 1.11	2.63 ± 0.43
4-F-Phe	22.0	33.5 ± 4.83	1.9 ± 0.29
F_2Phe	17.1	1631 ± 96	1.95 ± 0.35
F_3Phe	12.9	8550 ± 303	1.55 ± 0.18
4-Br-Phe		9.2 ± 0.08	0.68 ± 0.12
4-MeO-Phe		6.6 ± 0.05	0.66 ± 0.09

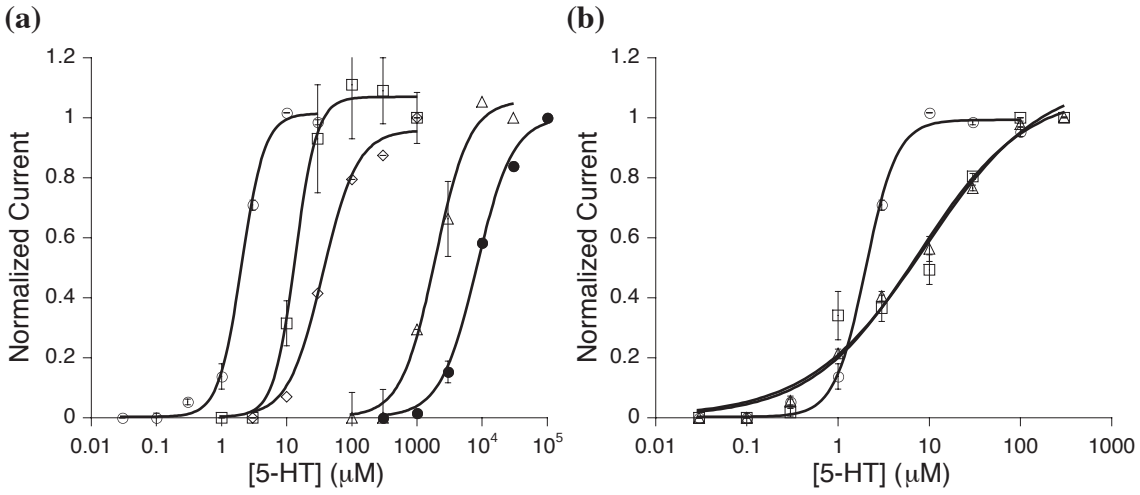

Figure 5.3. Dose-response relations for suppression experiments at 198 in $GABA_C$. (a) Tyr (*open circles*), Phe (*open squares*), 4-F-Phe (*open diamonds*), F_2Phe (*open triangles*), and F_3Phe (*filled circles*). (b) Tyr (*open circles*), 4-Br-Phe (*open squares*), 4-MeO-Phe (*open triangles*)

The dose-response data for incorporation of the fluorinated phenylalanine series shows a clear trend (Figure 5.3 and Table 5.1). Each additional fluorine leads to a concomitant rise in EC_{50}. As in previous work on the nAChR and 5-HT_3R, our measure for the cation-π binding ability of the fluorinated derivatives is the calculated binding

energy (kcal/mol) of a generic probe cation (Na^+) to the corresponding substituted benzene ring.[12-14] Extensive studies of the cation-π interaction establish that *trends* in cation-π binding ability across a series of aromatics are independent of the identity of the cation, justifying the use of a simple probe ion.[15] The calculations for Phe and 4-F-Phe were performed by Sandro Mecozzi and Anthony West[18], and the calculations for 3,5-F_2-Phe and 3,4,5-F_3-Phe were performed by Dennis Dougherty (unpublished results). The fluorination plot (a plot of log EC_{50} versus the calculated cation binding ability of the fluorinated derivatives; see Chapter 2 for details) for these data shows a compelling relationship (Figure 5.4). Over a range of greater than three orders of magnitude in EC_{50}, there is a linear correlation between log EC_{50} (using log EC_{50} to put the EC_{50} data on an energy scale) and the cation-π binding ability of the side chains. This provides substantial evidence that Tyr 198 binds GABA through a cation-π interaction arising from van der Waals contact between the agonist ammonium group and the aromatic side chain.

These findings provide further evidence that the cation-π interaction is a common recognition strategy for agonist binding in the Cys loop receptors. Four members in this family have now been shown to bind their respective ligands through a cation-π interaction.[12-14] Tyr 198 in $GABA_C$ represents the first tyrosine residue to be identified as a cation-π site using fluorinated unnatural amino acids. This study also emphasizes the uniqueness of MOD-1, as $GABA_C$ follows the trend of the nAChR and the 5-HT_3R with the location of the cation-π site in loop B (Figure 5.1). Inspection of the fluorination plot in Figure 5.4b shows that the line for GABA has a similar slope as 5-HT (in both the 5-HT_3R and MOD-1). This supports the idea that, given the large electrostatic component

of the cation-π interaction, primary ammonium groups (Figure 5.2) are more sensitive to electronic perturbation of their aromatic binding partner.[12]

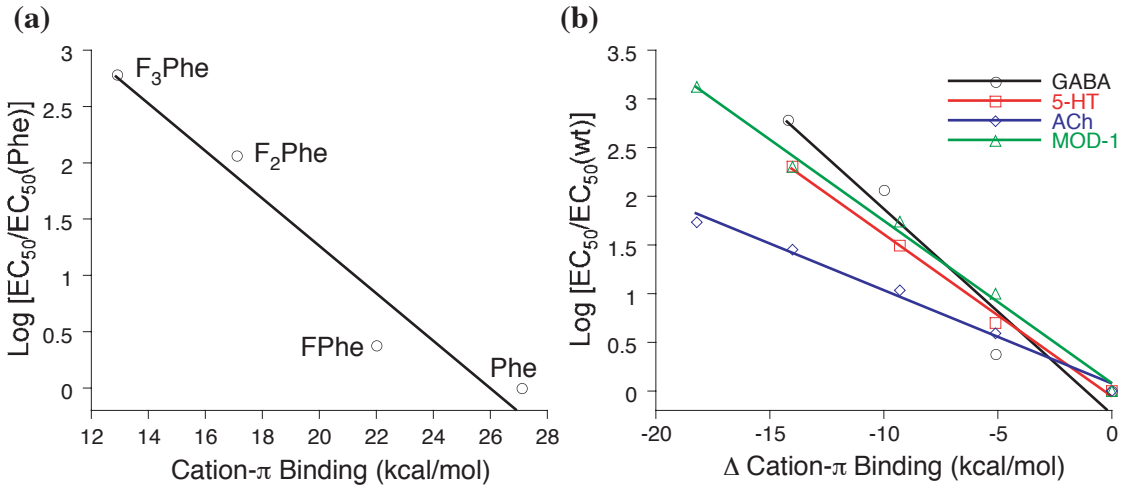

Figure 5.4. Analysis of the cation-π studies in Cys loop LGIC. (a) Fluorination plot for fluoro-Phe series at 198 in $GABA_C$ (the equation for the linear fit is $y = 5.5 - 0.21x$). (b) Fluorination plot for all LGICs with cation-π sites. Two different series of fluorinated aromatics are shown in this plot, thus the *x-axis* reflects the relative binding affinity of each residue in a series. For ACh, 5-HT, and MOD-1 (also 5-HT but different receptor) the data points correspond to fluoro-Trp series and right to left are: Trp, FTrp, F_2Trp, F_3Trp, and F_4Trp. For GABA the plot is for fluoro-Phe series and right to left are: Phe, Fphe, F_2Phe, and F_3Phe.

5.2 Phe 226 in the 5-HT_3R

In the 5-HT_3R, four of the five residues at the aromatic box are conserved (Figure 5.1). In previous work (Chapter 2 and 3), we have examined all but Phe 226.[12, 19] This residue is located in loop C and aligns with Tyr 190 in the nAChR. The functional role of Phe 226 was examined using a series of phenylalanine analogs incorporated via nonsense suppression methods (Figure 5.5).[16, 17]

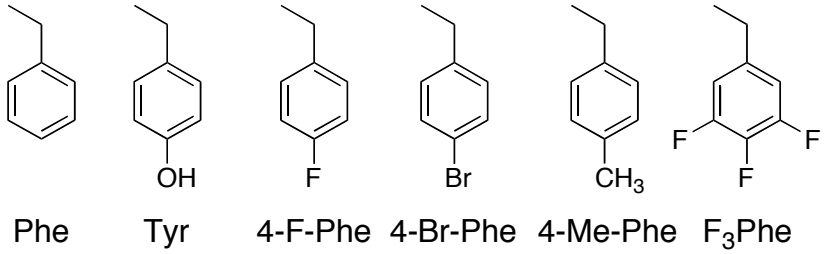

Figure 5.5. Residues used in the study of Phe 226 in 5-HT_3R

Reintroduction of phenylalanine at position 226 produced receptors with an EC_{50} value similar to wild type, 1.6 μM (Table 5.2). Injection of mRNA alone or with uncharged tRNA did not yield functional receptors. The dose-response results for substitution of Phe 226 indicate this is not an overly important position. Incorporation of 4-Me-Phe or 4-Br-Phe leads to a 9-fold increase in EC_{50}. The similarity in results observed for these two unnaturals suggests this increase in EC_{50} is likely a steric effect, and not due to modulation of electrostatic potential on the aromatic ring. This conclusion is supported by the small increase in EC_{50} seen in the 4-F-Phe mutant (4-fold increase.) Interestingly, incorporation of Tyr at 226 leads to a small decrease in EC_{50}. This group of mutations shows Phe 226 is quite tolerant to a variety of substitutions at the 4 position of the aromatic ring.

Table 5.2. Dose-response data for Suppression at 226

Residue	**EC_{50}±SEM (μM)**
Phe	1.6 ± 0.3
Tyr	1.0 ± 0.1
Ala	23.7 ± 5.3
4-Me-Phe	14.3 ± 3.2
4-Br-Phe	14.7 ± 2.4
4-F-Phe	7.1 ± 0.8
F_3-Phe	>300

Two mutations did, however, lead to larger increases in EC_{50}, Ala and F_3-Phe. These lead to 23- and >200-fold increases, respectively. The fact that Ala was less perturbing than F_3Phe is noteworthy in that completely removing the ring has a smaller effect than maintaining the steric size of the ring, but altering the electrostatic potential on the ring. It is also somewhat puzzling that electron–withdrawing groups at the 4 position of the ring are well tolerated, but either the combined effect of three such groups in F_3-Phe or their specific placement on the ring (at positions 3,4, and 5) leads to a large perturbation in receptor function. The latter possibility suggests a specific interaction with one of the ring hydrogens at position 3 or 5.

In the homology model of the 5-HT_3R with 5-HT computationally docked at the binding site, the side chain of Phe 226 is located very near the indole ring of 5-HT (Figure 5.6).[20] The model does not, however, point to any special role for Phe 226. The findings at Phe 226 are quite distinct from what was observed at Tyr 190 in nAChR.[21] Similar substitutions here ablate receptor function or cause large increases in EC_{50}, indicating both the hydroxyl and the aromatic group are critical. These studies demonstrate that there are subtle differences in the functional role of binding-site residues among the receptors in the Cys loop family.

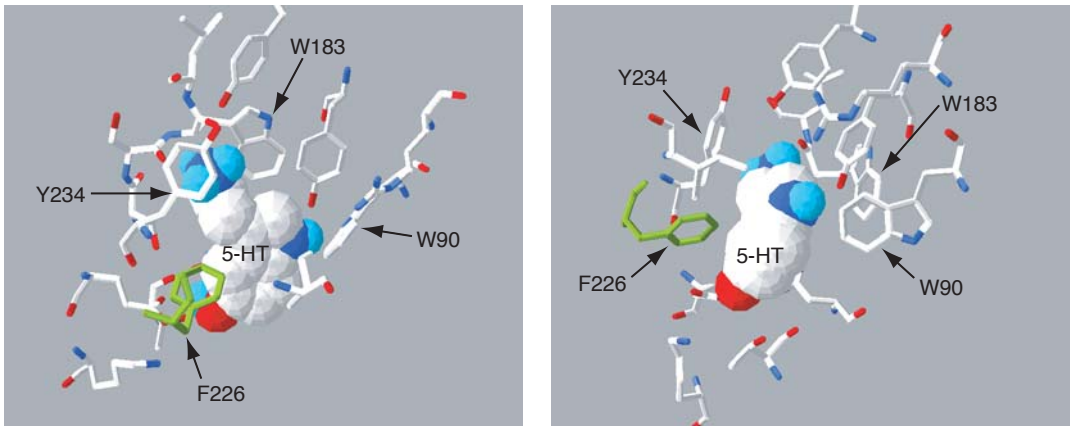

Figure 5.6. Homology model of the 5-HT_3R with 5-HT computationally docked at the ligand-binding site. Phe 226 is shown in green.

5.3 Efforts towards the incorporation of a backbone thioamide

5.3.1 Background

A powerful use of the nonsense suppression method is the introduction of backbone mutations. To date, the method has proven amenable to the incorporation of esters, aza-amides, and oxy-amides into the protein backbone (Figure 5.7a).[22-24] These mutations can be used to probe the hydrogen-bonding properties and local secondary structure at main chain sites. Thus far, the incorporation of backbone mutations has been limited to modifications at the amide nitrogen. Incorporation of a backbone thioamide group represents a potential backbone mutation with modification at the amide oxygen (Figure 5.7b).

The thioamide group has been widely used in the solid-phase synthesis of small peptides for peptidomimetic studies.[25-32] Introduction of a thioamide into the main chain of the protein alters the hydrogen-bonding properties of the protein backbone.[33] Relative to the standard peptide bond, the thioamide carbonyl is a weaker hydrogen-bond acceptor

and the thioamide NH is a stronger hydrogen-bond donor. Thus, in studies of backbone hydrogen-bonding, the thioamide would be a useful complement to main chain ester mutations which remove the hydrogen-bond donor at the amide nitrogen position. In addition, the increased C=S bond length (1.65 Å versus 1.2 Å for C=O) and larger van der Waals radius of the sulfur atom (0.45 Å greater than oxygen) lead to a widening of secondary structure and results in a loss of conformational freedom in the protein backbone.[31, 34, 35] Studies have demonstrated, however, that main chain thioamides do not significantly destabilize α-helices or β-sheets.[26, 27, 31] One particularly attractive feature of the thioamide group is that substitution of oxygen by sulfur in an amide bond leads to significantly red-shifted π–π* and n-π* absorptions, lowering the excitation energy needed for photoisomerization. Recent studies have shown that *cis*/*trans* isomerization of a thioamide group can be readily induced by 250-280 nm light.[36] This latter feature could be a potentially valuable tool for investigating protein conformational changes.

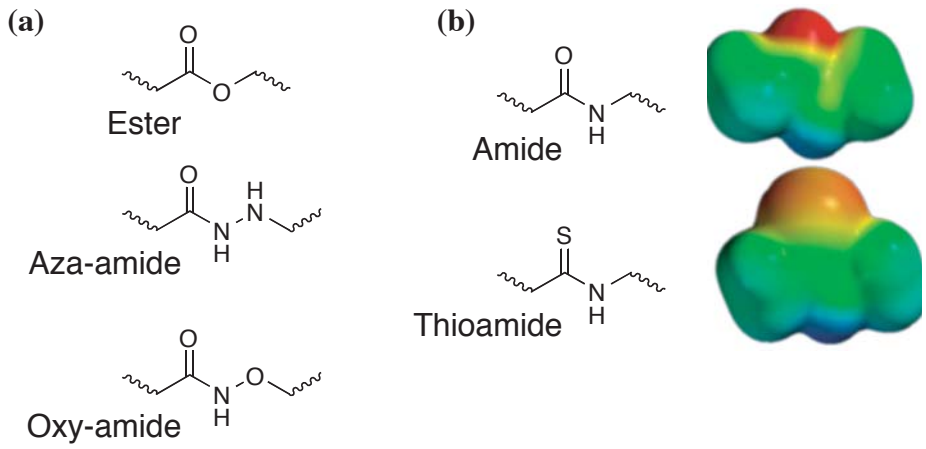

Figure 5.7. Protein backbone mutations. (a) Backbone mutations thus far incorporated by nonsense suppression. (b) Electrostatic potential surfaces for an amide and thioamide, illustrating the relative size of the two groups and the lesser negative potential of sulfur relative to oxygen (red = negative, blue = positive).

5.3.2 Synthetic concerns

Thionation— the conversion of a carbonyl group to a thiocarbonyl— is a widely used synthetic transformation for the preparation of organosulfur compounds. Typically this transformation is accomplished using either phosphorus pentasulfide (P_4S_{10}) or Lawesson's reagent (LR) (Figure 5.8).[37-40] Both of these reagents have a similar reactivity profile. In general, the ease of thionation for a given substrate with these reagents is determined by the electron density at the carbonyl oxygen. Thus, the thionation of amides is usually a fairly facile transformation, while thionation of esters often requires elevated temperatures, longer reaction times, and generally results in poor yields. LR is more commonly used for the thionation of amides as it tends to give higher yields with fewer side reactions.[37] In the case of esters, both reagents have their advantages and disadvantages. The longer reaction times and higher temperatures required for esters means that with either reagent there are significant side reactions. One

advantage of P_4S_{10}, however, is that many of the products from side reactions can be removed through aqueous work-up.[41] It should be noted, however, that because both reagents have highly electrophillic phosphorus species, reactions with either reagent require very dry conditions.

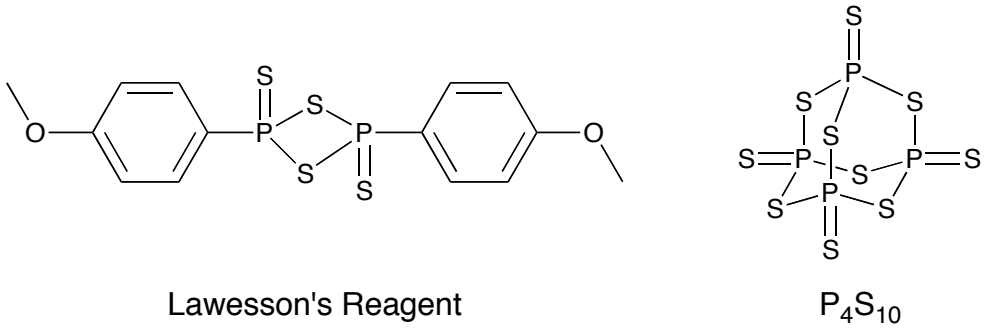

Figure 5.8. Thionation reagents.

Early work on the peptidyl-transfer reaction demonstrated that the ribosome can catalyze the formation of a main chain thioamide in a growing peptide chain.[42] This work used a tRNA where the typical ester linkage between the tRNA and amino acid was replaced by a thionoester— an ester in which the carbonyl oxygen is substituted with sulfur. This study provides evidence for the feasibility of using nonsense suppression to incorporate a backbone thioamide.

The central challenge in realizing suppression-mediated thioamide incorporation is the synthetic preparation of an amino-thionoacyl dCA, where analogous to the studies above the amino acid and dinucleotide are linked by a thionoester (Figure 5.9). There are two important issues in considering synthetic approaches to this thionoester linkage. First, the thionated residue must be activated in way that is compatible with dCA coupling, and second, thionation of the residue must be synthetically accessible. In solid-phase peptide synthesis thioamides are introduced by replacing the carboxylic acid with

an amide.[28, 29, 43, 44] This is then thionated with LR and activated so that the amine is a good leaving group during the peptide coupling reaction. This strategy avoids having to thionate the activated ester. Adapting this protocol for use with the standard dCA coupling chemistry used in preparation of aminoacyl dCA represents one possible approach to generating aminoacyl dCA with a thionoester linkage (Scheme 5.1).[43, 44] This method, however, would require the development of new dCA coupling chemistry. A second approach to this problem is to thionate the activated cyanomethyl ester and then couple the thionated ester with dCA (Scheme 5.2). This route uses the standard dCA coupling chemistry, but has the drawback of having to thionate an ester.

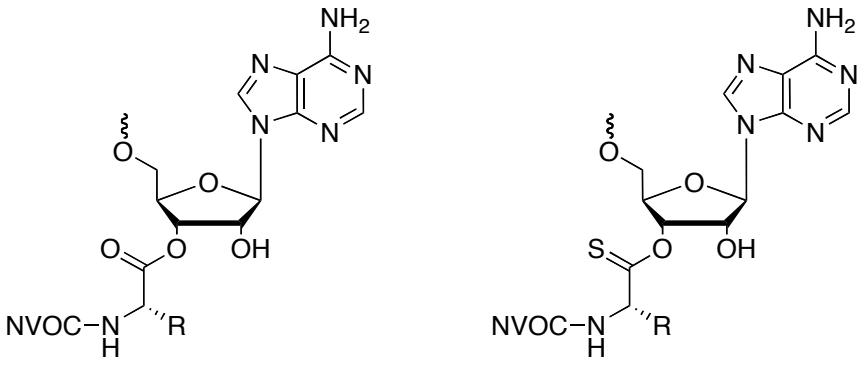

Aminoacyl dCA Amino-thionoacyl dCA

Figure 5.9. Schematic illustrating the ester linkage between the amino acid and the dinucleotide dCA and the thionoester linkage with dCA that is necessary for incorporation of a thioamide via nonsense suppression methods.

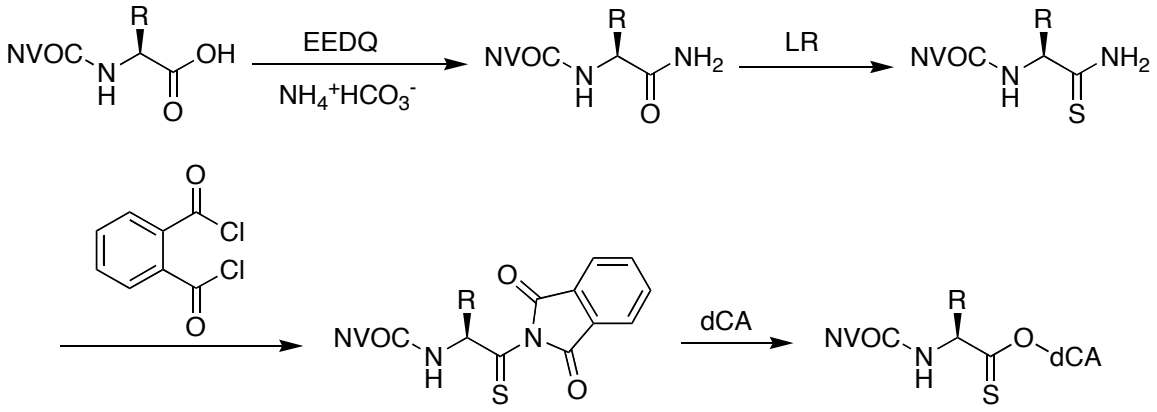

Scheme 5.1. Synthetic route to amino thionoacyl dCA, adapted from strategies used in the solid-phase synthesis of peptides containing thioamides.

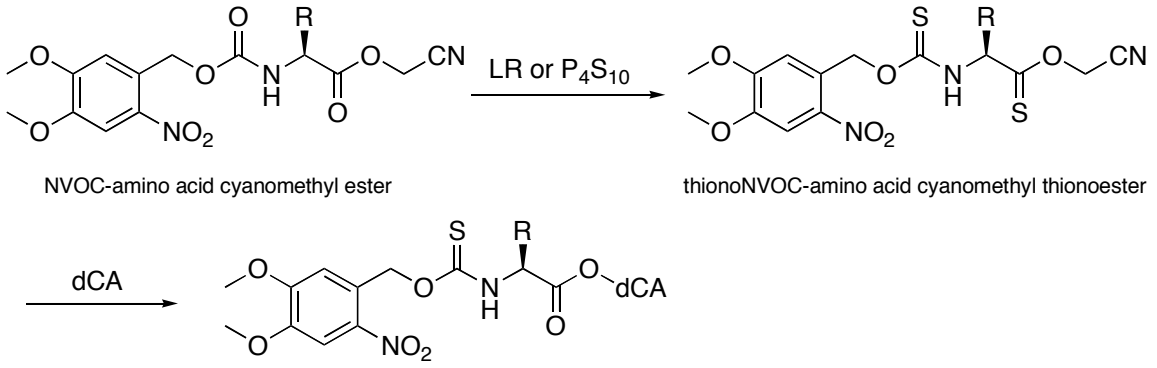

Scheme 5.2. Synthetic route to amino thionoacyl dCA, using standard dCA coupling chemistry.

5.3.3 Experiments

5.3.3.1 Synthesis of thionoNVOC-Pro cyanomethyl thionoester

Initial attempts to synthesize amino thionoacyl dCA followed the route shown in Scheme 5.2. In the end, it was decided that remaining with the standard chemistry used in nonsense suppression represented a better strategy. It is also a shorter route, as it requires only one additional step to be added to the standard amino acid activation and dCA coupling protocol. It should be noted that carbamates are generally quite reactive

with LR, and thus, it is anticipated that the NVOC carbonyl will also be thionated.[37] This does not seem to be problematic, as the thionated species should not substantially perturb the photolysis reaction. The first thionation reaction used NVOC-Pro cyanomethyl ester as the substrate and LR as the thionating reagent. Proline was selected for the potential use of the thiono-analog in studies of the M2-M3 loop (Chapter 4). NVOC-Pro cyanomethyl ester was synthesized in the usual manner.

NVOC-Pro cyanomethyl ester (150 mg, 0.39 mmol) was placed in an oven-dried flask. To this was added 2 mL of dry toluene and 3.6 molar equivalents of LR (568 mg, 14 mmol). The reaction was run under positive argon pressure, heated to reflux in an oil bath, and stirred. The reaction was stopped after 12 hours and applied directly to a flash chromatography column (silica, hexanes/ethyl acetate 1:1). NMR analysis of the column fractions showed no product, but did reveal that the column fractions contained multiple compounds. The diagnostic assay for thionation of an ester is ^{13}C NMR.[30] Thionation leads to ~30 ppm upfield shift in the carbonyl carbon signal. A very typical ^{13}C chemical shift for the carbonyl carbon in a cyanomethyl ester is ~170 ppm. Thus it was expected the product would show a peak near 200 ppm. Thionation of an ester does not typically lead to diagnostic chemical shifts in the ^{1}H NMR spectrum.

The reaction was repeated using identical conditions. This time, however, the reaction was monitored by reverse-phase HPLC and UV spectroscopy. Purification was carried out using semi-preparative reverse-phase HPLC. The chromatogram showed two peaks with significant 350 nm absorption (NVOC group). One matched the elution profile of NVOC-Pro cyanomethyl ester. Fractions corresponding to the other peak were isolated and lyophilized yielding a yellow/brown powder (24 mg, 14% yield). ^{1}H NMR

(300 MHz, $CDCl_3$) δ = 1.95-2.04 (4H, m), 2.21-2.29 (2H, m), 3.88 (3H, s) 3.90 (3H, s), 4.33-4.37 (1H, m), 4.97 (2H, q), 5.45 (2H, dd), 6.88 (1H, s), 7.63 (1H, s). ^{13}C NMR (75 MHz, $CDCl_3$) δ = 25.4, 30.4, 30.8, 47.3, 56.1, 57.4, 60.5, 65.7, 69.8, 108.3, 110.2, 128.3, 140.8, 148.6, 154.3, 156.2, 172.3. MS Calcd for $C_{17}H_{19}N_3O_6S_2$ 425.48. Found: (ESI^+) 426.8 $[M+H^+]^+$.

The mass spectroscopy data correspond to thionoNVOC-Pro cyanomethyl thionoester, with thionation at both the ester carbonyl and the carbamate carbonyl as was expected. Interestingly, the ^{13}C data do not show a shift in the carbonyl carbon peaks for the ester or the carbamate, 172.3 and 156.2 ppm, respectively. The corresponding peaks in NVOC-Pro cyanomethyl ester for the ester and carbamate carbons are 171.9 and 155.4 ppm, respectively. The ^{13}C and ^1H NMR spectra do show differences in the chemical shifts between the two compounds, but the origin of these differences was not able to be determined. Ultimately the spectral data are ambiguous as to the identity of the isolated product. The mass spectroscopy analysis indicates it is thionoNVOC-Pro cyanomethyl thionoester, but the ^{13}C NMR data do not show the diagnostic shifts. Despite this uncertainty, the product was taken on to the dCA coupling step. For comparison the spectral data for NVOC-Pro cyanomethyl ester are shown below: ^1H NMR (300 MHz, $CDCl_3$) δ = 1.68-1.88 (4H, m), 2.07-2.15 (2H, m), 3.69 (3H, s) 3.77 (3H, s), 4.20-4.23 (1H, m), 4.59 (2H, q), 5.25 (2H, dd), 6.74 (1H, s), 7.42 (1H, s). ^{13}C NMR (75 MHz, $CDCl_3$) δ = 24.7, 29.5, 31.0, 36.3, 49.8, 54.3, 56.2, 58.8, 64.8, 110.1, 114.2, 128.7, 139.8, 148.4, 154.3, 155.4, 171.9. MS Calcd for $C_{17}H_{19}N_3O_8$ 393.35. Found: (ESI^+) 394.4 $[M+H^+]^+$

5.3.3.2 dCA coupling

Coupling of the speculative thionoNVOC-Pro cyanomethyl thionoester to dCA was done in the usual manner. To a dry flask was added thionoNVOC-Pro cyanomethyl thionoester (24 mg, 0.056 mmol), dCA (20 mg), and 0.8 mL of dry DMF, and the reaction was stirred under argon. The reaction was monitored by reverse-phase HPLC. After 6 hours no product formation was seen, so tetrabutylammonium acetate (10 mg) was added to the reaction. The reaction immediately turned scarlet red. After 48 hours no product formation was observed and the chromatogram for the reaction showed a multitude of side reactions.

5.3.3.3 Attempts using microwave irradiation

The reactions detailed above revealed several problems with the initial strategy. The reactions showed a significant number of side reactions. The use of excess LR as is required in the thionation of esters made the purification problematic by either flash chromatography (insufficient purification) or reverse-phase HPLC (time consuming), and ultimately, the results were ambiguous.[37] Recently, several groups have reported facile thionation of esters using solvent-free microwave reactions.[45, 46] These studies reported high yields, required only minutes to run, and were able to thionate recalcitrant substrates. These studies also adapted a procedure commonly used in P_4S_{10} thionations, where it has been noted that inclusion of the scavenger hexamethyl-disiloxane (HMDO) in the reaction mix reduces the number of side products and improves the yield.[38, 41]

For the solvent-free microwave-assisted reactions described below, NVOC-Gly cyano methyl ester was used as the substrate. This was done to simplify the NMR

spectra and for potential proof of principle experiments involving the *Shaker* potassium channel (discussed in 5.3.4 Future directions).

In the first reaction, NVOC-Gly cyanomethyl ester (100 mg, 0.28 mmol) and LR (183 mg, 0.45 mmol) were placed in a test tube and thoroughly mixed with a spatula. The test tube was placed in an alumina bath (alumina in a beaker) and irradiated with an unmodified household microwave at maximum wattage (1000 W) for 3 minutes (continuous radiation). This reaction yielded black charred material. The second reaction was set up in an identical manner and irradiated for 5 minutes (10 x 30 s). Following irradiation, the reaction mix was dissolved in methylene chloride and loaded on a flash chromatography column (silica, hexanes/ethyl acetate 1:1). Neither product nor starting material was isolated. In the third attempt, HMDO (73 mg, 95 μL, 0.45 mmol) was included in the reaction mix and the reaction was irradiated for 5 min. (10 x 30 s). Again, neither products nor starting materials were isolated by flash chromatography.

5.3.4 Future directions

There are several possible directions that can be taken to address the problems encountered in trying to synthesize amino thionoacyl dCA. The first is the use of model compounds. This would allow a better estimation of the proper reaction conditions. As noted in the introductory section, thionation reactions with LR or P_4S_{10} are very sensitive to water. It may be that the conditions were not dry enough. In addition, the reactions were run with 3.6 molar equivalents of LR. This excess— although standard in thionations of esters— certainly must lead to more side products as well as making purification in general more difficult.[37, 39] It would also be worthwhile to include HMDO

in the standard LR reactions, and reactions using P_4S_{10} should be considered. If none of these steps prove sufficient, then the route illustrated in Scheme 5.1 offers an alternative that avoids having to thionate an ester.

Once the synthetic issues are worked out, the early studies on the peptidyl-transfer reaction indicate this mutation is compatible with the ribosome and thus, should be amenable to incorporation by nonsense suppression methods. Once incorporated into the protein, backbone thioamides can be readily cleaved by treatment with trifluoracetic acid.[47] The mechanism for this cleavage proceeds in a similar manner to the Edman degradation. This would provide a direct means for verifying the successful incorporation of a backbone thioamide, as the full-length protein and the cleaved protein would show different gel mobilities. Finally, a nice proof of principle experiment would be the incorporation of a thionoGly at the selectivity filter of the *Shaker* potassium channel. The selectivity filter in potassium channels is composed of several backbone carbonyls that point into the channel lumen. The carbonyl oxygen atoms serve to coordinate the potassium ion as it enters the channel. Thus, replacement of the oxygens with the less electronegative sulfur atom should alter the ion selectivity and permeation properties of these channels.

5.4 References

1. Bormann, J., The 'ABC' of GABA receptors. *Trends in Pharmacological Sciences* **2000,** 21, (1), 16-19.
2. Enz, R., GABA(C) receptors: A molecular view. *Biological Chemistry* **2001,** 382, (8), 1111-1122.
3. Jentsch, T. J.; Stein, V.; Weinreich, F.; Zdebik, A. A., Molecular structure and physiological function of chloride channels. *Physiological Reviews* **2002,** 82, (2), 503-568.
4. Cutting, G. R.; Lu, L.; Ohara, B. F.; Kasch, L. M.; Montroserafizadeh, C.; Donovan, D. M.; Shimada, S.; Antonarakis, S. E.; Guggino, W. B.; Uhl, G. R.; Kazazian, H. H., Cloning of the Gamma-Aminobutyric-Acid (Gaba) Rho-1 Cdna - a Gaba Receptor Subunit Highly Expressed in the Retina. *Proceedings of the National Academy of Sciences of the United States of America* **1991,** 88, (7), 2673-2677.
5. Zheng, W.; Xie, W. R.; Zhang, J. H.; Strong, J. A.; Wang, L.; Yu, L.; Xu, M.; Lu, L., Function of gamma-aminobutyric acid receptor/channel rho(1) subunits in spinal cord. *Journal of Biological Chemistry* **2003,** 278, (48), 48321-48329.

6. Amin, J. a. W., D.S., Homomeric r1 GABA channels: activation mechanisms and domains. *Receptors and Channels* **1994,** 2, 227-236.
7. Chang, Y. C.; Covey, D. F.; Weiss, D. S., Correlation of the apparent affinities and efficacies of gamma-aminobutyric acid(C) receptor agonists. *Molecular Pharmacology* **2000,** 58, (6), 1375-1380.
8. Martinez-Torres, A.; Demuro, A.; Miledi, R., GABA rho 1/GABA(A)alpha 1 receptor chimeras to study receptor desensitization. *Proceedings of the National Academy of Sciences of the United States of America* **2000,** 97, (7), 3562-3566.
9. Wotring, V. E.; Chang, Y. C.; Weiss, D. S., Permeability and single channel conductance of human homomeric rho 1 GABA(C) receptors. *Journal of Physiology-London* **1999,** 521, (2), 327-336.
10. Zhang, D. X.; Pan, Z. H.; Awobuluyi, M.; Lipton, S. A., Structure and function of GABA(c) receptors: a comparison of native versus recombinant receptors. *Trends in Pharmacological Sciences* **2001,** 22, (3), 121-132.
11. Brejc, K.; van Dijk, W. J.; Klaassen, R. V.; Schuurmans, M.; van der Oost, J.; Smit, A. B.; Sixma, T. K., Crystal structure of an ACh-binding protein reveals the ligand-binding domain of nicotinic receptors. *Nature* **2001,** 411, (6835), 269-276.
12. Beene, D. L.; Brandt, G. S.; Zhong, W. G.; Zacharias, N. M.; Lester, H. A.; Dougherty, D. A., Cation-pi interactions in ligand recognition by serotonergic (5-HT3A) and nicotinic acetylcholine receptors: The anomalous binding properties of nicotine. *Biochemistry* **2002,** 41, (32), 10262-10269.
13. Zhong, W. G.; Gallivan, J. P.; Zhang, Y. N.; Li, L. T.; Lester, H. A.; Dougherty, D. A., From ab initio quantum mechanics to molecular neurobiology: A cation-pi binding site in the nicotinic receptor. *Proceedings of the National Academy of Sciences of the United States of America* **1998,** 95, (21), 12088-12093.
14. Mu, T. W.; Lester, H. A.; Dougherty, D. A., Different binding orientations for the same agonist at homologous receptors: A lock and key or a simple wedge? *Journal of the American Chemical Society* **2003,** 125, (23), 6850-6851.
15. Ma, J. C.; Dougherty, D. A., The cation-pi interaction. *Chemical Reviews* **1997,** 97, (5), 1303-1324.
16. Nowak, M. W.; Kearney, P. C.; Sampson, J. R.; Saks, M. E.; Labarca, C. G.; Silverman, S. K.; Zhong, W.; Thorson, J.; Abelson, J. N.; Davidson, N.; Schultz, P. G.; Dougherty, D. A.; Lester, H. A., Nicotinic Receptor-Binding Site Probed with Unnatural Amino-Acid-Incorporation in Intact-Cells. *Science* **1995,** 268, (5209), 439-442.
17. Nowak, M. W.; Gallivan, J. P.; Silverman, S. K.; Labarca, C. G.; Dougherty, D. A.; Lester, H. A., In vivo incorporation of unnatural amino acids into ion channels in Xenopus oocyte expression system. In *Ion Channels, Pt B* **1998**, 293, 504-529.
18. Mecozzi, S.; West, A. P.; Dougherty, D. A., Cation-pi interactions in simple aromatics: Electrostatics provide a predictive tool. *Journal of the American Chemical Society* **1996,** 118, (9), 2307-2308.
19. Beene, D. L.; Price, K. L.; Lester, H. A.; Dougherty, D. A.; Lummis, S. C. R., Tyrosine residues that control binding and Gating in the 5-hydroxytryptamine(3) receptor revealed by unnatural amino acid mutagenesis. *Journal of Neuroscience* **2004,** 24, (41), 9097-9104.
20. Reeves, D. C.; Sayed, M. R. F.; Chau, P. L.; Price, K. L.; Lummis, S. C. R., Prediction of 5-HT3 receptor agonist-binding residues using homology modeling. *Biophysical Journal* **2003,** 84, (4), 2338-2344.
21. Kearney, P. C.; Nowak, M. W.; Zhong, W.; Silverman, S. K.; Lester, H. A.; Dougherty, D. A., Agonist binding site of the nicotinic acetylcholine receptor: Tests with novel side chains and with several agonists. *Molecular Pharmacology* **1996,** 50, (5), 1401-1412.
22. Koh, J. T.; Cornish, V. W.; Schultz, P. G., An experimental approach to evaluating the role of backbone interactions in proteins using unnatural amino acid mutagenesis. *Biochemistry* **1997,** 36, (38), 11314-11322.
23. Eisenhauer, B. M.; Hecht, S. M., Site-specific incorporation of (aminooxy)acetic acid into proteins. *Biochemistry* **2002,** 41, (38), 11472-11478.
24. Killian, J. A.; Van Cleve, M. D.; Shayo, Y. F.; Hecht, S. M., Ribosome-mediated incorporation of hydrazinophenylalanine into modified peptide and protein analogues. *Journal of the American Chemical Society* **1998,** 120, (13), 3032-3042.
25. Levesque, G.; Arsene, P.; Fanneau-Bellenger, V.; Pham, T. N., Protein thioacylation. 1. Reagents design and synthesis. *Biomacromolecules* **2000,** 1, (3), 387-399.
26. Miwa, J. H.; Patel, A. K.; Vivatrat, N.; Popek, S. M.; Meyer, A. M., Compatibility of the thioamide functional group with beta-sheet secondary structure: Incorporation of a thioamide linkage into a beta-hairpin peptide. *Organic Letters* **2001,** 3, (21), 3373-3375.

27. Miwa, J. H.; Pallivathucal, L.; Gowda, S.; Lee, K. E., Conformational stability of helical peptides containing a thioamide linkage. *Organic Letters* **2002,** 4, (26), 4655-4657.
28. Shalaby, M. A.; Grote, C. W.; Rapoport, H., Thiopeptide synthesis. alpha-amino thionoacid derivatives of nitrobenzotriazole as thioacylating agents. *Journal of Organic Chemistry* **1996,** 61, (25), 9045-9048.
29. Shalaby, M. A.; Rapoport, H., A general and efficient route to thionoesters via thionoacyl nitrobenzotriazoles. *Journal of Organic Chemistry* **1999,** 64, (3), 1065-1070.
30. Sifferlen, T.; Rueping, M.; Gademann, K.; Jaun, B.; Seebach, D., beta-Thiopeptides: Synthesis, NMR solution structure, CD spectra, and photochemistry. *Helvetica Chimica Acta* **1999,** 82, (12), 2067-2093.
31. Tran, T. T.; Zeng, J.; Treutlein, H.; Burgess, A. W., Effects of thioamide substitutions on the conformation and stability of alpha- and 3(10)-helices. *Journal of the American Chemical Society* **2002,** 124, (18), 5222-5230.
32. Zacharie, B.; Lagraoui, M.; Dimarco, M.; Penney, C. L.; Gagnon, L., Thioamides: Synthesis, stability, and immunological activities of thioanalogues of Imreg. Preparation of new thioacylating agents using fluorobenzimidazolone derivatives. *Journal of Medicinal Chemistry* **1999,** 42, (11), 2046-2052.
33. Aleman, C., On the ability of modified peptide links to form hydrogen bonds. *Journal of Physical Chemistry A* **2001,** 105, (27), 6717-6723.
34. Artis, D. R.; Lipton, M. A., Conformations of thioamide-containing dipeptides: A computational study. *Journal of the American Chemical Society* **1998,** 120, (47), 12200-12206.
35. Tran, T. T.; Treutlein, H.; Burgess, A. W., Conformational analysis of thiopeptides: derivation of Sp(2) sulfur parameters for the CFF91 force field. *Journal of Computational Chemistry* **2001,** 22, (10), 1010-1025.
36. Helbing, J.; Bregy, H.; Bredenbeck, J.; Pfister, R.; Hamm, P.; Huber, R.; Wachtveitl, J.; De Vico, L.; Olivucci, M., A fast photoswitch for minimally perturbed peptides: Investigation of the trans -> cis photoisomerization of N-methylthioacetamide. *Journal of the American Chemical Society* **2004,** 126, (28), 8823-8834.
37. Cava, M. P.; Levinson, M. I., Thionation Reactions of Lawesson Reagents. *Tetrahedron* **1985,** 41, (22), 5061-5087.
38. Curphey, T. J., Thionation of esters and lactones with the reagent combination of phosphorus pentasulfide and hexamethyldisiloxane. *Tetrahedron Letters* **2002,** 43, (3), 371-373.
39. Pedersen, B. S.; Scheibye, S.; Nilsson, N. H.; Lawesson, S. O., Studies on Organophosphorus Compounds .10. Syntheses of Thioketones. *Bulletin Des Societes Chimiques Belges* **1978,** 87, (3), 223-228.
40. Sudalai, A.; Kanagasabapathy, S.; Benicewicz, B. C., Phosphorus pentasulfide: A mild and versatile catalyst-reagent for the preparation of dithiocarboxylic esters. *Organic Letters* **2000,** 2, (20), 3213-3216.
41. Curphey, T. J., Thionation with the reagent combination of phosphorus pentasulfide and hexamethyldisiloxane. *Journal of Organic Chemistry* **2002,** 67, (18), 6461-6473.
42. Victorova, L. S.; Kotusov, V. V.; Azhaev, A. V.; Krayevsky, A. A.; Kukhanova, M. K.; Gottikh, B. P., Synthesis of Thioamide Bond Catalyzed by Escherichia-Coli Ribosomes. *Febs Letters* **1976,** 68, (2), 215-218.
43. Josse, O.; Labar, D.; Marchand-Brynaert, J., A convenient synthesis of ethyl 3-aminopropanedithioate (beta- alanine ethyl dithioester). *Synthesis-Stuttgart* **1999**, (3), 404-406.
44. Brain, C. T.; Hallett, A.; Ko, S. Y., Thioamide synthesis: Thioacyl-N-phthalimides as thioacylating agents. *Journal of Organic Chemistry* **1997,** 62, (12), 3808-3809.
45. Varma, R. S.; Kumar, D., Microwave-accelerated solvent-free synthesis of thioketones, thiolactones, thioamides, thionoesters, and thioflavonoids. *Organic Letters* **1999,** 1, (5), 697-700.
46. Filippi, J. J.; Fernandez, X.; Lizzani-Cuvelier, L.; Loiseau, A. M., Solvent-free thionation of gamma-lactones under microwave irradiation. *Tetrahedron Letters* **2003,** 44, (35), 6647-6650.
47. Miwa, J. H.; Margarida, L. A.; Meyer, A. E., Improved acidolytic deprotection conditions for the Fmoc-based solid-phase synthesis of thioxo peptides. *Tetrahedron Letters* **2001,** 42, (41), 7189-7191.